Pilot Compartment
Airbag Restraint Program

Final Report

MARTIN

Pilot Compartment
Airbag Restraint Program

Final Report

NASw-877

ER 13551

July 1964

AVAILABLE TO U.S. GOVERNMENT AGENCIES ONLY

MARTIN
BALTIMORE DIVISION
BALTIMORE, MARYLAND 21203

FOREWORD

This report was prepared by Carl C. Clark, Carl Blechschmidt and Fay Gordon of the Life Sciences and Structures Departments, Space Systems Division of the Martin Company. It presents the testing and analytical results of the Pilot Compartment Airbag Restraint System.

This program was conducted in partial fulfillment of the National Aeronautics and Space Administration Contract Number NASw-877 and under the technical direction of Mr. John M. Fuscoe, Biotechnology Branch (Code RBB) of the Office of Advanced Research and Technology, NASA Headquarters.

A report covering the work under Amendments Nos. 1 and 2 will be presented at a later date.

CONTENTS

SUMMARY

Manned impact tests of airbag restraint systems in a preliminary experimentation box, a spacecraft simulator, and a passenger airplane simulator have been carried out to show the feasibility of such active elastic restraint systems, in which restoring forces can be varied by varying bag pressures to ensure the prevention of "bottoming." These systems can isolate from high frequency (above 5 cps) vibration and impact loads, transmitting less than 50%, and often less than 25%, of the loads on the "vehicle." Rebound effects occur at a low enough frequency (near 3 cps) that they are physiologically acceptable, without any bag pressure dumping or valving.

A total of 57 experimental impact tests were carried out in the spacecraft simulator with manned impact tests up to impact velocities of 9.8 m/sec (32 ft/sec). The impact vehicle was a container about 1.8 m (6 ft) in diameter and 3.7 m (12 ft) long. The subject lies in the vehicle parallel to its longitudinal axis and is sandwiched between 2 airbags 203 cm (80 in.) long with airbags above his head and below his feet 60 cm (24 in.) and 80 cm (32 in.) long, respectively. For a vertical or level attitude drop from 4.9 m (16 ft), maximum vehicle loads of 69 G_x were measured while the head load peaked at 21.8 G_x, chest load at 14.6 G_x and hip load at 18.0 G_x. For the 45° feet-down attitude drop from 4.9 m (16 ft) with a load of +72 G_x and +27 G_z on the vehicle (77 G resultant), the load on the man's head was less than 16 G_x and 9 G_z, and on the chest and hip less than 9 G_x and 11 G_z. Maximum vehicle loads of 68 G perpendicular to the impact plane were measured for the 45° left-side attitude drop from 3.1 m (10 ft) with maximum loads of 18.7 G_x head, 10.5 G_x chest, and 9.3 G_x hip measured on the subject. The maximum calculated deflection for any of the above drops did not exceed 24 in. Impact tests were also conducted using the restrained anthropomorphic dummy at the maximum drop height capability of the overhead crane, 8.6 m (28 ft). The measured accelerations were high but physiologically acceptable in an emergency. Technical film report No. 8[23] summarizes the entire test program.

Analog simulation of the airbag restraint system duplicated the experimental vertical drops and allowed predictions beyond the experimental effort. The experimental system as represented on the analog has a resonant frequency of 2.05 cps with a transmissibility of 4.8 at resonance. This system will attenuate all frequencies above 3 cps. The analog model permitted solution of typical launch and re-entry as well as impact loads.

11515

Indications from both the experimental program and the analog program are that the airbag-type restraint system would provide excellent isolation from spacecraft landing impacts and launch and re-entry vibrations with the astronaut in any attitude. This spacecraft restraint study also led to the development of an active elastic airbag restraint system for aircraft passenger protection. Information on this testing program will be presented in a later report covering the effort under addendum to NASA contract NASw 877.

author

CONCLUSIONS

(1) A single-subject "pilot compartment airbag restraint system" has been built and tested to demonstrate the excellent vibration and impact load isolation characteristics of such a restraint. Indeed, the isolation is so good that the airbag design is viewed as representing a significant new approach in restraint development, predicted by others (as documented in the report) but, here, experimentally demonstrated by dummy, manned and analog computer tests. It is recommended that this restraint be further developed for use in spacecraft, aircraft and automobiles, both for its load isolation aspects and for its potentially light weight and ease of stowage when not in use.

(2) The previous view that rebound in the elastic restraint must be eliminated, by a pressure-dumping blow-out valve for example, has been shown to be wrong. With good restraint during rebound, motion at a physiologically well-accepted frequency of two or three cycles per second, and amplitudes well within tolerance levels because of the restraint load isolation properties, the very brief rebound events are physiologically and subjectively well accepted. The crash is experienced as a slight ripple loading rather than a single event. Leaving the restraint inflated allows it to protect against subsequent impacts, from whatever direction, retaining its isolation capabilities. Note that deformable solids, such as honeycomb, lose much of their load isolation capabilities after an initial impact.

(3) With resonance frequencies near two or three cycles per second, airbag restraint systems provide good vibration isolation for vehicle frequencies above five cycles per second. (Figure 64 of this report shows no five cycles per second load isolation, but further analysis shows that ±3 G at 10 cps of the vehicle would be reduced to ±0.15 G at the crew by the restraint.) It is noted that rocket vehicle structural and aerodynamic vibration frequencies are generally above five cycles per second.

(4) "Bottoming" of restraints onto less yielding structures must be prevented to avoid potential load amplification rather than isolation. Whereas rigid restraints cannot provide load isolation, they also avoid this potential bottoming load amplification hazard. At a certain increasing impact load level, passive elastic restraint systems, such as cushions, will bottom, and if these large loads are possible (as in aircraft ejection seats) use of a rigid restraint (seat) is advised over the use of the passive elastic restraint (cushion), at the expense of losing the comfort of the load isolation of the passive elastic restraint for all loads in which it does not bottom.

On the other hand, with airbag restraint systems, which we call active elastic restraint systems because of the ease of changing their properties, bag pressure can be adjusted to ensure that bottoming will

not occur for the anticipated impact load (or measured approach velocity). Indeed, by inserting restraining straps through the bags, the pressure can be increased without volume expansion to make the airbag system essentially rigid, if an extreme load is to be experienced. Hence, airbag restraint systems provide the advantage of load isolation of elastic systems for moderate loads yet with adjusted pressure can avoid the hazard of bottoming and potential load amplification for extreme loads. In this program of 57 impacts, "bottoming" loads did not occur with human subjects but occurred five times with the dummy, twice when the dummy slid to the side between the bags prior to a side impact (Runs 48 and 51) and three times when pressure was too low for the severe impact (Runs 54, 55 and 57), the last two of which were at the impact velocity of 42 feet per second. Note, however, that in all five of the "bottoming" cases, the loads on the dummy were less than those on the vehicle.

(5) Airbag restraints provide load isolation by an allowed motion of the subject with respect to the vehicle. This amplitude of motion depends on the applied impact velocity (↑), the mass of the subject or subjects (↑), the subject surface area (↓), the bag absolute pressure (↓), bag wall stretchability (↑), and bag volume (↑). Some of these functions, trending up or down as indicated by the arrows, have only briefly been analyzed in this report; a more complete analysis will appear in the final report on the addendum to this contract, particularly concerning the airline passenger airstop restraint. Experimentally, it is possible to decelerate a subject at less than 20 G for an impact velocity of 32 feet per second by a simple anterior and posterior latex bag restraint pressurized to just a few inches of water pressure above atmospheric pressure with a stopping distance of less than two feet. From theoretical analysis, the motion of the subject with respect to the vehicle is maximum for an instantaneous stopping of the vehicle, and is decreased as the vehicle stopping distance is increased. Under conditions in which a reduced "stopping distance" is available of allowed motion of the subject with respect to the vehicle before he "bottoms" on more rigid structure, increased bag pressure would be required for this simple restraint design to produce the required increased deceleration to stop the subject in the shorter distance.

(6) In the addendum part of the contract, to be reported shortly, rubberized nylon, vinyl chloride, and mylar bags have been examined in addition to latex bags of differing wall thicknesses. Materials studies can significantly affect the weight of a finally selected operational restraint system, but it is felt that the general acceleration isolation capabilities of airbag restraints can be shown with these few materials. We feel that it is important first to demonstrate these general capabilities for the particular conditions of number of crew members, vehicle volume and geometry, allowable crew motions, vehicle deceleration, etc. Then, after a decision to perfect an airbag system for a particular operational situation, a materials selection study would be highly desirable.

ILLUSTRATIONS

ILLUSTRATIONS (continued)

ILLUSTRATIONS (continued)

ILLUSTRATIONS (continued)

ILLUSTRATIONS (continued)

ILLUSTRATIONS (continued)

I. INTRODUCTION

In designing and testing human restraint systems, the classical approach of John Paul Stapp[1], Eli Beeding[2], Ellis Taylor[3], John Swearingen[4], Neville Clarke[5], Martin Webb[6], Flanagan Gray[6], Carter Collins[6], and others has been to determine the human tolerance limits in the particular restraint, with attempts to modify the restraint to allow the human to tolerate higher and higher acceleration, particularly by limiting "body distortion[7]." For low frequency or steady accelerations, this is the necessary approach, for the human must either accept the acceleration of the vehicle or be left behind by it. But for accelerations approaching 1 cps or above, we are exploring an alternative approach of designing the human restraint system to isolate the human from these high frequency accelerations of the vehicle, by allowing the human to move in a controlled way with respect to the vehicle. In previous work, passive elastic or loose restraints have been mistrusted in restraint systems because of the "acceleration overshoot" or "bottoming effect" experienced by the human when reaching elastic or displacement limits of the component, and because of concern for rebound or "backlash" effects. Recent work has emphasized increasingly rigid restraint systems with, at best, a passive mechanical load limiter external to the man-rigid couch restraint system. Our work is exploring the concept based on the use of pressurized airbags about the human to form an active elastic restraint system having elastic properties that can be varied to ensure that bottoming will not occur for the acceleration event of concern, and to provide high frequency acceleration isolation. We wish to be isolated from rather than simply tolerate vibration and impact loads.

Airbags have been used previously to limit vehicle impact loads, including: those to recover Mace missiles fired for training[8] (Fig. 1); the mat landing system used with an arresting wire and airplane hook for minimum length landing[9] (Fig. 2); the bags used under the Mercury vehicles[10], filled by lowering the heat shield from the capsule prior to landing; those under the B-58 escape capsule[11]; and those of theoretical studies[12, 13]. Inflated components in tested human restraint systems include the Goodyear airmat restraint[14] (Fig. 3), which used a high enough pressure to be essentially rigid during operation, and the low pressure fit-adjustment bags used in the Vykukal-Ames (Fig. 4) restraint system[15]. Proposed human restraints involving airbags include the "freedom-restraint concept (Fig. 5) of Douglas[16], with bags inflated around a lap shelf which Al Mayo says[17] he did try in a crash simulation test, and the "caterpillar restraint" (Fig. 6) design of Ling-Temco-Vought[18], involving a series

of inflatable fabric bags supported by semi-circular metal formers, which was considered and rejected for development. Since doing most of the work described in this report, we have heard of airbag designs for airplane passenger restraint by Assen Jordanoff* (Figs. 7 and 8) and for an automobile passenger restraint by General Motors[19], but have not located written reports. Apparently the development work on these systems did not include manned crash simulation tests.

A number of patents[20] (Fig. 9) involving airbag restraints have been located, but these also apparently did not involve human crash tests.

*Jordanoff, Assen: From personal communications, Mr. Jordanoff's airbag conception and first model was in 1953 (Fig. 7). A demonstration and paper, "Passenger Crash Protection Device," was presented at the 8th Annual International Air Safety Seminar of the Flight Safety Foundation, Palm Beach, Florida, December 1956. An improved protection device was made with the U.S. Rubber Company in February, 1957 (Fig. 8). This was demonstrated by running on foot into walls, but not tested in crash simulation.

II. PILOT COMPARTMENT AIRBAG RESTRAINT PROGRAM

A. IMPACT TESTS

1. Physical Setup

The impact vehicle, shown diagramatically in Fig. 11, was fabricated from a surplus Mace warhead section shipping container about 1.8 m (6 ft) in diameter and 3.7 m (12 ft) long (Figs. 12 and 13). Modification consisted of: reinforcements in the areas of high stress loadings; addition of 45° feet-down (Fig. 14) and 45° left-side (Fig. 15) impact skids; addition of lifting lugs and adjustable three point sling for pickup and attitude control (Fig. 13); provision for ingress-egress by two doors [one located near the head of the subject on the subject's right side, the other near the feet on the subject's left side (Fig. 16)]; and providing ports for pressurizing and evacuating the airbags. The subject lies in the vehicle parallel to its longitudinal axis (Fig. 16), supported on a semi-cylindrical lower latex airbag (Fig. 17), 203 cm (80 in.) long and covered by a semi-cylindrical upper bag. Above his head and below his feet are head and foot cylindrical bags 60 cm (24 in.) and 80 cm (32 in.) long, respectively. This provides for displacements of 76 cm (30 in.) in any test direction before "bottoming." Emergency "bottoming" protection was provided by an additional 12.7 cm (5 in.) of polyurethane foam and felt secured to the inside bottom and foot end of the container. Lacing ties were provided around the internal periphery for attaching the airbags. Provisions were made for two types of "body stiffening," one a plywood board 71 x 175 cm (28 x 69 in.) laced to the lower bags, and the other a "body bag" (Fig. 18) in which the subject zippers himself and which is inflatable to a higher pressure than the surrounding bags. This body bag is a multiple walled inflatable structure allowing the outer wall to be pressurized to a pressure higher than the surrounding bags, while the inner walled low pressure bag allows comfort and universal fit. In a spacecraft utilization, the body bag functions would be provided by a pressure suit. Hoisting and dropping was accomplished with a 25,000-lb rated, servo actuated quick release hook attached to a 5-ton manned overhead cab crane. The impacting surface for all conditions was an 18-in. bed of bank grade sand with a high concentration of clay and gravel except for the 45° feet-down attitude test where a 2.54-cm (1-in.) thick steel plate was placed 12.7 cm (5 in.) below the surface (for increased vehicle loading).

2. Instrumentation

Vehicle and airbag. The instrumentation schematic of Fig. 19 shows the basic setup used. Vehicle accelerations were measured using two types of transducers, Endevco Model 2235 and Statham Model A5A. These accelerometers were oriented for measurement in the G_x, G_y and

G_z (Fig. 20) axes, depending on the impact attitude of concern, and were located on the base structure of the vehicle near the point of impact (Fig. 21). The output from these accelerometers was amplified by Dyna-Monitor Model 2702B for the Endevco accelerometers and "Bridge Balance Units" for the Statham accelerometers. The amplified accelerometer output was recorded on a CEC direct writing oscillograph (Fig. 13). All airbags were instrumented with CEC Model 4-312-5 psid pressure pickups shock mounted in the pressurizing ports of the vehicle. The output from these transducers was conditioned by "Bridge Balance Units" and recorded on a CEC direct writing oscillograph.

Subject or anthropomorphic dummy accelerations. Subject instrumentation consisted of Statham F-50-300 accelerometers mounted generally on the head, chest and hip for measurement of G_x, G_y and G_z accelerations (Fig. 22). Dummy instrumentation consisted of Statham A5A accelerometers mounted in the head, chest and pelvic cavities, for measurement of G_x, G_y and G_z accelerations. The output from these accelerometers was amplified through a "Systems D" carrier amplifier and recorded on a CEC direct writing oscillograph. A manual marker was employed to synchronize the two oscillographs.

Physiological parameters. Physiological monitoring, in addition to communications, consisted of the electrocardiograph using standard limb electrodes taped to the right and left sides of the chest (Fig. 22) and body temperature recordings with the temperature sensor affixed to the axillary region where temperature approximates that of the core. The ECG was recorded both by hardware (Sanborn Model 150-1600 ECG preamplifier and recorder) and telemetry (Telemedics RKG100) techniques. The body temperature was monitored with a telethermometer (Yellow Springs Instrument) and also recorded on the Sanborn Model 150 recorder using a Model 760-50 temperature bridge with a Model 150-1100 carrier preamplifier.

Tape recordings were made of all subject-test monitor conversations and subjective remarks.

3. Experimental Procedure

Before placing the test subject in the container, all physiological sensors were affixed (ECG and body temperature) (Fig. 22) and accelerometers secured to the head, chest (Fig. 22) and hip. Communications and recording were checked out as well as the ventilation-breathing air supply. A vacuum pump was attached to the upper airbag to evacuate the bag against the upper wall of the container to provide an open access area. The lower airbag was partially filled with air to support the subject. The subject was then positioned on the lower airbag, either on

the support board (Fig. 16), in the body bag (Fig. 18), or without any support depending on the condition to be tested. Instrumentation leads from the subject were then connected to the recording equipment. The upper airbag was then partially pressurized and final checks made on the status of the subject and airbag installation. The two doors were then locked in place and the airbags were pressurized to the testing pressure. The automatic release mechanism was secured to the overhead crane hook and then attached to the test vehicle pickup sling. The test vehicle was then raised to the test drop height (Figs. 23, 24 and 25), instrumentation was checked and recording started, final subjective check was made, and release effected (Figs. 26, 27 and 28). Immediately after impact, subjective comments were solicited and recorded.

4. Discussion and Results

The magnitude of the elastic restraint problem can be discerned by using two equations. For sinusoidal vibrations of frequency, f, in cycles per second and peak acceleration, a, in g units, the double amplitude of displacement, d, in centimeters is given by

$$d = 2\ ag/4\ \pi^2 f^2 = 50\ a/f^2 . \qquad (1)$$

The goal of the elastic restraint is to allow the body to stay still (i.e., move along the mean vehicle flight path) while the vehicle vibrates about it. This "decoupling" from the vehicle vibration will require an allowable distance of body motion with respect to the vehicle of rather more than d, since it is difficult to attain perfect decoupling, and "bottoming" at the end of the elastic restraint stroke must be avoided.

For impacts of velocity, v, imposing a tolerable load, a, on the body, the stopping distance, d, of the body is given by

$$d = v^2/2\ ag. \qquad (2)$$

To the extent that the vehicle stops other than instantaneously, the body motion with respect to the vehicle would be decreased. A practical system does not provide a square wave restoring load, a circumstance reducing concern for onset rates of change of acceleration. For a haversine restoring load of the same peak acceleration and period as the square wave, a stopping distance twice as great as that for the square wave load case is required.

Consider a vehicle with a possible vibration during launch or reentry of ±5 g at 10 cps and a parachute landing impact onto rock at 1000 cm/sec (400 in./sec). From Eq (1)

$$d = 50\ (5)/10^2 = 2.5\ \text{cm}\ (1\ \text{in.}). \qquad (3)$$

From Eq (2), for a 20-g landing,

$$d = 1000^2/2(20)(980) = 26 \text{ cm } (10 \text{ in.}). \quad (4)$$

For the more typical haversine deceleration, 2d = 52 cm (20 in.). It can be seen that for this vehicle, the landing sets the more severe requirement for body motion with respect to the vehicle.

Preliminary work on the airbag restraint system was carried out as a Martin-funded program, using a 56- x 86- x 214-cm (22- x 34- x 84-in.) wooden box containing two full length latex bags between which the subject lay (Fig. 10), with a clearance from the "vehicle" bottom of about 18 cm (7 in.). Respiration was maintained through an opening in the upper bag and box cover. Vibrations were applied in the range from 5 to 2000 cps using a C-25H electrodynamic shaker. At all frequencies studied, the acceleration on the man was less than that on the vehicle; for example, with 8.9 cm (3.5 in.) of water pressure in the lower bag, a vehicle acceleration of 1 ±3 G_x at 11 cps became 1 ±0.4 G_x at the subject's hip. The resonance frequency of the man-airbag system should be lower than any significant amplitude vehicle vibration frequency in order to provide vibration isolation. Low bag pressures provided such isolation. In the flight situation, a lower bag pressure increased through a "G-valve" in proportion to the "steady state" acceleration of launch or re-entry might be required to maintain body position with respect to instruments; it is not necessarily low pressure but a fairly flat force versus displacement curve for oscillations about the steady-state force that is required for vibration isolation.

The box "vehicle" was impacted into sand from heights up to 1.5 m (5 ft). With the limited stroke available in this system, it was considered safer to eliminate body bending by having the subject on a 3-cm thick sand mattress (for contouring) on a 2-cm thick 640- x 1400-cm (25- x 55-in.) area plywood "back-board" on top of the lower airbag. At the start of this work, it was considered important to eliminate rebound, by abruptly dropping the pressure of the lower bag at its maximum stroke. In the developed system, a 30-cm (12-in.) diameter port was opened into the lower bag when a shear pin yielded at a lower bag overpressure of 38 cm (15 in.) of water. With this system, with initial lower bag pressure of 25 cm (10 in.) of water and upper bag pressure of 15 cm (6 in.) of water, a 1.5-m (5-ft) drop, giving an impact velocity of 5.5 m/sec (17.9 ft/sec) and an impact load of 440 G_x on the structure, gave a load on the man's head of 16.7 G_x and a load on his hip of 13.2 G_x. Subjectively, this impact was quite acceptable, without any headache or other sequela.

The procedure of dropping bag pressure to reduce rebound, of course, releases the restraint--an undesirable procedure in the operational

situation in which multiple impact loads and tumbling may occur. Hence, several impacts were made without releasing pressure. Rebounds occurred, but with successive cycle peaks attenuated about 50% and at a frequency below 5 cps; subjectively, these impacts were also quite acceptable; however, the concern for "bottoming" or acceleration overshoot at stroke limits of the elastic system must remain. The desirable system was therefore identified as an airbag restraint supporting the subject in all directions and remaining inflated throughout impact. Bottoming would be prevented either by using a high enough bag pressure required for the measured velocity prior to impact or preferably by having available a long enough stroke at the lower bag pressure. For bag pressures above 25 cm (10 in.) of water, the body, for comfort, would have to be isolated within a limited compression shell such as an inflated pressure suit.

Table 1 (pg 71) summarizes the 57 experimental impact tests conducted on the Pilot Compartment Airbag Restraint System under NASA Contract NASw-877. Fourteen of these tests were manned, the remaining being conducted with a 95th percentile anthropomorphic dummy. Figures 29 through 40 present the time-history accelerations for the primary manned impact test and a portion of the anthropomorphic dummy impact tests for comparison purposes. Figures 47 through 53 present a graphical summary of the body accelerations versus impact velocity for the three types of drops (level, 45° feet down, and 45° left side). Figures 54 through 56 present a graphical summary of body accelerations versus initial bag pressures at various impact velocities for the anthropomorphic dummy impact tests.

For the vertical or level attitude drop (with the subject on the backboard) from 4.9 m (16 ft) giving an impact velocity of 9.8 m/sec (32 ft/sec) (Fig. 32), maximum vehicle loads of 69 G_x were measured with the vehicle sinking into the stony sand about 15 cm (6 in.) (Fig. 21). With an average pressure in the bags of 7.6 cm (3 in.) of water before drop, the head load peaked at 21.8 G_x, chest load at 14.6 G_x, and hip load at 18.0 G_x, with rapidly damping (approximately 50% attenuation per cycle) rebounds at about 3 cps. Double integration of the hip acceleration curve gives a computed displacement of 50 cm (19.7 in.) (x direction).

For the 45° feet-down attitude drop from 4.9 m (16 ft), the subject was inside the body bag, pressurized to 25 cm (10 in.) of water. This gave an impact velocity of 9.8 m/sec (32 ft/sec) (Fig. 35). Maximum vehicle loads of 72 G_x were measured at initial impact at a 45° angle (Fig. 27) and 17 G_x at secondary head-end slap-down (Fig. 35). With an average pressure in the bags of 7.6 cm (3 in.) of water before the drop, the head load peaked at 16.5 G_x, chest load at 9.4 G_x and hip load at 7.4 G_x. Double integration of the hip acceleration curve gives a computed displacement of 58 cm (22.8 in.) (x direction) and 43 cm (16.9 in.) (z direction).

For the 45° left-side attitude drop from 3.1 m (10 ft), the subject was inside the body bag, pressurized to 25 cm (10 in.) of water. This drop gave an impact velocity of 7.6 m/sec (25 ft/sec) (Fig. 36). Maximum vehicle loads of 68 G perpendicular to the impact plane were measured (Fig. 28). With an average pressure in the bags of 15 cm (6 in.) of water before the drop, the head load peaked at 18.7 G_x, chest load at 10.5 G_x, and hip load at 9.3 G_x. Double integration of the chest acceleration gives a computed displacement of 37 cm (14.6 in.) (x direction) and 61 cm (24.0 in.) (y direction).

The 45° left-side drop from 4.9 m (16 ft) was conducted only with the anthropomorphic dummy since door failure and increasing vehicle strain (Figs. 41, 42, 43, 44, 45) made safety of manned drops from this height less certain in the damaged vehicle. Moreover, body position within the bags must be determined with care; in runs 48 and 51 the dummy was found on post-run examination to have slid far to the left, and bottoming did occur. A manned drop was carried off from 3.1 m (10 ft) giving an impact velocity of 7.6 m/sec (25 ft/sec). Before drop, care was taken to ensure a central position within the bag by having the subject observe marks on the upper airbag centerline.

It is emphasized that frequency components higher than the 3 cps resonant frequency are observed on the acceleration traces (Figs. 32 and 34) particularly with the backboard system, suggesting some body slap against the backboard. Three impact tests were conducted without any form of body stiffening at impact velocities up to 5.5 m/sec (17.9 ft/sec) with accelerometers on the chest, hip and knee of the subject. Table 1, runs 33, 34 and 35 and Fig. 30 show that very little body buckling was present so that further improvements of the restraint to remove the higher frequency components might reduce the body loads to about half these peak values without significantly increasing body displacement.

For control during the period of restraint, it was found that the zipper closure of the body bag is such that there is a mid-line gap several inches wide from the head down, allowing some arm motion and complete wrist motion as in operating controls. In an operational system used with a pressure suit, such lacunae for controllers could be easily provided (see Figs. 66 and 67). Preliminary work has been done with a transparent plastic upper airbag, to allow an astronaut full view of his displays while restrained. Switch operation on the panel is precluded while restrained, but such operations could be provided by a stepping switch at the hand which is indexed on the panel.

Figures 42, 43, 44 and 45 reflect some of the damage incurred during impact testing. Damage to the structure and in particular to the ingress-egress doors was determined to be serious enough to preclude the pressurization and water filling tasks as originally planned.

In no case was bag pressure dumped on impact as in previous Martin experimental work[21 and 22] (Fig. 10), so that the system would provide essentially full protection for successive impacts as was demonstrated in the 45° feet-down drops where initial impact occurred at 45°, at which point the vehicle pitched head down for the secondary impact. In all cases, drops with an instrumented anthropomorphic dummy preceded drops with an instrumented man, for the same conditions, using a build-up drop series of 1.5, 3.0, and 4.9 m (5, 10, and 16 ft) for each vehicle attitude.

Three impact tests were conducted at the maximum drop height capability of the overhead crane, 8.6 m (28 ft). These tests were conducted using the anthropomorphic dummy in the vertical impact orientation and, even though the measured accelerations are high (Table 1, test Nos. 55, 56 and 57), they are physiologically acceptable in an emergency situation. Figure 40 presents the acceleration-time history of the final 8.6 m (28 ft) drop. Two tests (Nos. 55 and 57) were conducted at lower initial bag pressures that permitted acceleration overshoot. For this drop the subject was inside the body bag but unpressurized (used only to prevent any sliding tendencies). This gave an impact velocity of 12.8 m/sec (42 ft/sec). Maximum vehicle loads of 101 G_x were measured (Fig. 40) with an average pressure in the bags of 64 cm (25 in.) of water before the drop. The head load peaked at 29 G_x, the chest load at 26.3 G_x, and the hip load at 32 G_x.

Biomedical monitoring was conducted during several of the manned impact tests. A physician was present for all manned test operations. The electrocardiogram obtained by telemetry (Telemedics RKG100) during test No. 53 are shown in Fig. 46. Heart rates are tabulated in Table 2. Note that the heart rate was maximum at the time of impact but returned toward normal in several minutes. Body temperatures, monitored during all manned tests showed very little variation throughout restraint periods exceeding 1-1/2 hr.

TABLE 2

Heart Rate
Pilot Compartment Airbag Restraint System

Date: 6/18/64
Drop: No. 53--45° left side from 10 ft
Subject: C. C. C.

Time (min)	Heart Rate (beats/min)
-35	90
-30	100

TABLE 2 (continued)

Time (min)	Heart Rate (beats/min)
-8	90
-3	100
-2	100
-1	105
-0.5	105
-0.1	110
0 (impact)	115
+0.5	115
+1	95
+2	90
+2.5	90

Martin-Baltimore Life Sciences Technical Film Report No. 8[23] presents the key tests of the astronaut version airbag restraint experimental program.

5. Conclusions

The impact testing results show satisfactory attenuation properties at impact velocities up to 9.8 m/sec (32 ft/sec) in vehicle attitudes of 45° feet-down and 45° roll left and in the level or 0° attitude up to 12.8 m/sec (42 ft/sec) that result in vehicle accelerations as high as 100 G. The impacts from a height of 8.6 m (28 ft) resulting in impact velocities of 12.8 m/sec (42 ft/sec) show the need for adjusting the bag pressure for the acceleration event of concern. (The anthropomorphic dummy bottomed during two tests before a pressure was reached to prevent this occurrence.) Acceleration loads on the subject were less than 22 G in all cases except the 8.6 m (28 ft) drop. This case demonstrated the need for higher initial bag pressures to prevent bottoming (i.e., adjustable for the acceleration event), thereby accepting higher but physiologically acceptable accelerations on the subject.

The rapidly damping rebounds at 3 cps with about 50% attenuation per cycle were subjectively quite acceptable, with the most noticeable feature being the cheek slap on the upper bag.

Indications from the testing program are that the airbag type restraint system would provide excellent isolation from spacecraft landing impacts and launch and re-entry vibrations with the astronaut in any attitude.

B. ANALOG PROGRAM

1. Mathematical Model

Analog simulations[24] were made for both the Airbag Restraint System and for the Airstop System. The Airbag Restraint System is discussed in this report and the Airstop System analog simulation will be discussed in a later report. The analog schematic for both systems is shown in Fig. 57.

The Airbag Restraint System with the subject sandwiched horizontally between an upper and lower airbag with additional airbags at his feet and head make the detailed mathematical model very complex. However, with a few reasonable assumptions, the model of the complex system can be reduced to a much simpler model which gives results that compare favorably with experimental data and allows extrapolation. The following assumptions were made to simplify the model of the complex system.

(1) Consider uncoupled inputs only. (In this analysis only vertical inputs were considered.)

(2) For vertical inputs the head and foot bags do not contribute to the system except to serve as immovable surfaces for the upper and lower bags to push against.

(3) The subject was considered as a rigid mass. (For most of the vertical drops the subject was lying on a backboard. Experimental results indicated that even without the backboard, body buckling did not seem to be a problem.)

The Airbag Restraint System can now be represented by the following system:

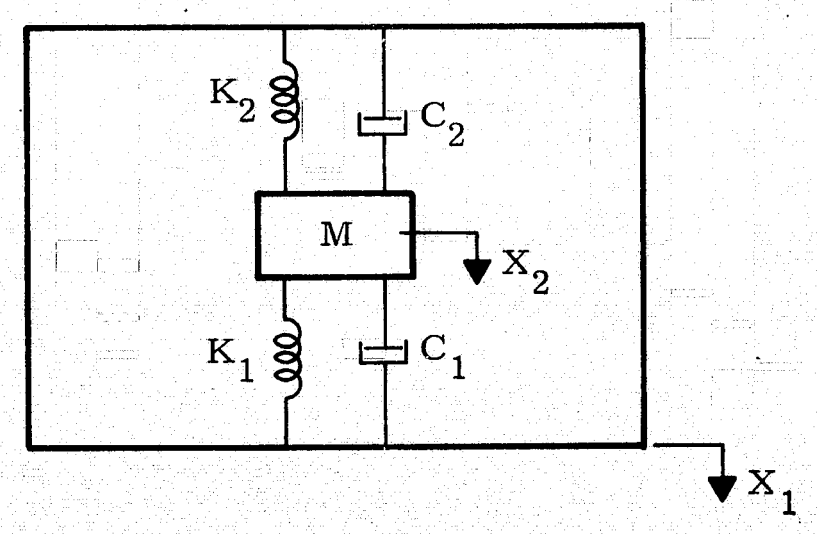

The equation of motion for this system can be expressed as

$$M \ddot{X}_r + (C_1 + C_2) \dot{X}_r + (K_1 + K_2) X_r + F_p = F(t)$$

or

$$\frac{M\, d^2 X_r}{dt^2} = F(t) - F_1(t, \dot{X}_r) - F_2(X_r) - F_p$$

where

$X_r = X_2 - X_1$ motion of the body mass relative to the vehicle

$F(t)$ = the forcing function

$F_1(t, \dot{X}_r)$ = the damping force

$F_2(X_r)$ = the spring force

M = mass of subject and support board.

2. Parameters

a. The forcing function--F (t)

During the study there were five separate types of inputs. These were classified as:

(1) Initial velocity.

(2) Sine wave.

(3) Steady force plus sine wave.

(4) Step.

(5) Haversine.

(1) Initial velocity

The impact loads were supplied by assigning an initial velocity to the mass and allowing the systems oscillations to damp out. The initial velocity supplied an impact load analogous to dropping the system from a specified height. These results then can be compared to the experimental drops.

(2) Sine wave

This input was used to obtain a transmissibility curve for the non-linear system. This input represents vibration of the system.

(3) Steady force plus sine wave

This input is shown in Fig. 58 and is an envelope of sinusoidal force superimposed on an increasing linear force. This input represents a simultaneous vibration and steady acceleration, such as in a spacecraft launch or re-entry.

(4) Step

A step input was used in the process of obtaining damping of a given value.

(5) Haversine

This function is shown in Fig. 58 and is a 240 sec, 10-g max pulse used to simulate re-entry.

b. Static pressure force--F_p

This is the pressure force required to balance the gravity force when the system is at rest. The pressure force at any time, for the simple model, is taken as PA where A is the backboard area of 1.02 m^2 (11 ft^2).

c. Damping--$F(t, \dot{X}_r)$

Damping as determined from experimental data was 11% of critical damping. (That is, successive cycle amplitudes were about half of the previous cycle amplitudes.) The time dependent portion of the damping function is a low pass filter with a small time constant $F(t, \dot{X}_r) = \frac{c\dot{X}_r}{1 + \tau s}$ where $\tau = 0.03$ sec. This was intended to simulate a time delay corresponding to zero damping at the instant of impact followed by rapid increase as the subject started initial displacement into the restraint system. In the analog computer studies, it was found that a zero delay of damping ($\tau = 0$) also provided good simulation of experimental data.

d. Spring force--$F_2(X_r)$--"Load Deflection Curves"

The load deflection curve used on the analog, to simulate the experimental restraint system, was obtained by double integration of the accelerations ($\ddot{X}_r$) from experimental runs 13 (1.5 m drop height) (5 ft),

16 (3.1 m) (10 ft), 25 (4.9 m) (16 ft) to get displacements (X_r). The corresponding time values of $\ddot{X}_r$ and $\dot{X}_r$ were read from the analog traces and a single best fit total load versus deflection of the three curves was drawn. This load deflection curve was adequately represented by a cubic equation of the form $L = Ax^3 + Bx^2 + Cx + D$ and is shown in Fig. 59.

The bag pressures were recorded during the experimental impact tests; and when plotted (after multiplication by backboard area) as load versus deflection, they account for about one-third of the total experimental load deflection curve. This suggests that pressure forces according to this simple model are not the total supporting forces as the subject moves into the bag. Both backboard side entrainment effects and perhaps stretch or some other undetermined force contribute the remaining part of the load deflection curve. This aspect will need additional consideration in future studies.

In addition to the cubic load deflection curve, analog models were examined with several other load deflection curves. The load deflection curves used were: cubic, cubic limited load, constant slope, constant slope limited load, and adiabatic. These load deflection curves are shown in Fig. 59. The use of these curves allows extrapolation of the experimental results and also gives results for a much stiffer (adiabatic, i.e., $PV^n = C$) system, a linear (constant slope) system, and a limited load system. The limited load represents a system that vents at a given load. The experimental system is much softer than the simple adiabatic model which assumes that the subject moves into the restraint like a piston and displaces a volume equal to the contact area times the displacement. The experimental system is also stiffer than the model obtained using the experimental pressure times the backboard area as the only restoring force.

3. Discussion and Results

There were a total of 239 separate analog runs in the study of the Airbag Restraint and the Airstop Restraint Systems. Only the Airbag Restraint System will be discussed here; a separate report will be written on the Airstop System. The results will be discussed under the headings of the various inputs.

a. Initial velocity

The analog simulation of the experimental 4.9-m (16-ft) drop is shown in Fig. 60. This figure shows the good correlation between experimental tests and the analog simulation. Figure 61 gives the maximum displacement into the different restraint systems at various impact velocities up to 30.5 m/sec (100 ft/sec). Figure 62 shows the maximum G_x forces on the body mass for the different restraint systems at the same displacements found in Fig. 61.

The maximum possible vertical deflection before "bottoming" in the experimental system was 0.76 m (2.5 ft). Using the constant slope (Fig. 59) as the experimental system (cubic) extrapolated, it is seen that impact velocities up to 13 m/sec (43 ft/sec) would be possible without bottoming. This was borne out in the experimental testing with run 56 when the subject did not bottom when subjected to an initial impact velocity of 12.8 m/sec.

From Figs. 61 and 62 it is observed that the analog models which result in small deflections (e.g., adiabatic) also result in higher forces on the body. The desired system is one that allows maximum travel for the expected load input without bottoming. Figures 61 and 62 then give a feel for the type of restraint necessary to meet the displacement and acceleration requirements that might be imposed on the experimental system of this report. For example, if it were required to drop the experimental system from a higher height than 8.6 m (28 ft) (impact velocity exceeding 12.8 m/sec) (42 ft/sec) without bottoming of the subject, then the restraint of the experimental system would have to be stiffer. This increased stiffness would result in less deflection into the restraint system but higher G forces on the subject. The analog study does, however, reflect that the present experimental system is very adequate for impact velocities in the order of magnitude of parachute drop velocities.

b. Sine wave

A vibration survey was conducted on the analog to obtain the response of the experimental system to vibration. The resonant frequency of the cubic experimental system on the analog was found to be 2.05 cps with transmissibility of 4.8 at resonance. (This frequency agrees with the experimental data.) The plot of X_{out}/X_{in} for this system is given in Fig. 63. This cubic experimental system will attenuate input of frequencies above 3 cps.

The adiabatic model is stiffer than the cubic system and has a resonant frequency of 3.5 cps with a 1 G input. The adiabatic model attenuates frequencies above 5 cps.

c. Steady force plus sine wave

The top part of Fig. 64 shows an input of steady acceleration and simultaneous vibration to the vehicle system such as might occur in a spacecraft launch or re-entry. The solid diamond part of the input between 90 and 150 sec is a 5 cps vibration and only appears solid because of the time scale shown. This sinusoidal ±3 G-force superimposed on a constantly increasing steady G-force results in only a ±3.5 G-force on the subject. Since the resonance of the system is below 5 cps and has about a 1/1 transmissibility at 5 cps, the restraint will attenuate vibration above 5 cps with a transmissibility similar to that shown in Fig. 63.

The constantly increasing steady G-force causes the subject to increase his displacement into the restraint system, and, for the force input shown in Fig. 64, the maximum displacement is only 0.2 m (8 in.).

d. Haversine

The re-entry simulation input to the vehicle and the subject's response to this input are shown in Fig. 65. Because this type input is spread over such a long time interval (240 sec), the subject receives negligible acceleration (or deceleration) relative to the vehicle but just displaces into the restraint system with the increasing G force. The maximum displacement for the 10 G maximum haversine is 0.44 m (17 in.) which is well within the maximum possible vertical deflection of the experimental system.

4. Conclusions

(1) The analog model represented the experimental system adequately and allowed predictions beyond the experimental system.

(2) The experimental system as represented by the analog has a resonant frequency of 2.05 cps with a transmissibility of 4.8 at resonance. This system attenuates all frequencies above 5 cps.

(3) The analog simulation demonstrated the acceptable use of the experimental airbag restraint system not only for impacts up to 13 m/sec (43 ft/sec) but also demonstrated its use for a complete mission with launch and re-entry simulation.

C. MISCELLANEOUS TESTS

1. Twenty-Four Hour Habitation

A test subject was placed in the vehicle positioned on the back support board with the lower, foot, and head bags inflated at the start of the confinement. After approximately 1 hr the pressure in the lower bag was relieved, allowing the subject to rest on the bottom of the tank. The subject remained in a prone or sitting position throughout the 24-hr stay with electrocardiogram and body temperature being monitored at the beginning, at the 12-hr point and again at the conclusion of the test. The last hour of the test was spent under full restraint and with utilization of the inflated bags as an exerciser. The restraint was good yet not uncomfortable.

2. Universal Fit

Three individuals of various percentile groups were restrained in the system at various times throughout the testing program, and two individuals were in partial restraint a number of times during the test program. The size of the bags is such that 1 or 99 percentile people would be well restrained.

3. Pressurization and Water Filling

Two unmanned tests were planned: one to pressurize to 5 psi to briefly examine the emergency pressurization feature of the system and another to fill the airbags with water to examine the radiation shielding protection feature of the system. Damage to the vehicle after the completion of the impact test program was considered to be severe enough to preclude these tests because of the hazards involved. It is noted, however, that emergency pressurization and radiation shielding (on water filling) along with the exercise function could be useful secondary functions of airbag restraints.

III. APPLICATIONS OF AIRBAG RESTRAINTS

The test program conducted under NASA Contract NASw-877 and reported in this report clearly indicates the potential use of Airbag Restraint Systems. The program has shown by manned tests that the system does, in fact, isolate and protect from the expected impact loads of current capsule recovery systems; and unmanned tests have demonstrated the capability of isolating and protecting from emergency impact situations that may arise such as partial failure of the retro-thrust or parachute recovery system.

A. MULTIMANNED-TYPE VEHICLES

Figures 66 and 67 show the concept of an airbag-type restraint in two types of vehicles: a multimanned parachute landing vehicle and a multimanned retro-thrust-type landing vehicle, respectively. In the operational system, multiple airbags would be stored in spacecraft wall compartments. They would be inflated prior to launch with stored gases from the life support system (such as oxygen) to provide support in any direction from the astronauts to the spacecraft wall. The use of the airbags in multiple layers would allow rapid inflation of a backup layer if the primary layer bag should fail. The astronauts would attach their pressure suit restraint clamps to the top of the lower or back-side airbag to reduce sliding between the bags during the impact or vibration event. The upper bags in front of the astronaut would be partially or totally transparent to allow panel visibility. Technical Film Report No. 8[23], Life Sciences, Martin Company, entitled "Impact Tests of a Prototype Astronaut Airbag Restraint System," summarizes the entire test program and shows a configuration utilizing a transparent airbag. Free volumes would be provided within the bags for hand or foot control uses. If the few centimeters displacement into the lower bag is objectionable because of reduced visibility, a "G-valve" can be used to increase lower bag pressure in proportion to the launch or re-entry acceleration to prevent this displacement. Following launch, the airbags would be deflated and folded back into the wall compartments, freeing the entire central volume of the spacecraft. Restraint to hold the astronauts at the instrument panel during coasting flight could be provided by small attachments. Prior to re-entry the bags would be checked for pressure integrity and inflated during re-entry and landing.

B. EXTRAVEHICULAR IMPACT PROTECTION

Orbital maneuvers by a free-floating astronaut will be a reality in the not-too-distant future. The docking or rendezvous speed of the astronaut should be commensurate with that of walking[25] so that impact forces

will be small. At these recommended low speeds (approximately 3 mph) the impact force could readily be dissipated by landing feet first and using knee action as the absorber. However, for docking in attitudes other than ideal, such as would be encountered with an unstabilized propulsion unit, or having the stabilization system fail, the astronaut requires some form of impact protection. Figure 68 shows a concept of an inflatable extravehicular protective suit for astronauts. This suit when integrated with the pressure suit provides low pressure impact isolation as well as an outer garment to prevent direct tearing of the pressure suit should the astronaut encounter sharp cornered structures. In addition, this outer garment could be filled with spacecraft supply module liquids to provide emergency near-body shielding from solar storm radiation should it prove necessary to leave the spacecraft during such a period.

C. "AIRSTOP" PASSENGER CRASH PROTECTION

As a development from the spacecraft astronaut airbag restraint concepts, even prior to the initial contract, a commercial airline restraint called "Airstop" had been designed. Figure 69 shows the operational concept of this system. In the operational system, it is thought that the airbags could either be inflated for every takeoff and landing if they can be automatically rolled up on deflation, or inflated by the pilot if he suspects an emergency, or by some other emergency cue that proves feasible. The chest bags would come out from the seat backs, and the foot bags from below the seats. Landing impact would actuate a time delay switch of perhaps 10 sec, in case there are multiple impacts, to be followed by automatic deflation of the bags, aiding cabin ventilation. The low pressure in the bags (8 cm of water) allows head rotation and even arm escape, so that breathing is easily maintained in air pockets, even for children covered by the bags for the 1- or 2-min period of bag inflation. Babies and floor luggage are supported by this system. With improved plastics handling, transparent airbags appear feasible, allowing mothers to see babies, stewardesses to see passengers, etc.

The initial testing of this system was conducted under amendment to the contract work reported in this report. Technical Film Report No. 7[26], Life Sciences, Martin Company, entitled, "The Martin Airstop Commercial Airline Passenger Airbag Restraint System" summarizes the testing program to date. Results of this testing and further improvements will be reported in a later report.

D. AIRLITTER RESTRAINT SYSTEM

The transport of sick or injured persons and the impact protection of these persons continue to be a major problem. The application of restraint loads to the patient over the entire body, with an inflated sleeping bag type of airbag restraint appears more suitable than the application of these loads with restraint straps. A prototype "Airlitter" has been built with an outer nonelastic high pressure layer and an inner elastic low pressure layer, both meeting at a common front zipper for easy ingress. An opening is provided for the face; in future applications of tight packing, this also would be covered by the high pressure bag, perhaps with a transparent insert, with breathing and cooling air, and communications (including relaxation music) being provided by appropriate plug-ins. The high pressure outer bag supports the system against local loads, including those of external tie-down straps or local hand-carrying forces, so that the system can be put into trucks, helicopters or aircraft without special support racks. Indeed, Airlitters with plug-in ventilation could be piled on top of each other. The Airlitter system can also be deflated for logistics distribution.

This system is being further developed under an addendum to Contract NASw-877 and will be reported on at a later date.

E. AUTOMOBILE PASSENGER RESTRAINT SYSTEM

All of us in safety work are concerned with the 40,000 deaths a year in automobile accidents in the United States alone. Inflated airbags surrounding the passengers indeed could save many of these lives, but a problem is to safely inflate the bags in anticipation of a crash. The warning time is so short and the driver so involved in other things that, for manual initiation of the inflation, the bags would have to fill in a fraction of a second to be useful. This filling rate could, by itself, throw about the passengers not properly seated. Automatic initiation of filling, perhaps by any abrupt driver control, or, in a later period, by separation distance radar or malfunction of the automatic drive control expected on superhighways, could allow safe inflation rates. Abrupt restraint of the driver may also contribute to the accident; lap belt and shoulder straps for the drivers are probably preferable to airbags, at least until driver controls are put in handgrips, replacing large steering wheels.

The applications of airbag restraint systems to passenger protection, both aircraft and automobile, and in injured patient handling were outgrowths of the original astronaut space concept that was experimentally evaluated under this contract. It is emphasized that there remain many engineering details to solve before airbags are feasible and reliable for spacecraft or other applications that have been discussed here.

IV. BIBLIOGRAPHY

1. Stapp, J. P., "Human Tolerance to Accelerations of Space Flight," Chapter 29 in Physics and Medicine of the Atmosphere and Space, edited by O. O. Benson, Jr. and H. Strughold, John Wiley and Sons, Inc., New York, 1960.

2. Beeding, Eli L., Jr. and Moseley, John D., "Human Deceleration Tests," Technical Note 60-2, Air Force Missile Development Center, Holloman AFB, New Mexico, January 1960.

3. Taylor, Ellis R. and Rhein, Leroy W., "Physiological Effects of Abrupt Deceleration. I. Relative Bradycardia," Aerospace Med. 33:1442-1445, 1962.

4. Swearingen, John J., McFadden, E. B., Garner, J. D. and Blethrow, J. G., "Human Voluntary Tolerance to Vertical Impact," Aerospace Med. 31:989-998, 1960.

5. Clarke, N. P. and Bondurant, S., "Human Tolerance to Prolonged Forward and Backward Accelerations," Technical Report 58-267, Wright Air Development Center, Wright-Patterson Air Force Base, Ohio, July 1958.

6. Clark, C. C. and Gray, R. F., "A Discussion on Restraint and Protection of the Human Experiencing the Smooth and Oscillating Accelerations of Proposed Space Vehicles," in Bio-Assay Techniques for Human Centrifuge and Physiological Effects of Acceleration, edited by R. Bergeret, AGARDograph 48, Pergamon Press, New York, 1961.

7. Clark, Carl C., "Acceleration and Body Distortion," in Human Factors in Technology, edited by Edward Bennett, James Degan and Joseph Spiegel, McGraw-Hill Book Company, New York, 1963.

8. Idomir, Kenneth, "TM-76 Mace Landing Mat Design," Aerospace Engineering 19:28-33, 1960.

9. "Zelmal (Zero Length Launch-Mat Arrested Landing) Engineering Design Summary," Engineering Report 6793, Martin Company, February 1955.

10. "Results of the First United States Manned Orbital Space Flight," Manned Spacecraft Center, National Aeronautics and Space Administration, 1962.

11. Holcomb, Galen A., "Impact Studies of the United States Aerospace Industry," Impact Acceleration Stress: Proceedings of a Symposium with a Comprehensive Chronological Bibliography, Publication 977, National Academy of Sciences-National Research Council, Washington, D. C., 1962.

12. Martin, L. C. and Howe, J. T., "An Analysis of the Impact Motion of an Inflated Sphere Landing Vehicle," Technical Note D-314, National Aeronautics and Space Administration, Washington, D. C., April 1960.

13. Esgar, J. B. and Morgan, W. C., "Analytical Study of Soft Landing on Gas Filled Bags," Technical Report R-75, National Aeronautics and Space Administration, Washington, D. C., April 1960.

14. Angel, C. F., Bloetscher, Kervar, H. and Gold, A., "Proposed Program to Develop Techniques for Simulation of Physiological Sensations of Re-Entry and Landing of Boost-Glide Vehicles," Report TAP-8935, Goodyear Aircraft Corporation, Akron, Ohio, December 1959.

15. Vykukal, H. C.,Richard, G. P. and Stinnett, G. W., "An Interchangeable Mobile Pilot Restraint System, Designed for Use in High Sustained Acceleration Force Fields," Aerospace Med. 33: 279-285, 1962.

16. Carlyle, L., "Literature Survey on Aircrew Restraint," Report ES 29260, Douglas Aircraft Company, Inc., El Segundo, California, February 1959.

17. Mayo, Alfred, Personal communication to Carl Clark, Aerospace Medical Association meetings, Miami, May 1964.

18. Freeman, H. E., Boyce, W. C., McKinney, R. and Adams, C. R., "Personal Restraint System," Progress Report No. 2, Contract AF33(600)-41418, Chance-Vought Corporation, Dallas, Texas, September 1960.

19. Gadd, Charles, Personal communication to Carl Clark, May 1964, on General Motors' work on bags to inflate from the automobile dashboard for crash protection.

20. Bertrand, H. A., Safety device for passenger, United States Patent 2,834,606, 13 May 1958 (filed 5 October 1955). This involves multiple airbags inflated by the driver before impact.

21. Cooper, Bruce, Blechschmidt, Carl, McCloskey, Keith and Clark, Carl, "Human Vibration and Impact Isolation with a Full Length Airbag Restraint System," Research Memorandum 146, Martin Company, Baltimore, March 1963.

22. Clark, Carl C. and Blechschmidt, Carl, "Human Vibration and Impact Protection by Airbag Restraint Systems," ER 13539, Martin Company, Baltimore, June 1964--AIAA annual meeting, 29 June 1964.

23. Technical Film Report No. 8, "Impact Tests of a Prototype Astronaut Airbag Restraint System," Martin Company Life Sciences, Baltimore, Maryland.

24. Analog Problem No. 695, Airbag Restraint System, Martin Company, Baltimore, Maryland.

25. "Zero G Personal Unstabilized Propulsion Unit," Martin Company Research Proposal, ER 13387P, March 1964.

26. Technical Film Report No. 7, "The Martin Airstop Commercial Airline Passenger Airbag Restraint System," Martin Company Life Sciences, Baltimore, Maryland.

PRECEDING PAGE BLANK NOT FILMED

V. ILLUSTRATIONS AND TABLE

PRECEDING PAGE BLANK NOT FILMED

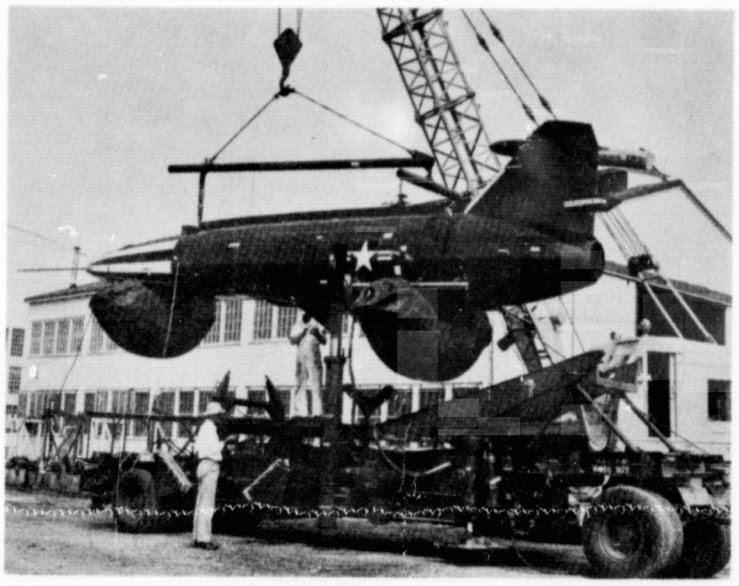

Fig. 1. The Martin Matador Airbag Recovery System

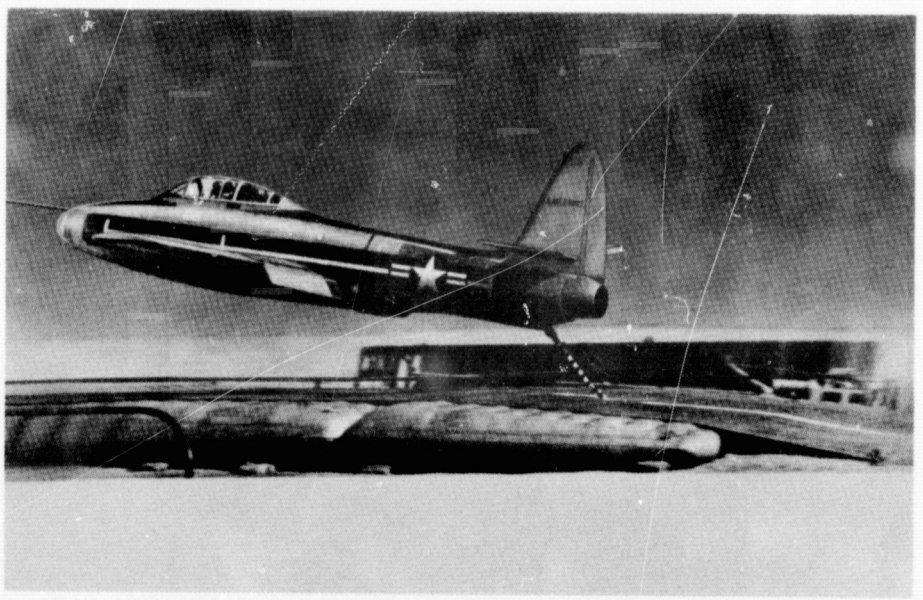

Fig. 2. The Martin "Zelmal" Airbag Airplane Landing System

Fig. 3. The Goodyear "Airmat" Restraint System

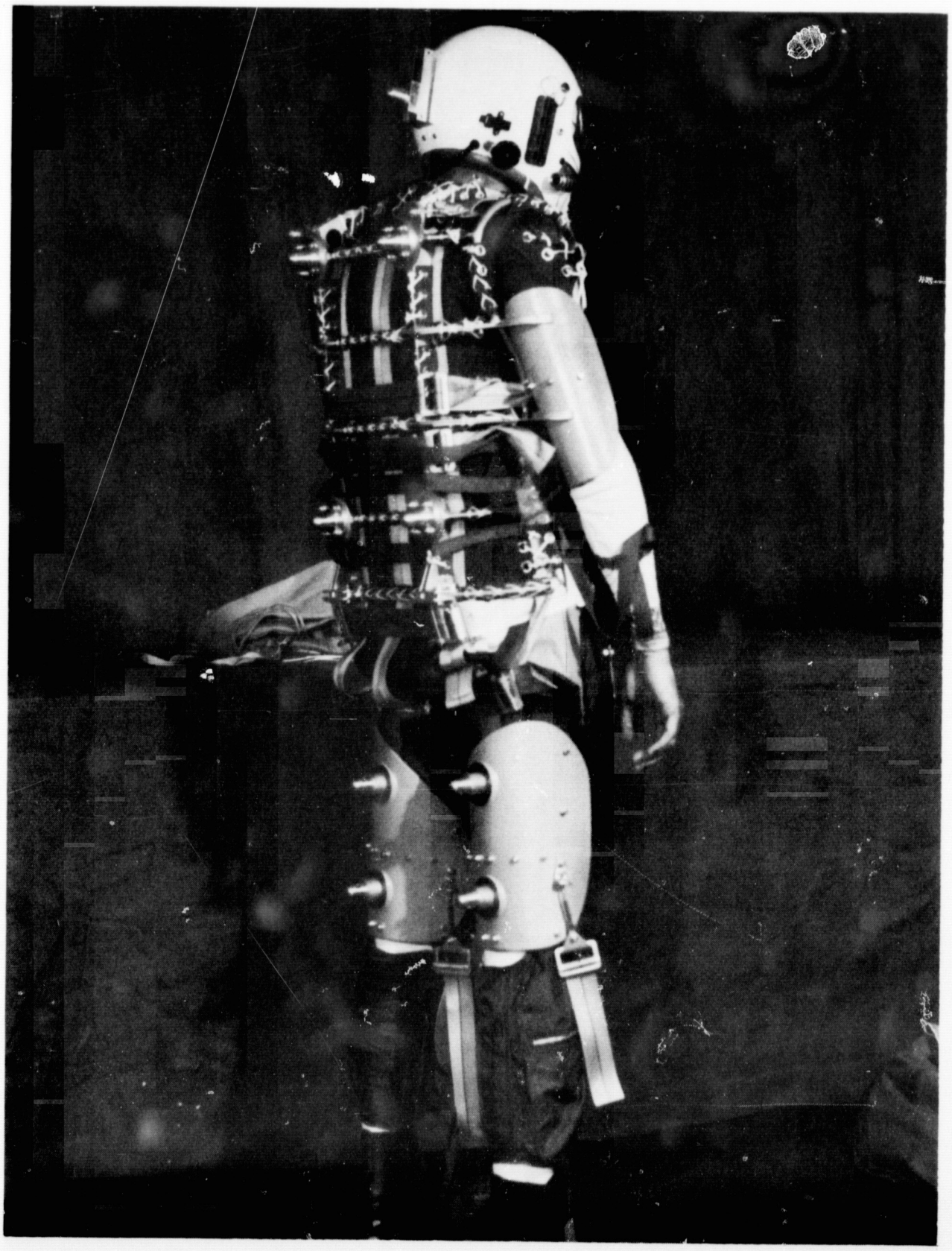

Fig. 4. The Vykukal-Ames Restraint System

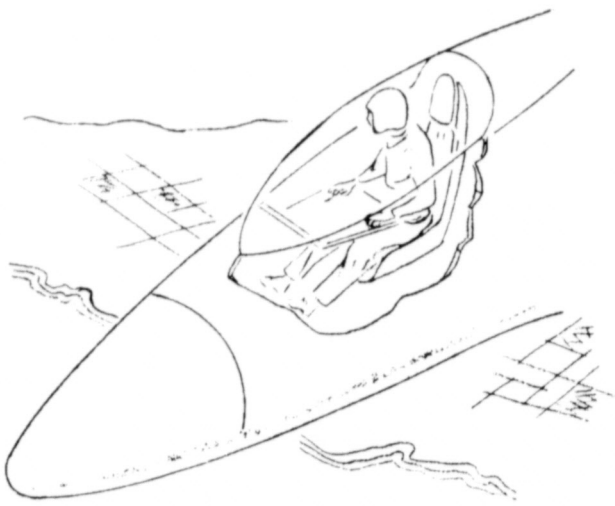

Pilot unencumbered
in normal flight

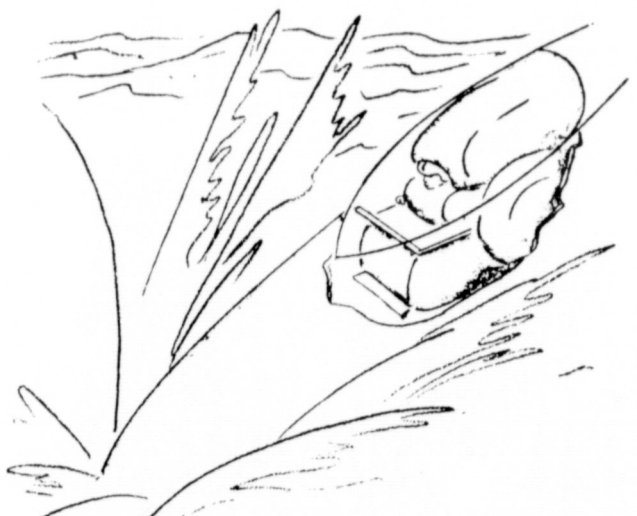

Pilot completely
encased during crash

Fig. 5. The Douglas "Freedom-Restraint" System

1. Head curtain inflated, showing vision opening. Slides down over head.
2. Shoulder holddown bladders.
3. Torso curtain--slides down over head and shoulders to meet lap curtain.
4. Lap curtain.
5. Forearm curtain.
6. Lower leg curtain.

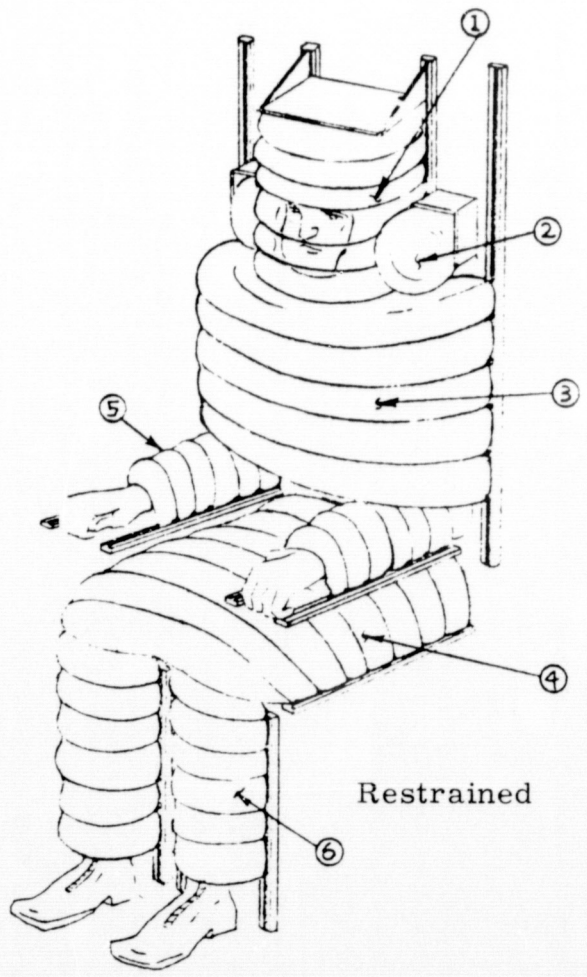

Fig. 6. The Ling-Tempco-Vought "Caterpiller" Restraint System

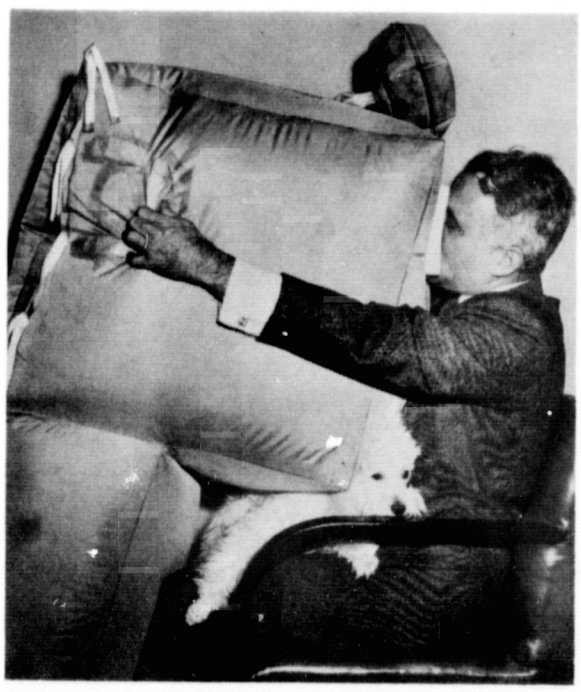

Fig. 7. Airbag Passenger Restraint Design by Assen Jordanoff

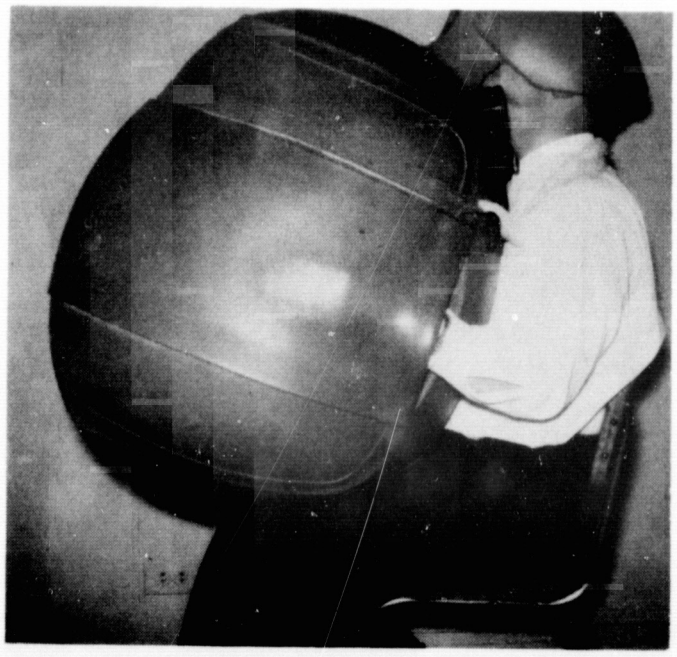

Fig. 8. Airbag Passenger Restraint Design by Assen Jordanoff

May 13, 1958 H. A. BERTRAND 2,834,606

SAFETY DEVICE FOR PASSENGERS

Filed Oct. 5, 1955 2 Sheets-Sheet 1

Fig. 1.

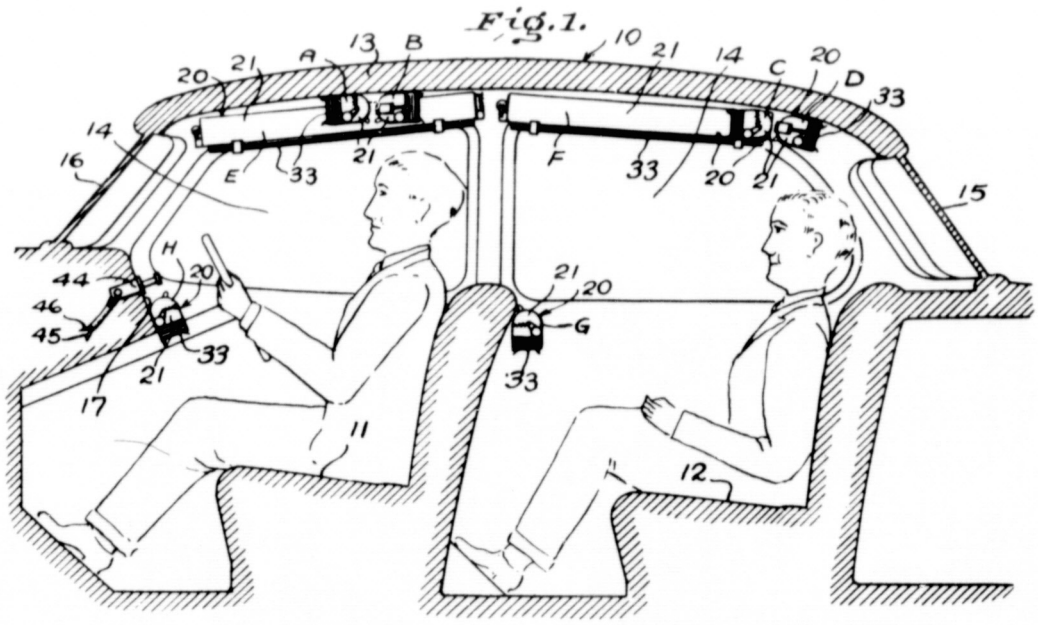

Fig. 2.

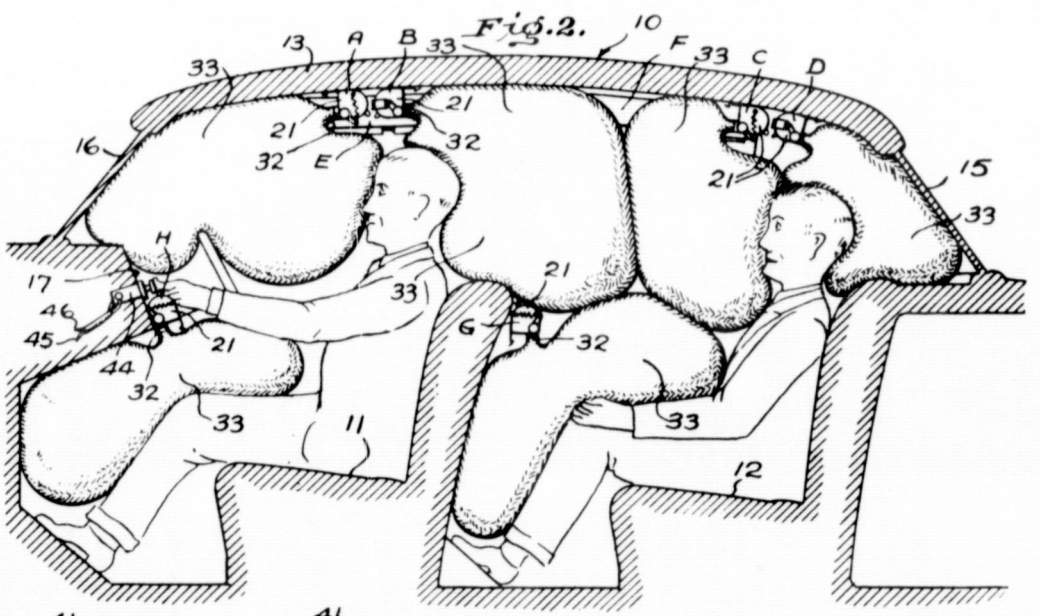

Fig. 9.

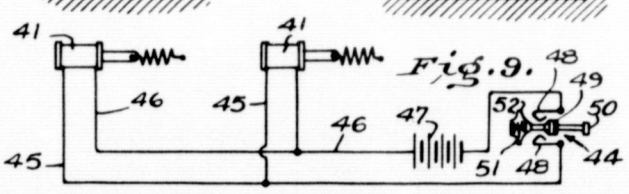

INVENTOR.
Harry A. Bertrand
BY Reginald W. Hoagland
ATTORNEY

Fig. 9. Airbag Restraint Safety Device for Passengers by H. A. Bertrand

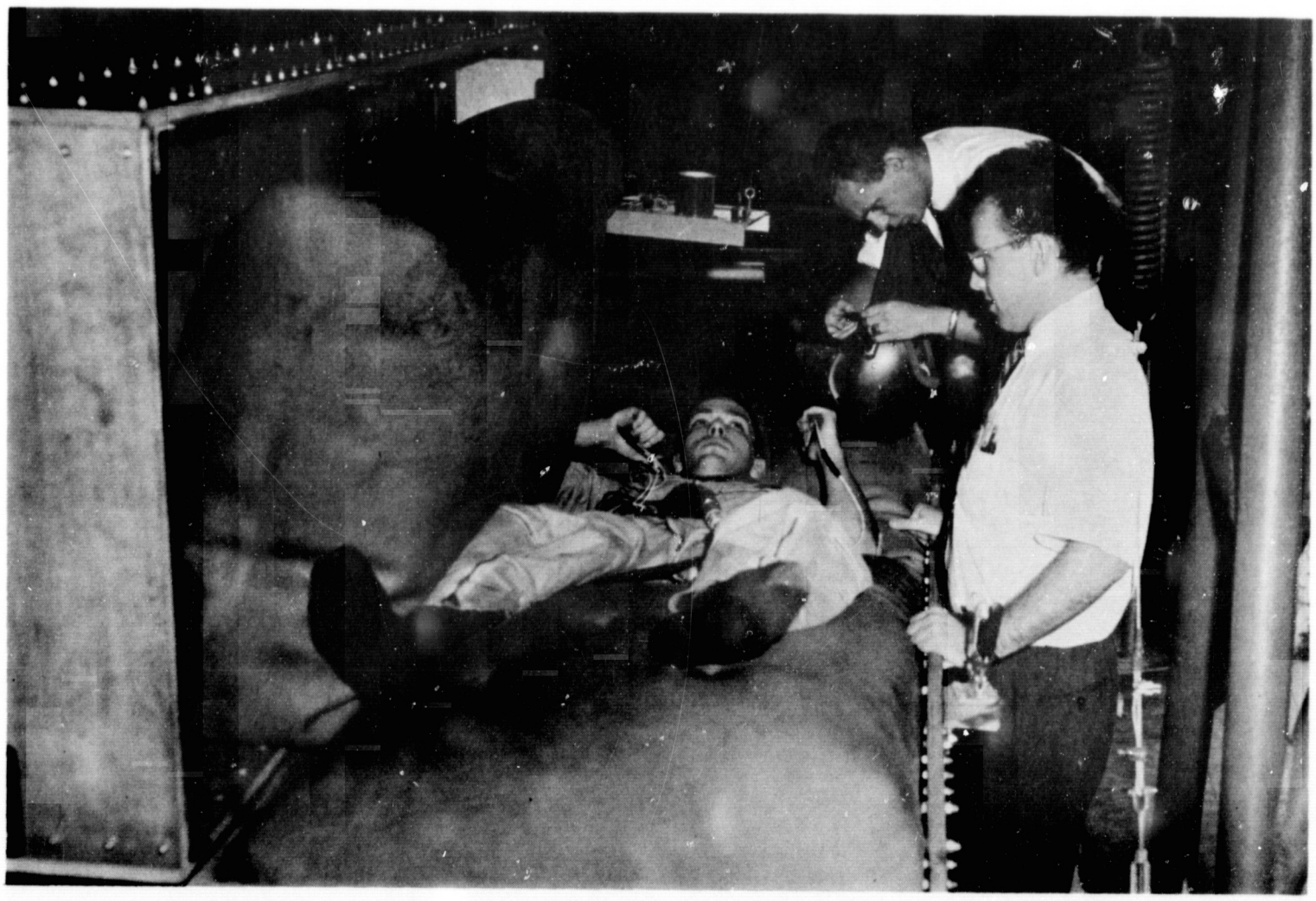

Fig. 10. The Martin Preliminary Experimentation Airbag Restraint System

Total weight incl airbags 2675 lb
Airbags weight 174 lb

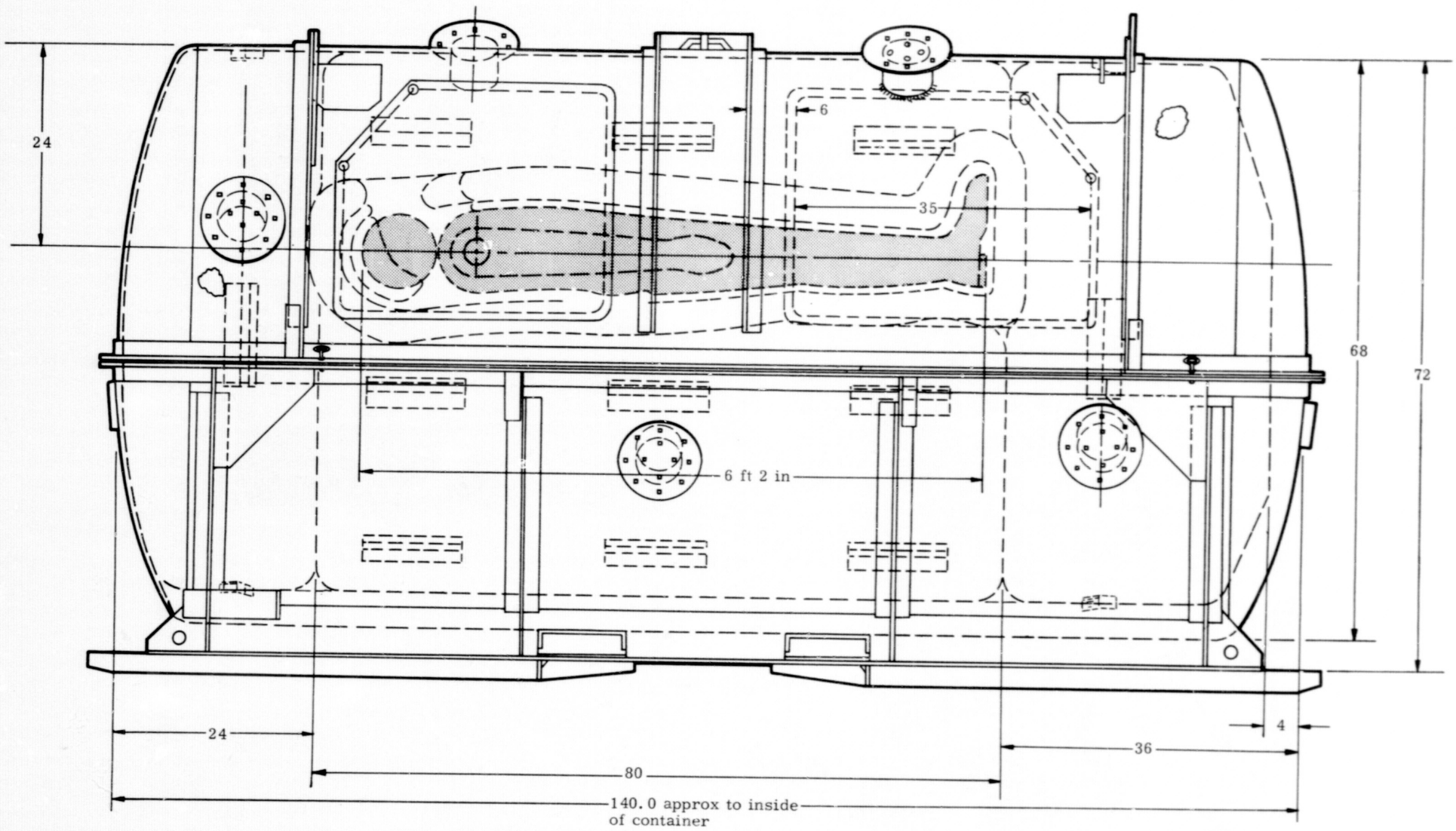

Fig. 11. Diagramatic Sketch of Test Vehicle--Pilot Compartment Airbag Restraint System

Fig. 12. Test Vehicle--Pilot Compartment Airbag Restraint System

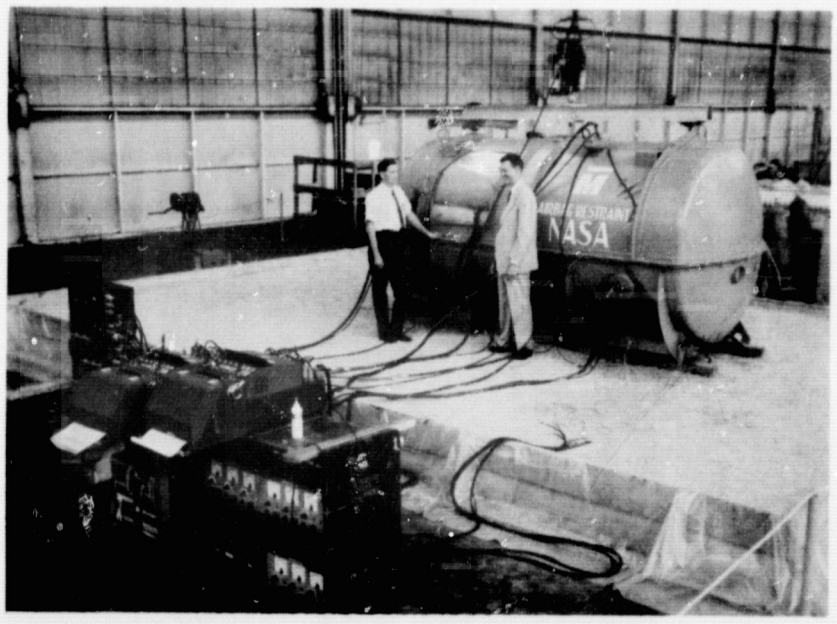

Fig. 13. Test Set-Up--Pilot Compartment Airbag Restraint System

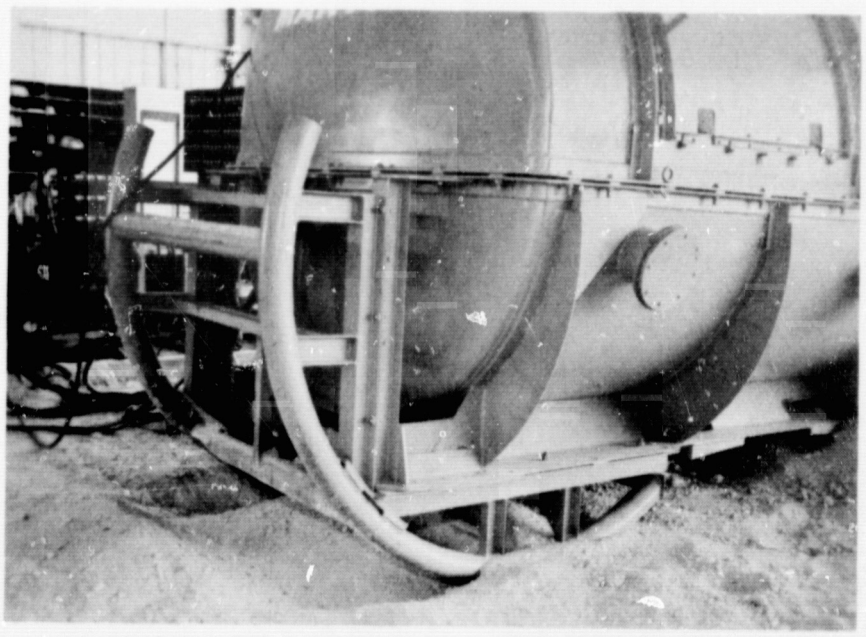

Fig. 14. Test Vehicle 45° Feed-Down Modification and Impact Pattern--Pilot Compartment Airbag Restraint System

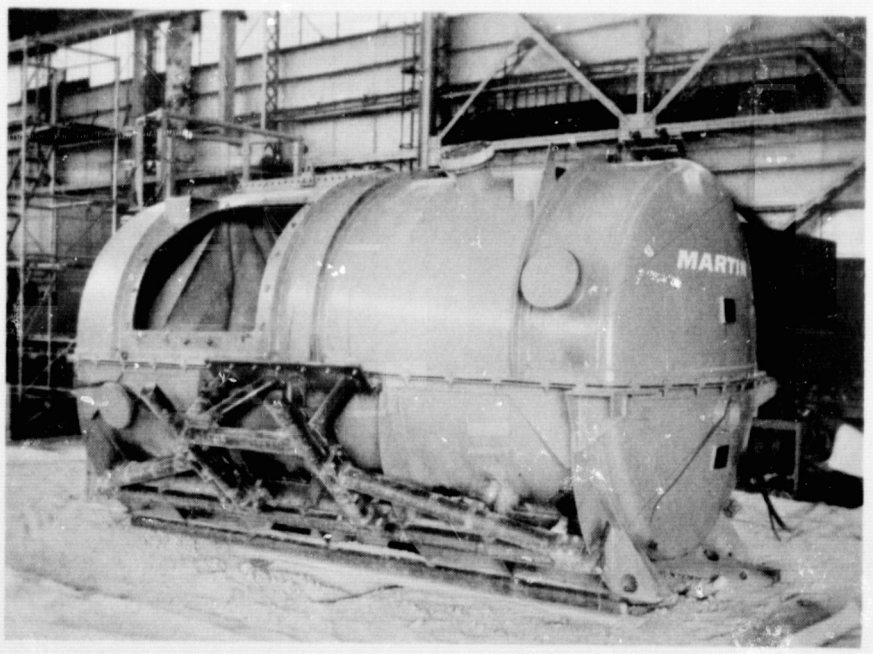

Fig. 15. Test Vehicle 45° Left-Side Modification--Pilot Compartment Airbag Restraint System

Fig. 16. Subject Positioned on "Backboard" on Lower Airbag--Vertical Impact Configuration--Pilot Compartment Airbag Restraint System

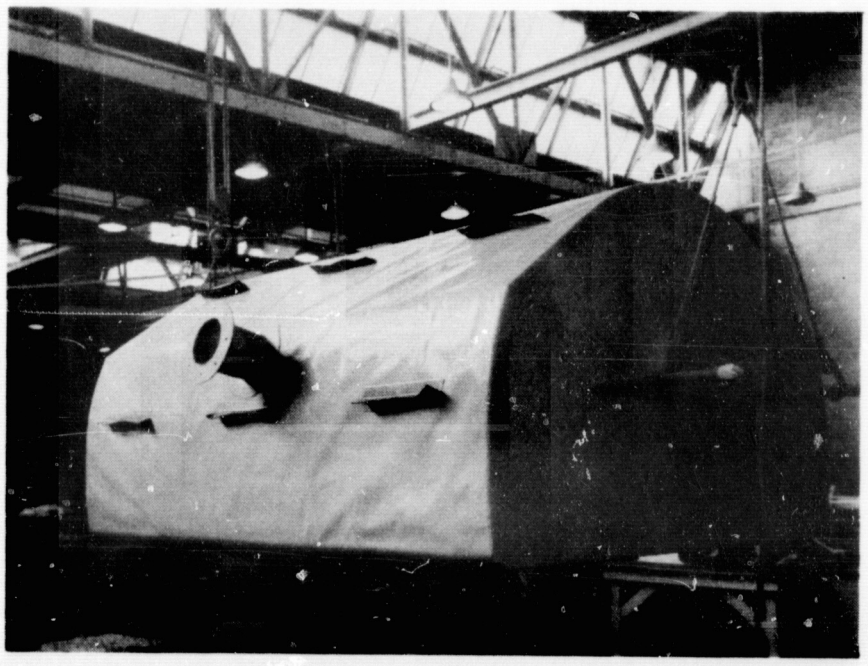

Fig. 17. Lower Airbag During Fabrication Process--Pilot Compartment Airbag Restrain System

Fig. 18. Subject Positioned Inside "Bodybag" on Lower Airbag--45° Feet-Down and 45° Left-Side Configuration--Pilot Compartment Airbag Restraint System

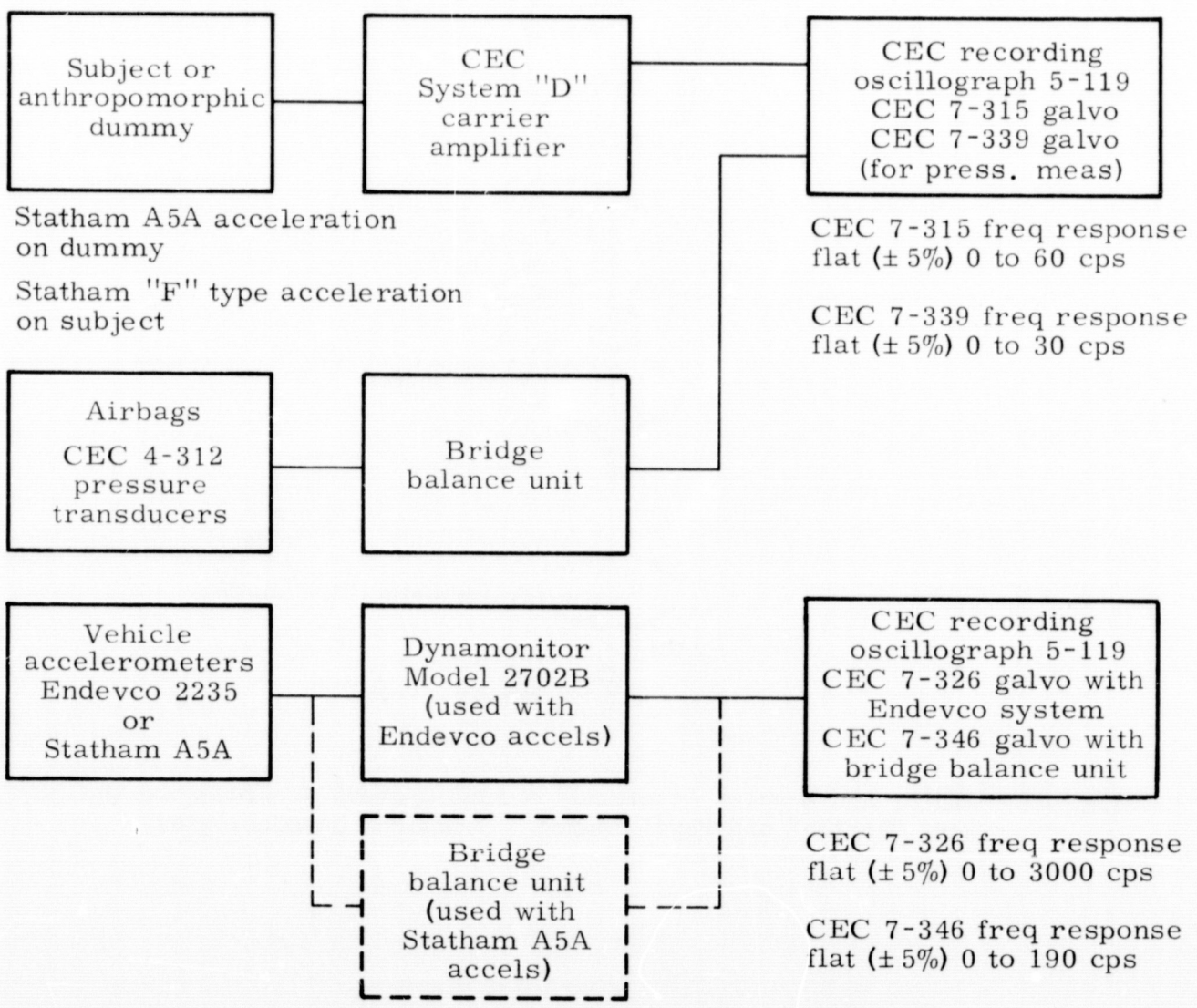

Fig. 19. Instrumentation System--Pilot Compartment Airbag Restraint System

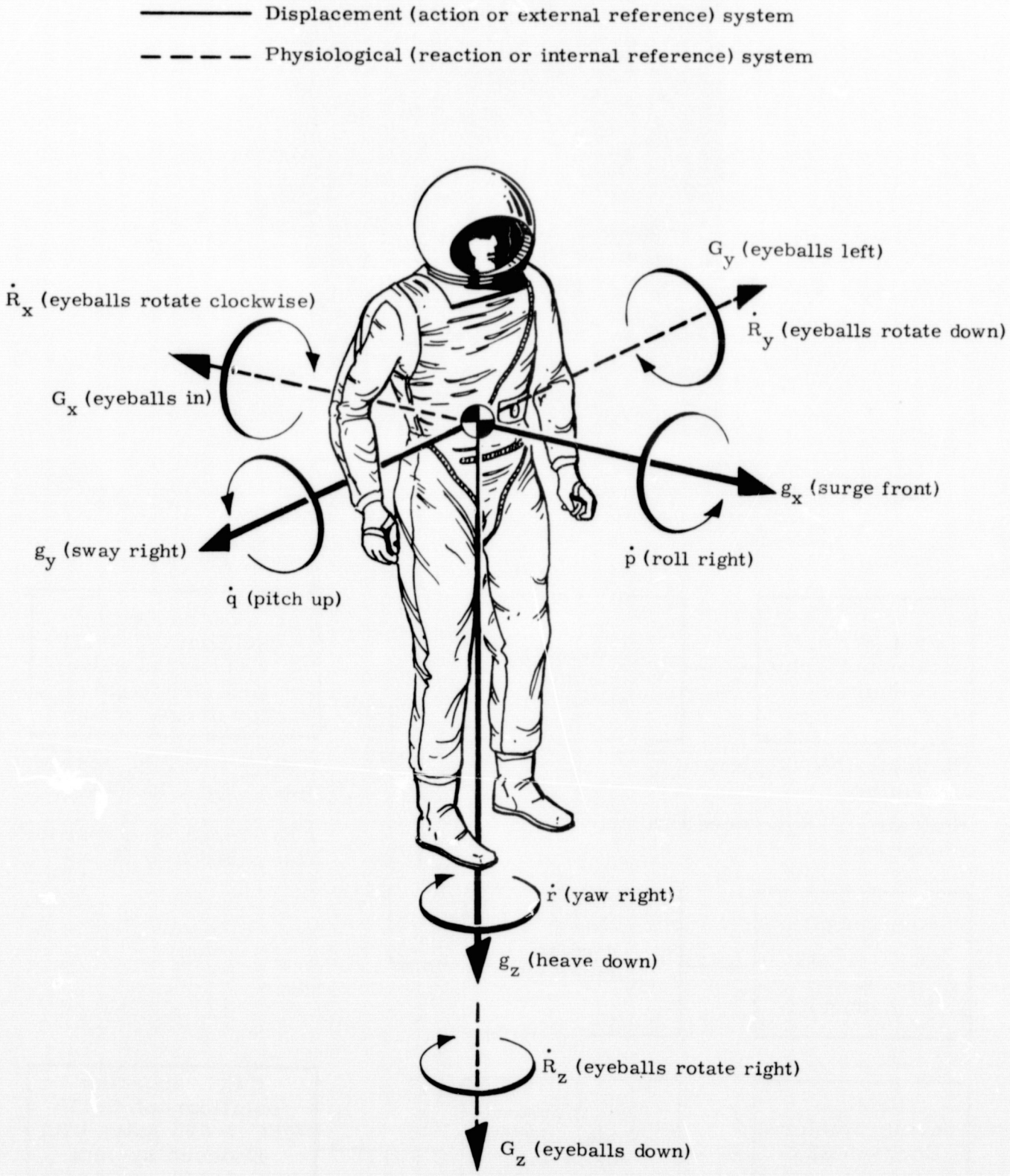

Fig. 20. Linear and Angular Acceleration Axis Systems According to the Body "Action" and Physiological "Reaction" Terminologies

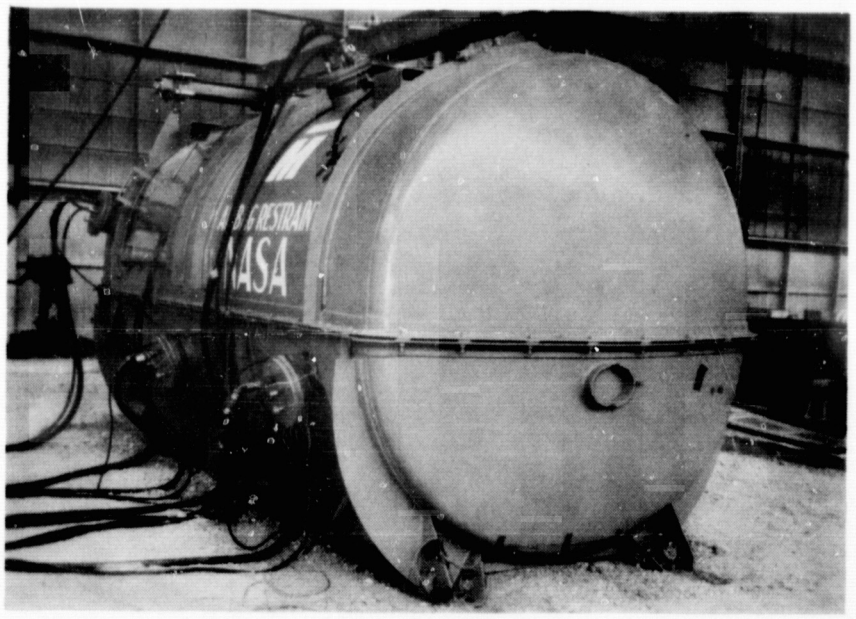

Fig. 21. Test Vehicle After Vertical Impact Showing Impact Pattern--Note Accelerometers Near Skid on Right Side--Pilot Compartment Airbag Restraint System

Fig. 22. Subject Instrumentation--ECG Electrodes, ECG Transmitter (Telemedics RKG-100) in Left Hand, and Chest Accelerometer (G_x shown partially secured for photo clarity)--Pilot Compartment Airbag Restraint System

Fig. 23. Test Vehicle Shown Positioned for Impact in the Vertical Attitude Configuration--Pilot Compartment Airbag Restraint System

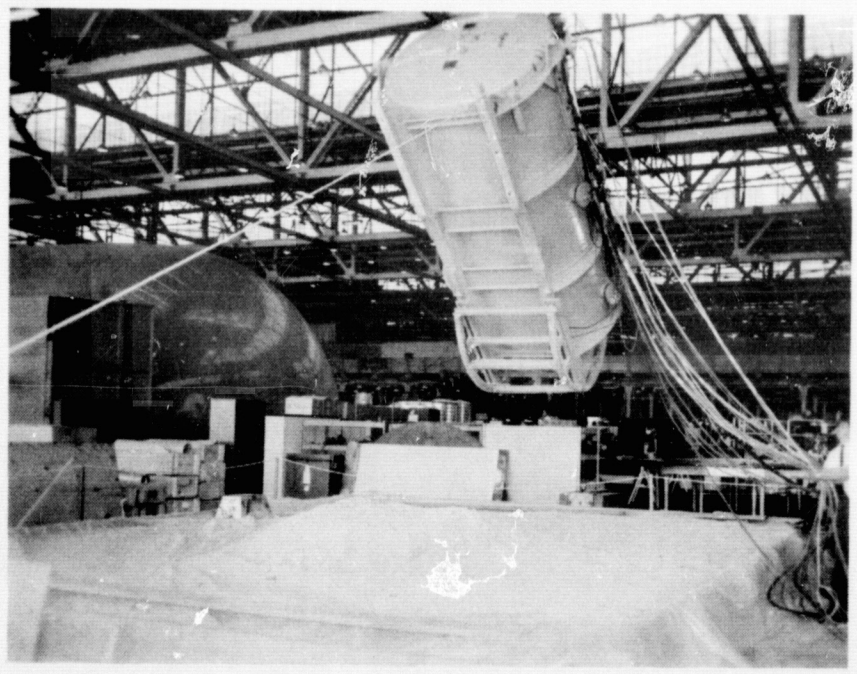

Fig. 24. Test Vehicle Shown Positioned for Impact in the 45° Feet-Down Attitude Configuration--Pilot Compartment Airbag Restraint System

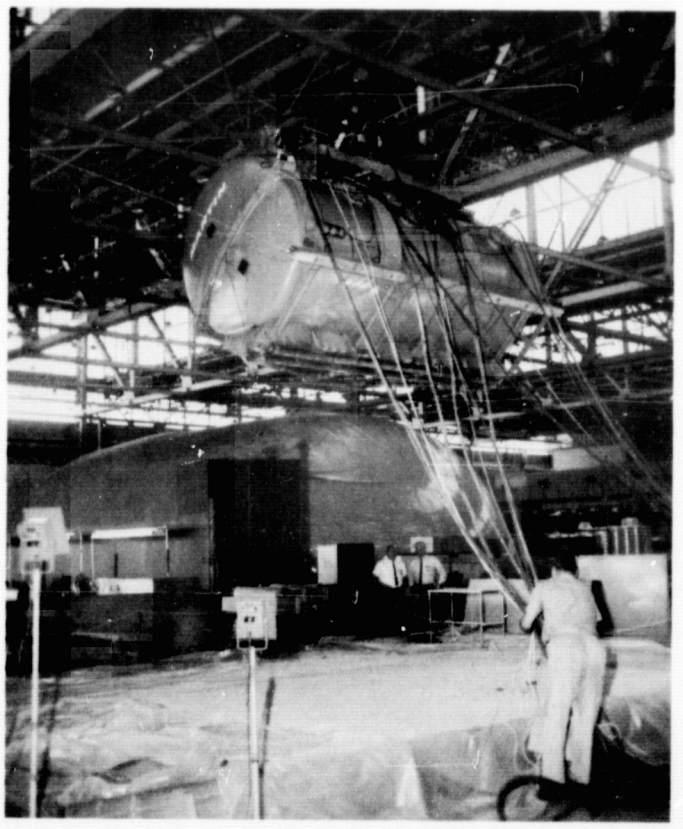

Fig. 25. Test Vehicle Shown Positioned for Impact in the 45° Left-Side Attitude Configuration--Pilot Compartment Airbag Restraint System

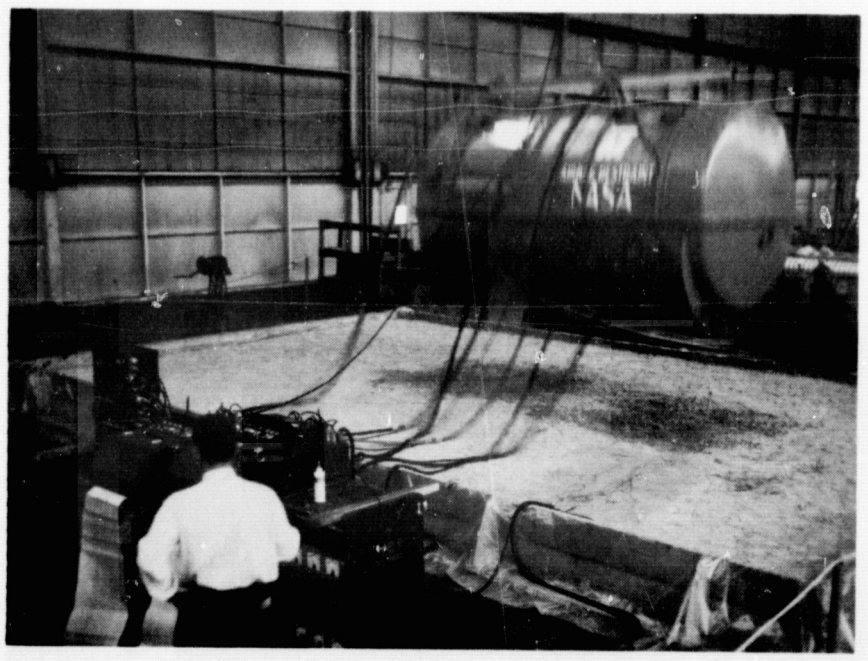

Fig. 26. Test Vehicle Shown just Prior to Impact--in Vertical Attitude Configuration--Pilot Compartment Airbag Restraint System

Fig. 27. Test Vehicle Shown just After Initial Contact in 45° Feet-Down Attitude Configuration--Note Head-Down Pitch Occurring--Pilot Compartment Airbag Restraint System

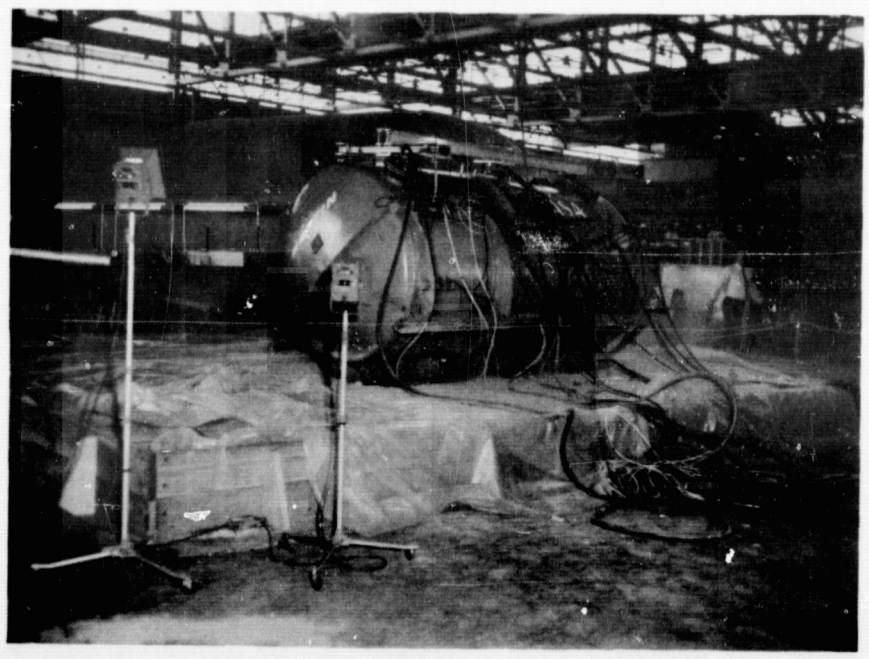

Fig. 28. Test Vehicle Shown just After Impact in the 45° Left-Side Attitude Configuration--Pilot Compartment Airbag Restraint System

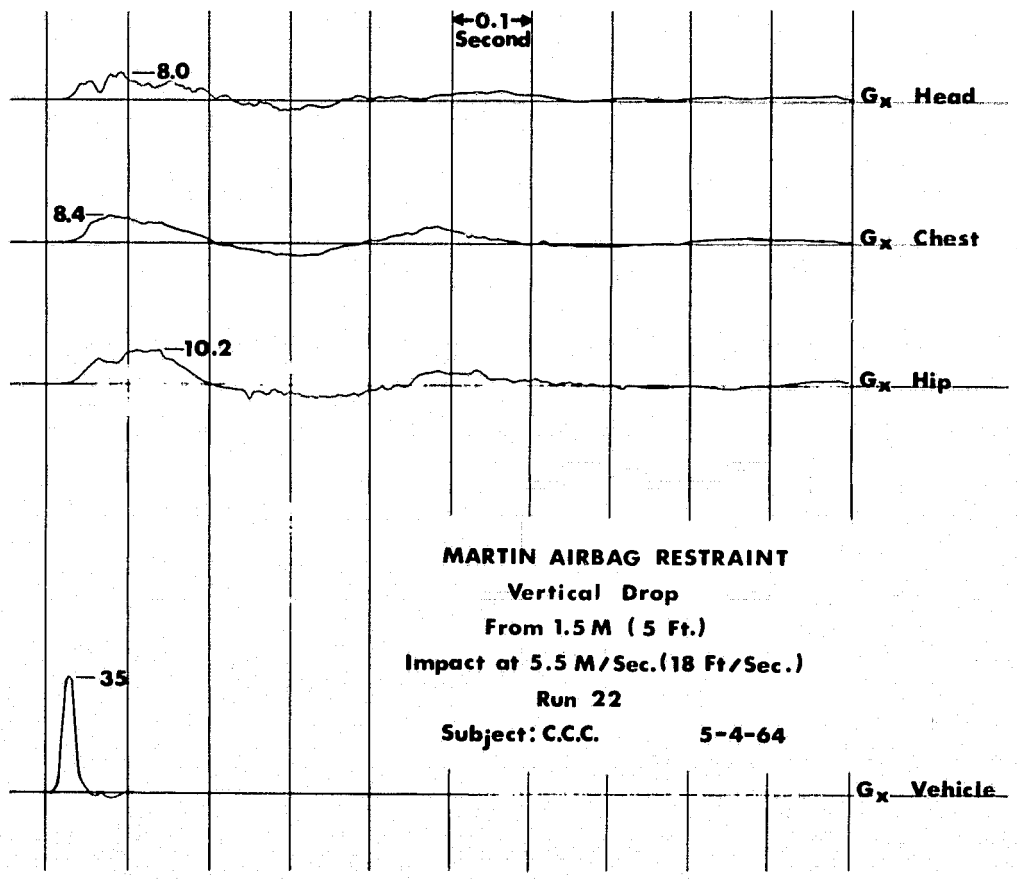

Fig. 29. Acceleration Time-History--Vertical Drop from 1.5 m (5 ft)--Human Subject

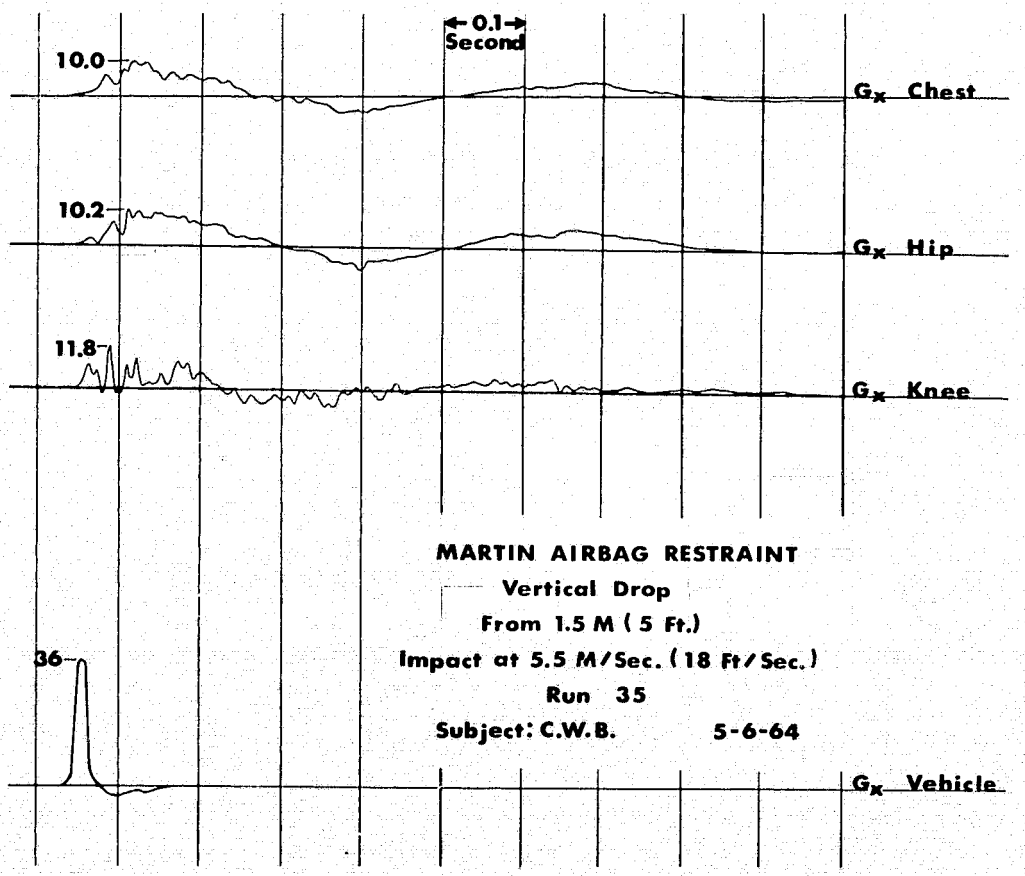

Fig. 30. Acceleration Time-History--Vertical Drop from 1.5 m (5 ft)--Human Subject

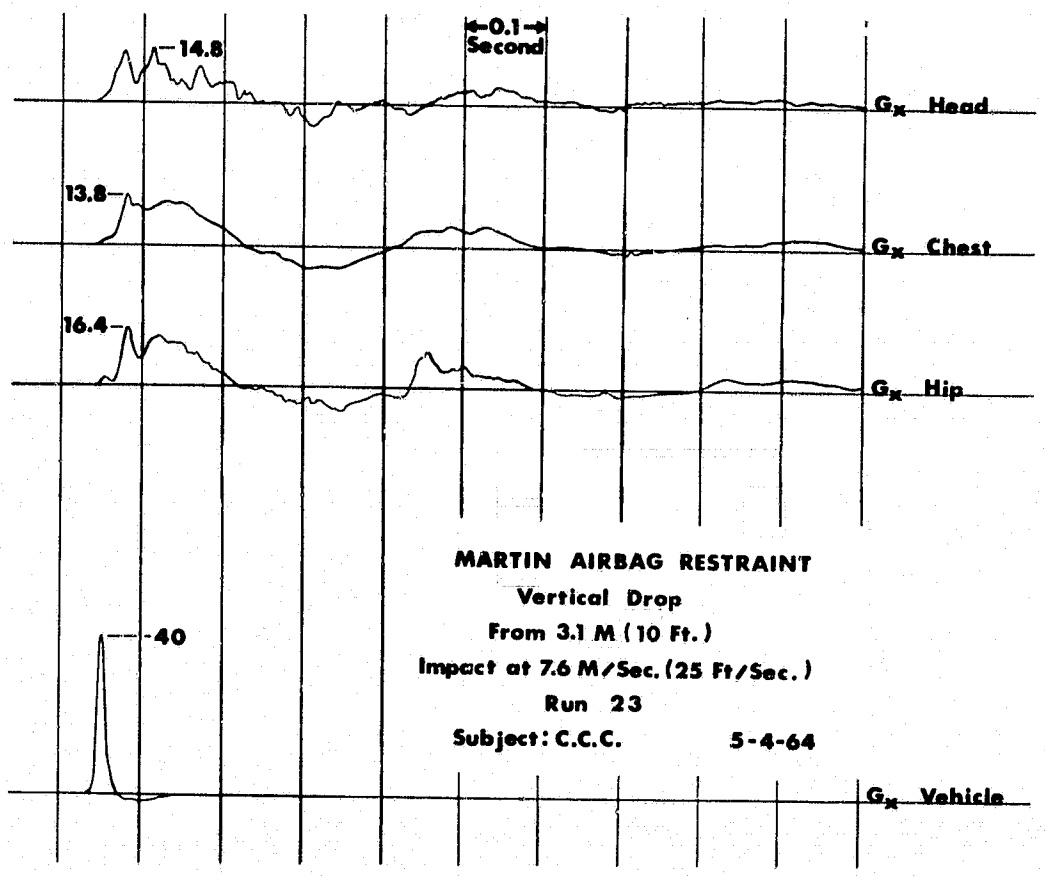

Fig. 31. Acceleration Time-History--Vertical Drop from 3.1 m (10 ft)--Human Subject

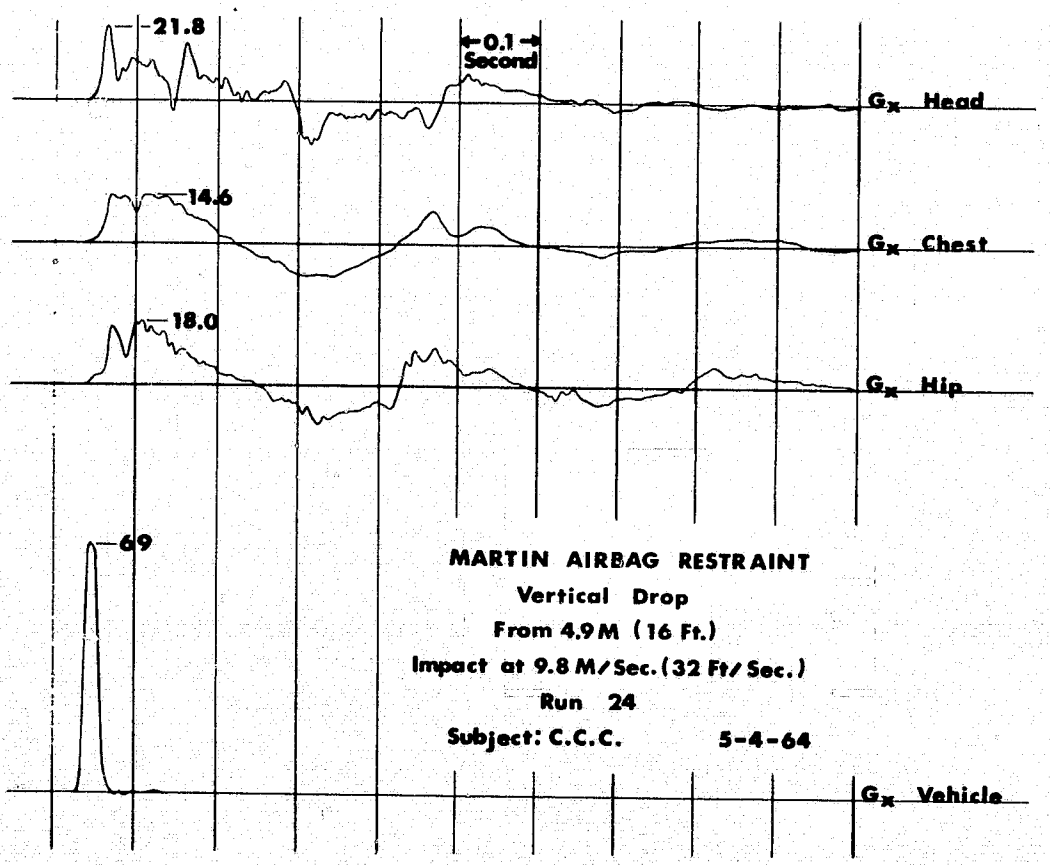

Fig. 32. Acceleration Time-History--Vertical Drop from 4.9 m (16 ft)--Human Subject

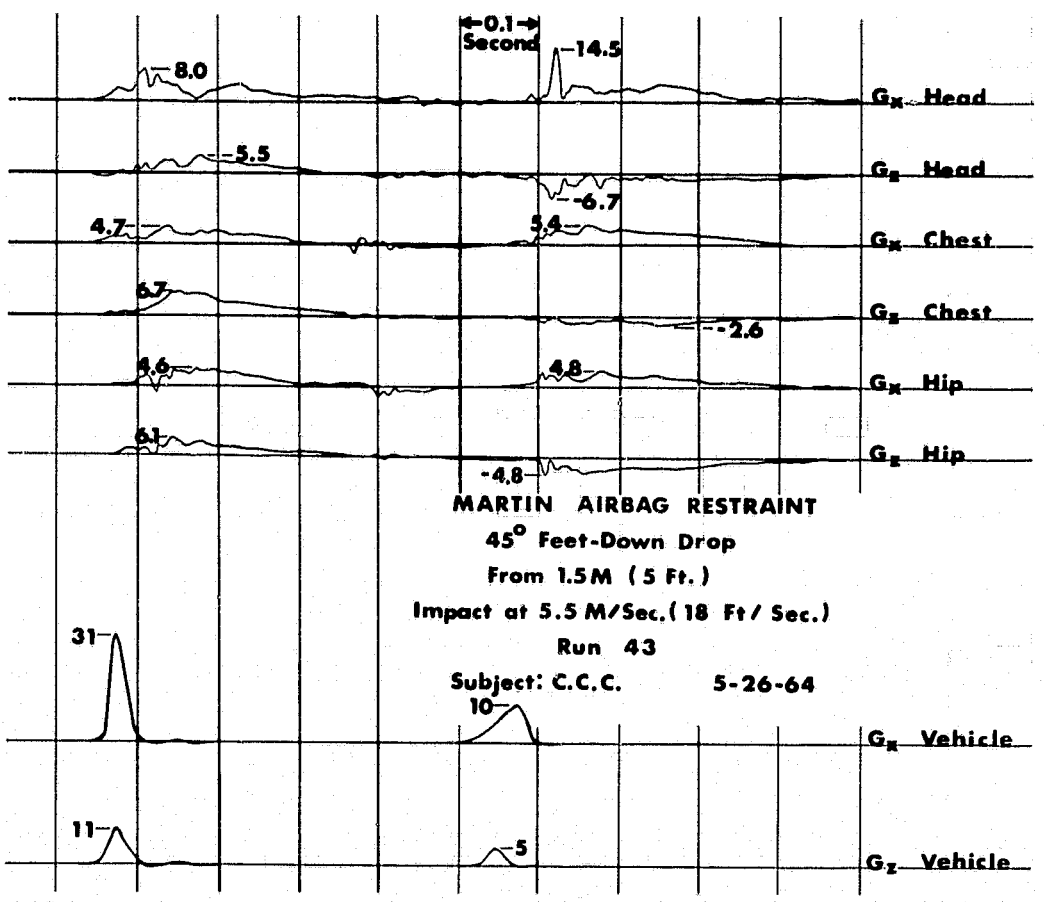

Fig. 33. Acceleration Time-History--45° Feet-Down Drop from 1.5 m (5 ft)--Human Subject

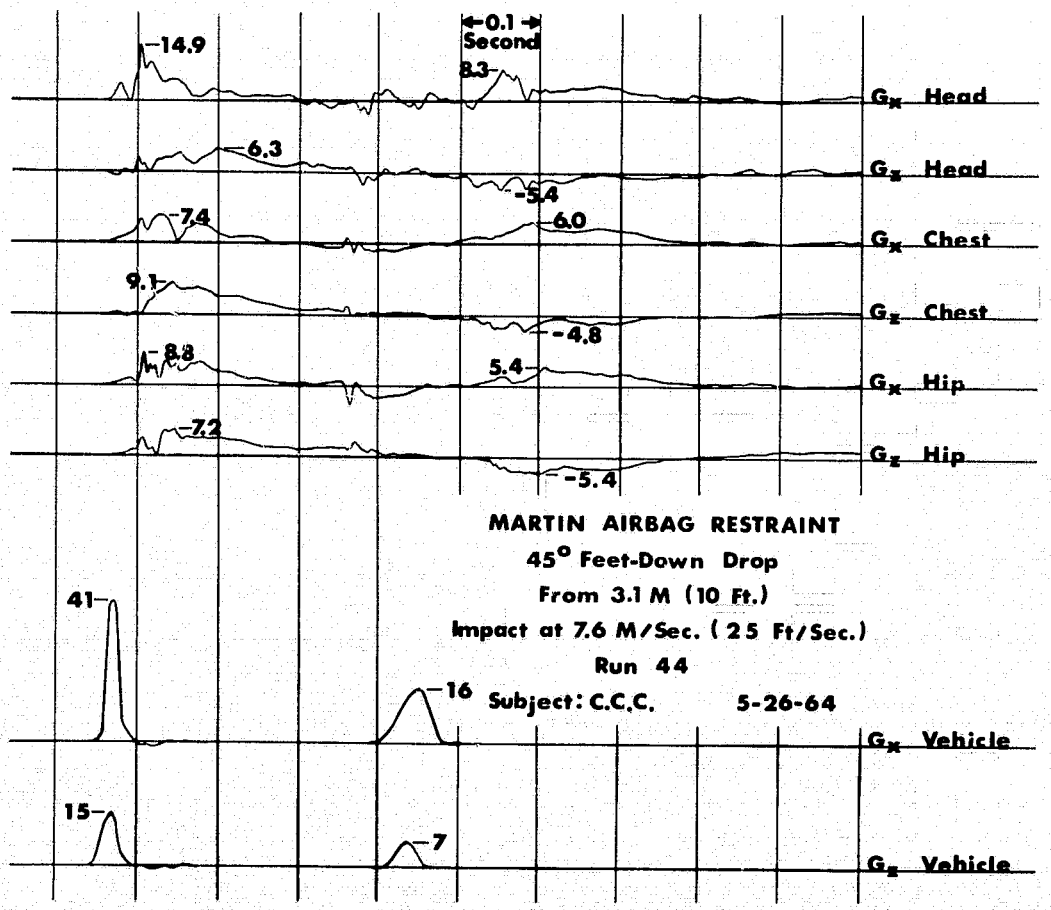

Fig. 34. Acceleration Time-History--45° Feet-Down Drop from 3.1 m (10 ft)--Human Subject

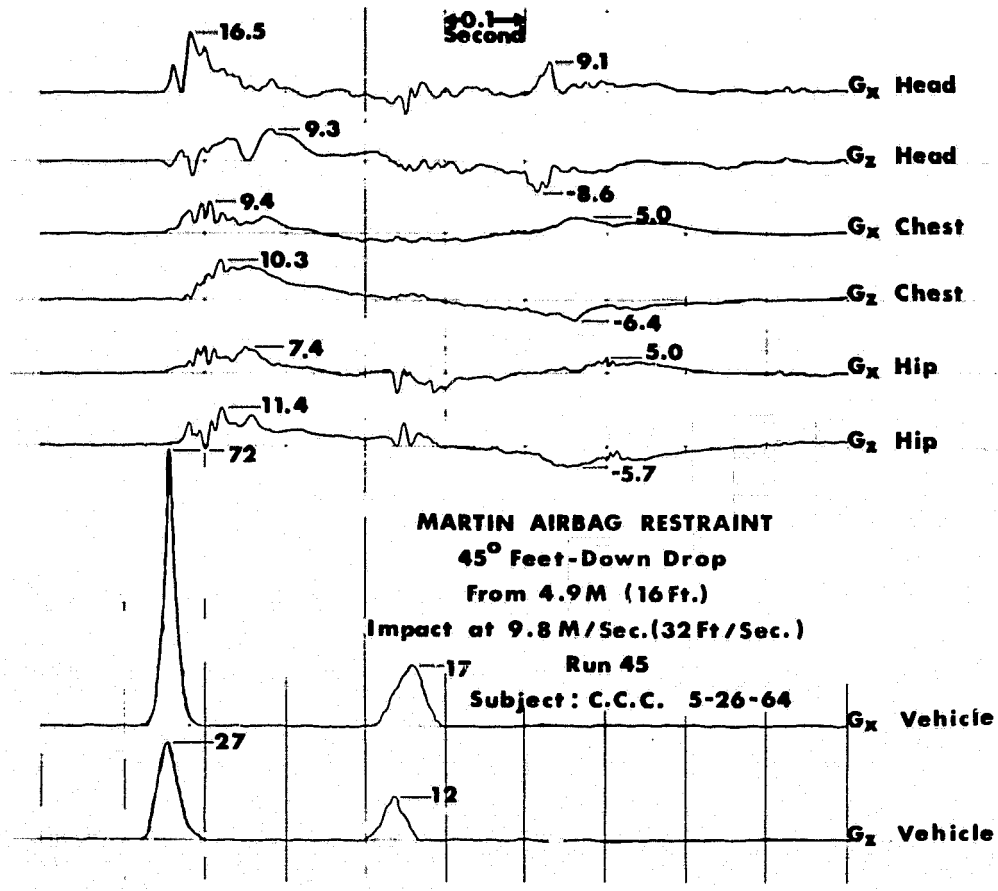

Fig. 35. Acceleration Time-History--45° Feet-Down Drop from 4.9 m (16 ft)--Human Subject

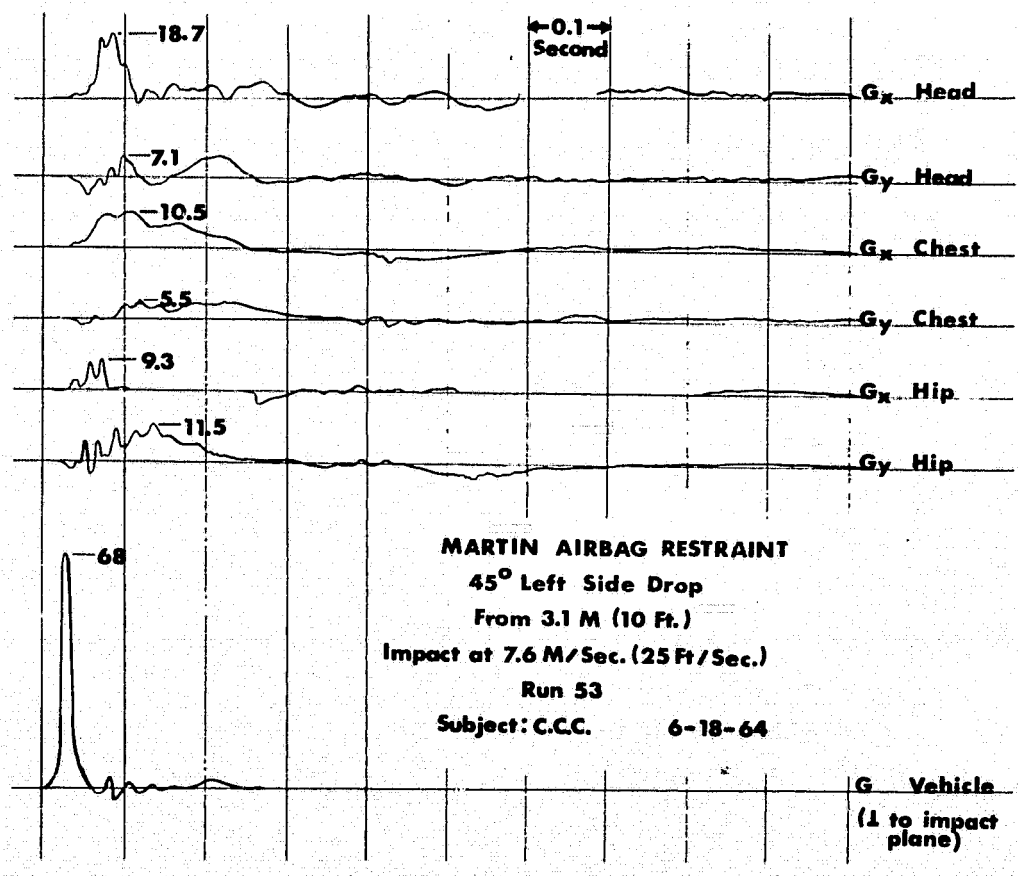

Fig. 36. Acceleration Time-History--45° Left-Side Drop from 3.1 m (10 ft)--Human Subject

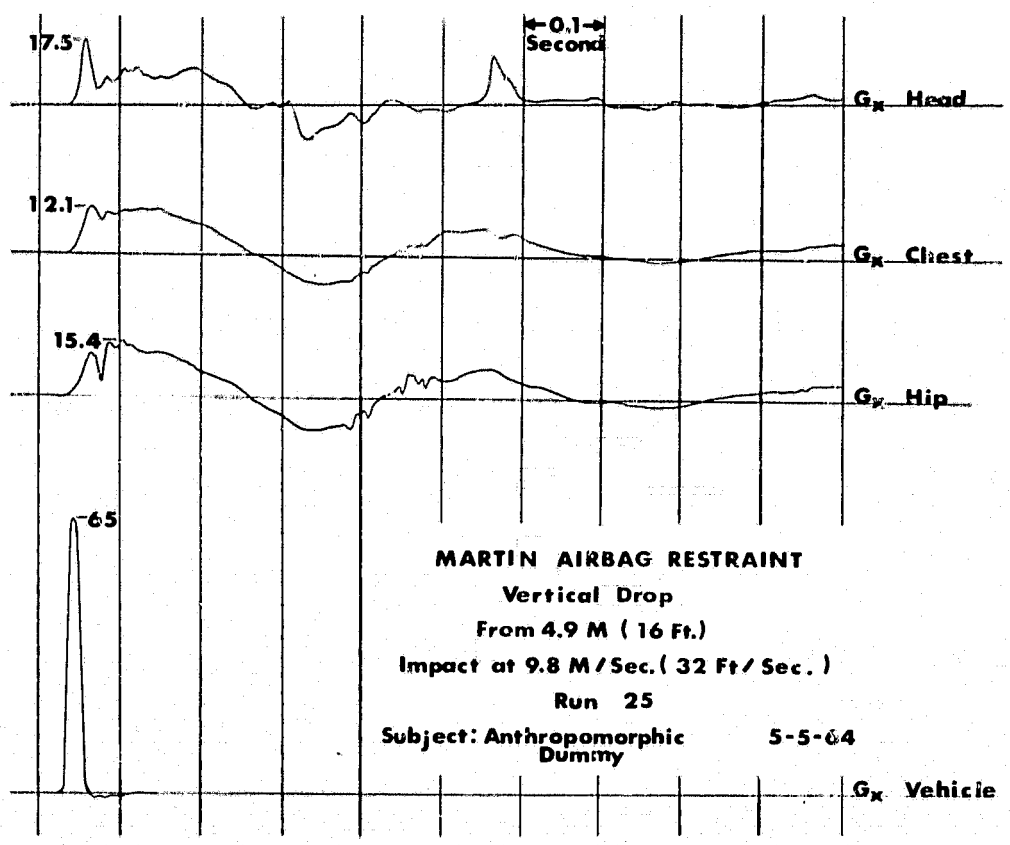

Fig. 37. Acceleration Time-History--Vertical Drop from 4.9 m (16 ft)--Dummy Subject

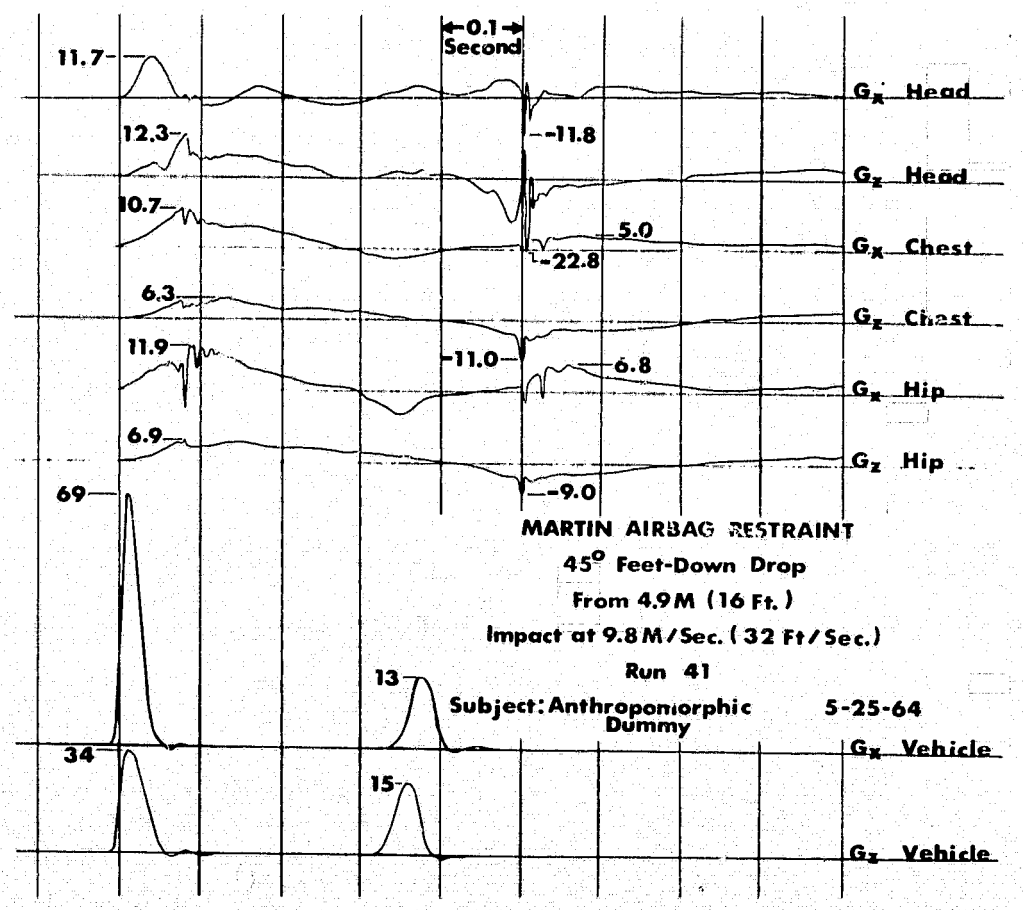

Fig. 38. Acceleration Time-History--45° Feet-Down Drop from 4.9 m (16 ft)--Dummy Subject

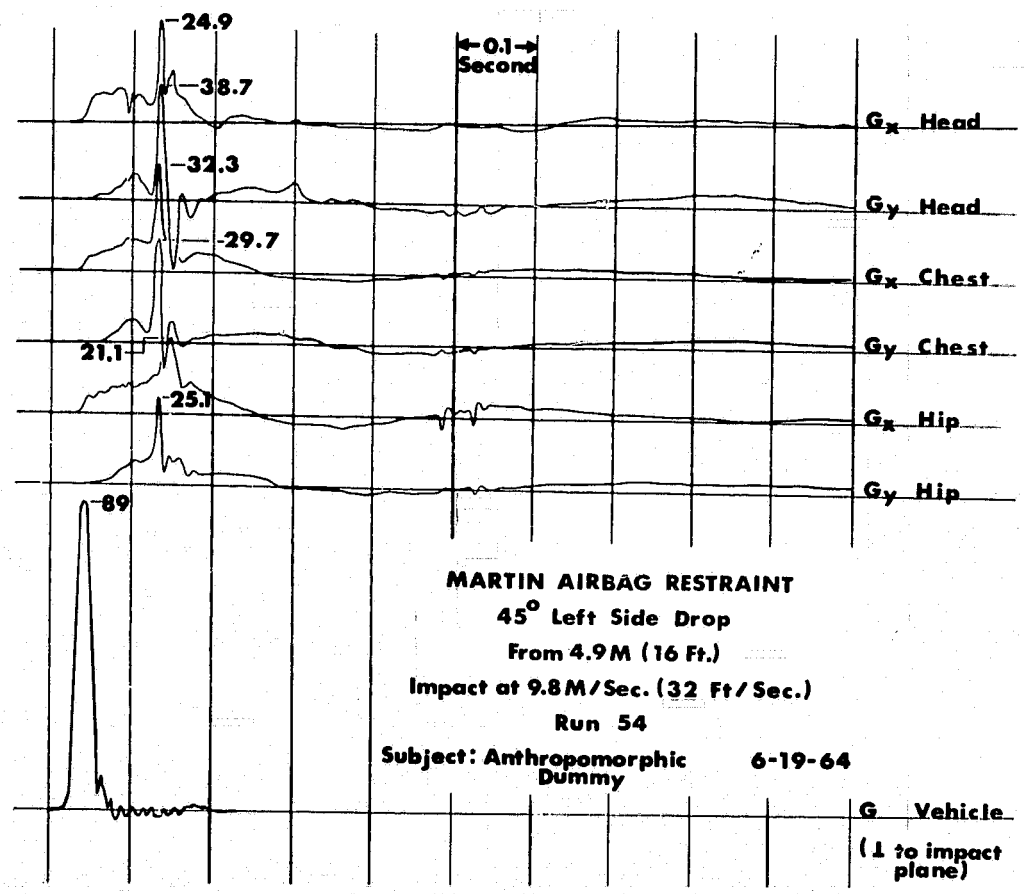

Fig. 39. Acceleration Time-History--45° Left-Side Drop from 4.9 m (16 ft)--Dummy Subject

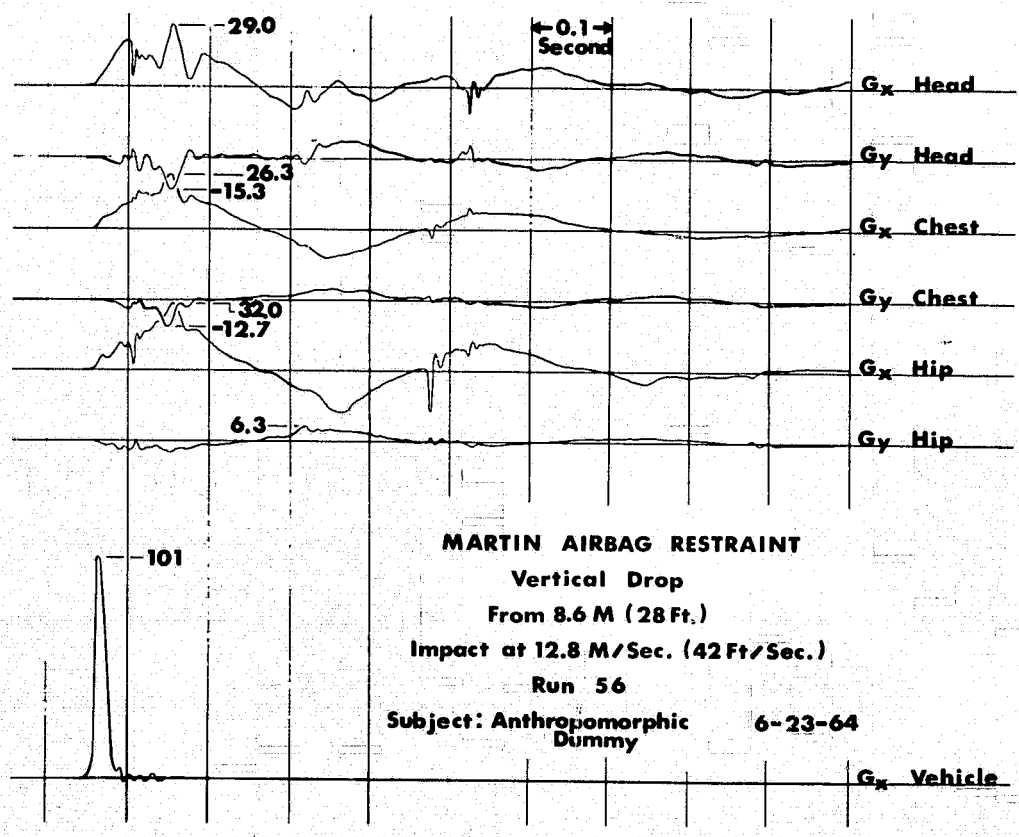

Fig. 40. Acceleration Time-History--Vertical Drop from 8.6 m (28 ft)--Dummy Subject

20

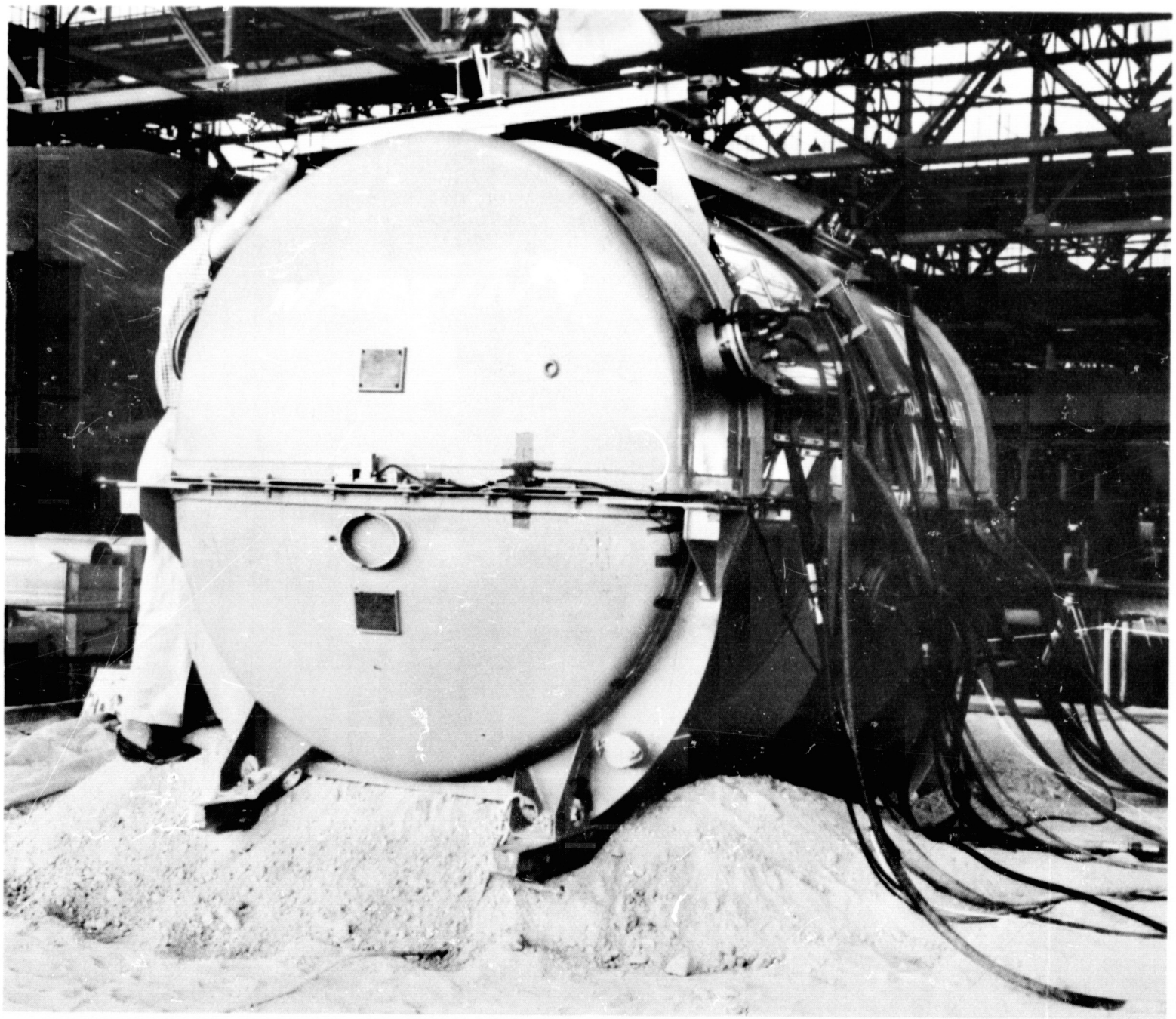

Fig. 41. Test Vehicle Shown After 45° Feet-Down Impact--Pilot Compartment Airbag Restraint System

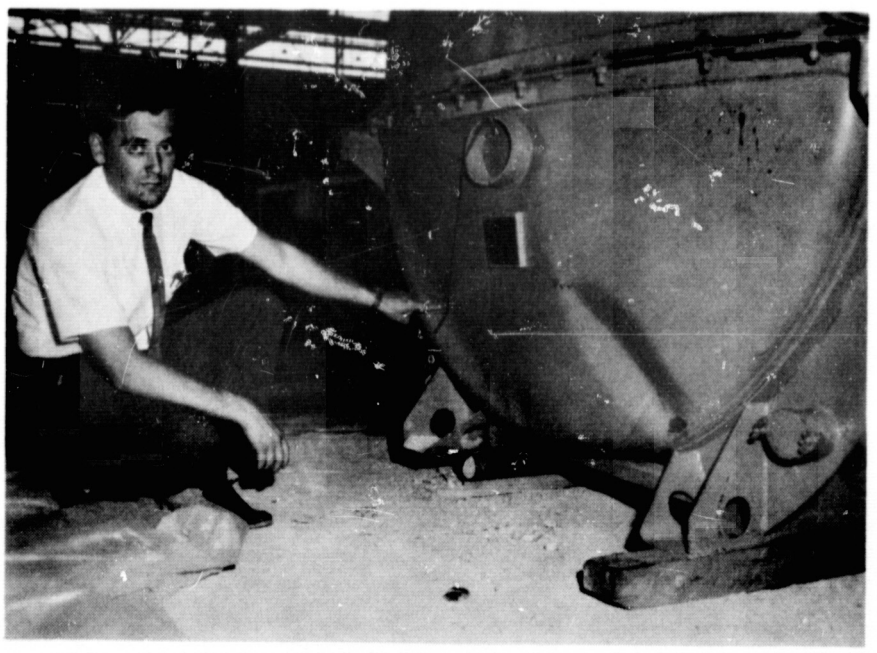

Fig. 42. Test Vehicle--Structural Damage After Impact Test Program--Pilot Compartment Airbag Restraint System

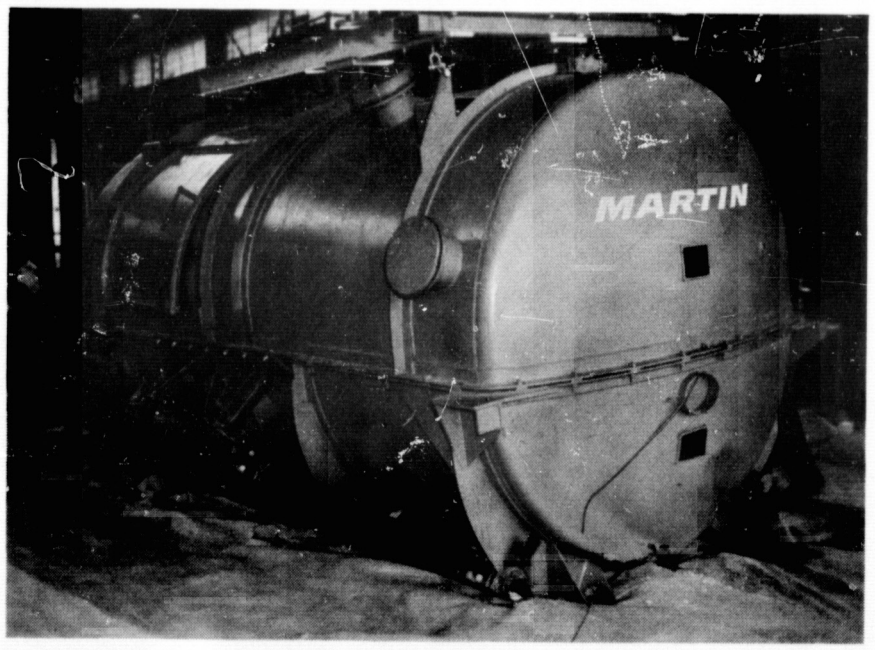

Fig. 43. Test Vehicle--Structural Damage After Impact Test Program--Note Door Failure--Pilot Compartment Airbag Restraint System

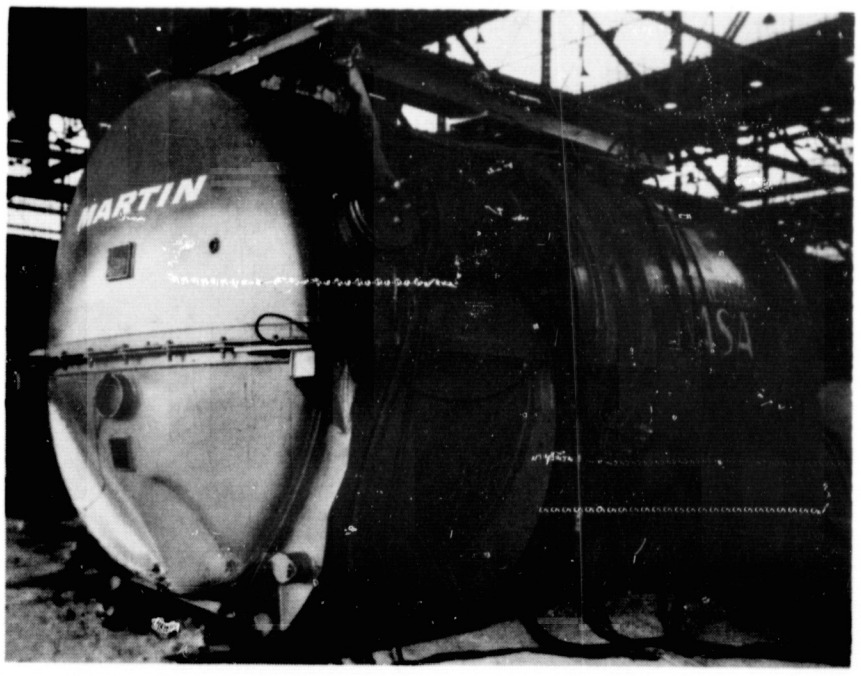

Fig. 44. Test Vehicle--Structural Damage After Impact Test Program--Pilot Compartment Airbag Restraint System

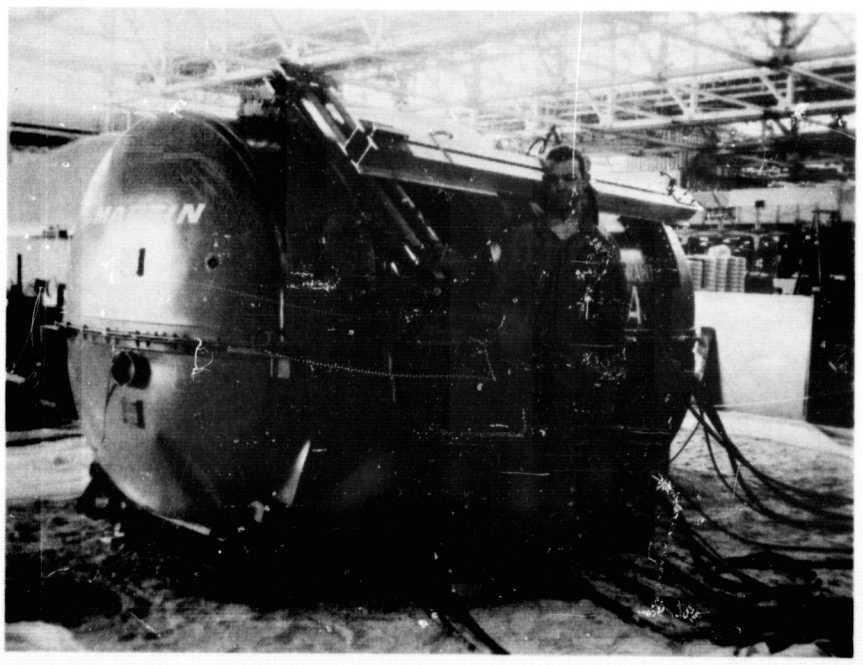

Fig. 45. Test Vehicle and Test Subject at the Completion of the Human Impact Tests--Pilot Compartment Airbag Restraint System

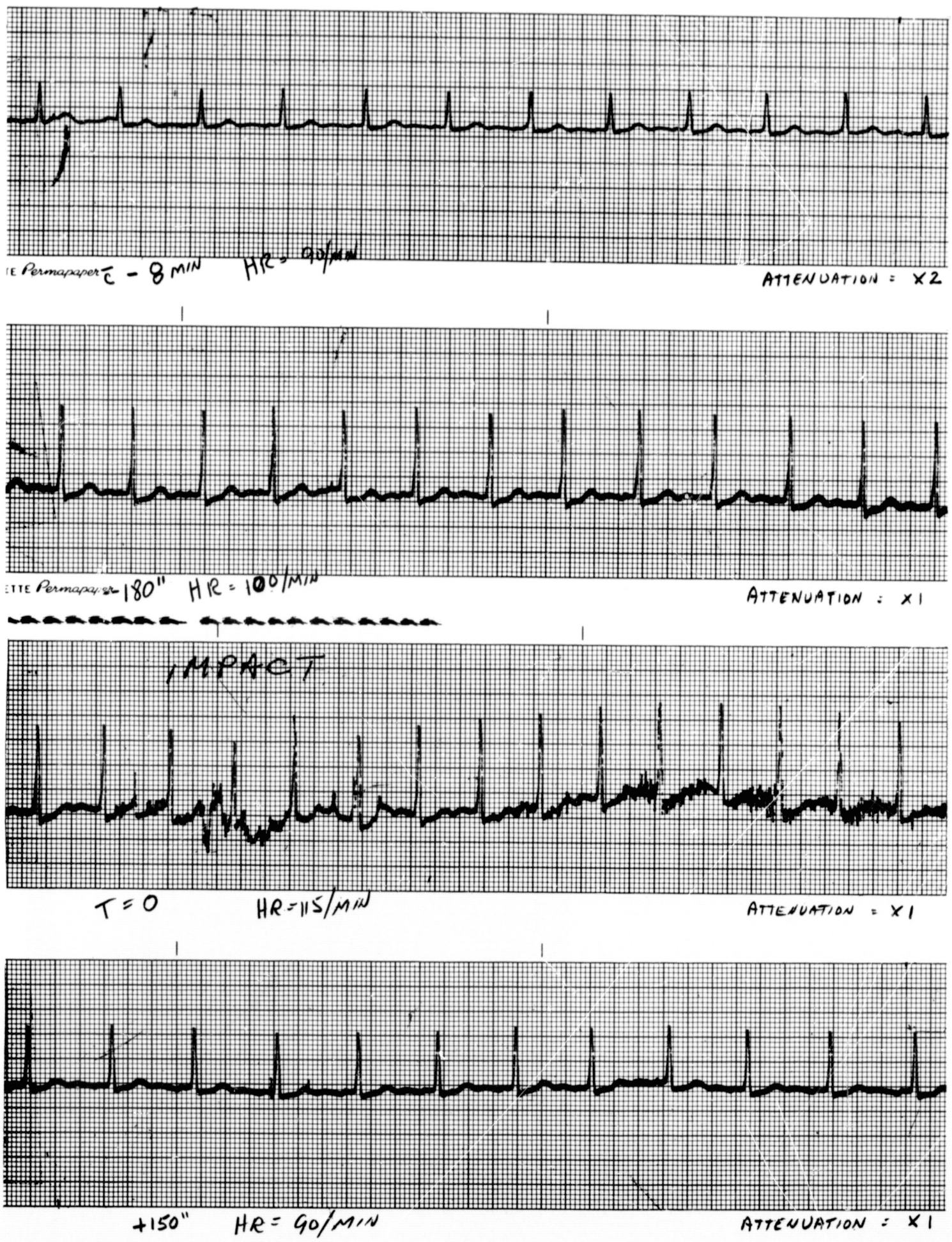

Fig. 46. Electrocardiograms--Test Number 53, Vehicle 45° Left-Side Drop from 3.1 m (10 ft)--Pilot Compartment Airbag Restraint System

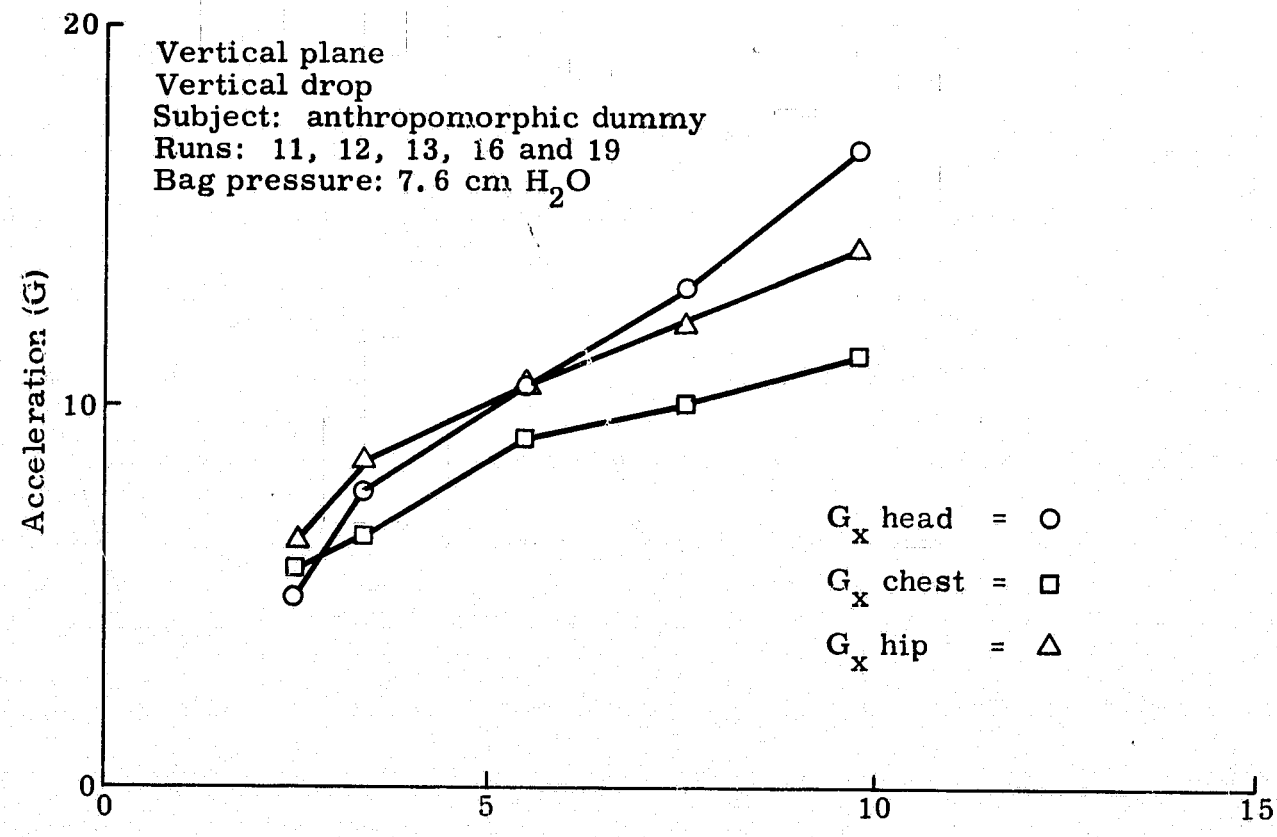

Fig. 47. Body Accelerations Versus Impact Velocity--Anthropomorphic Dummy

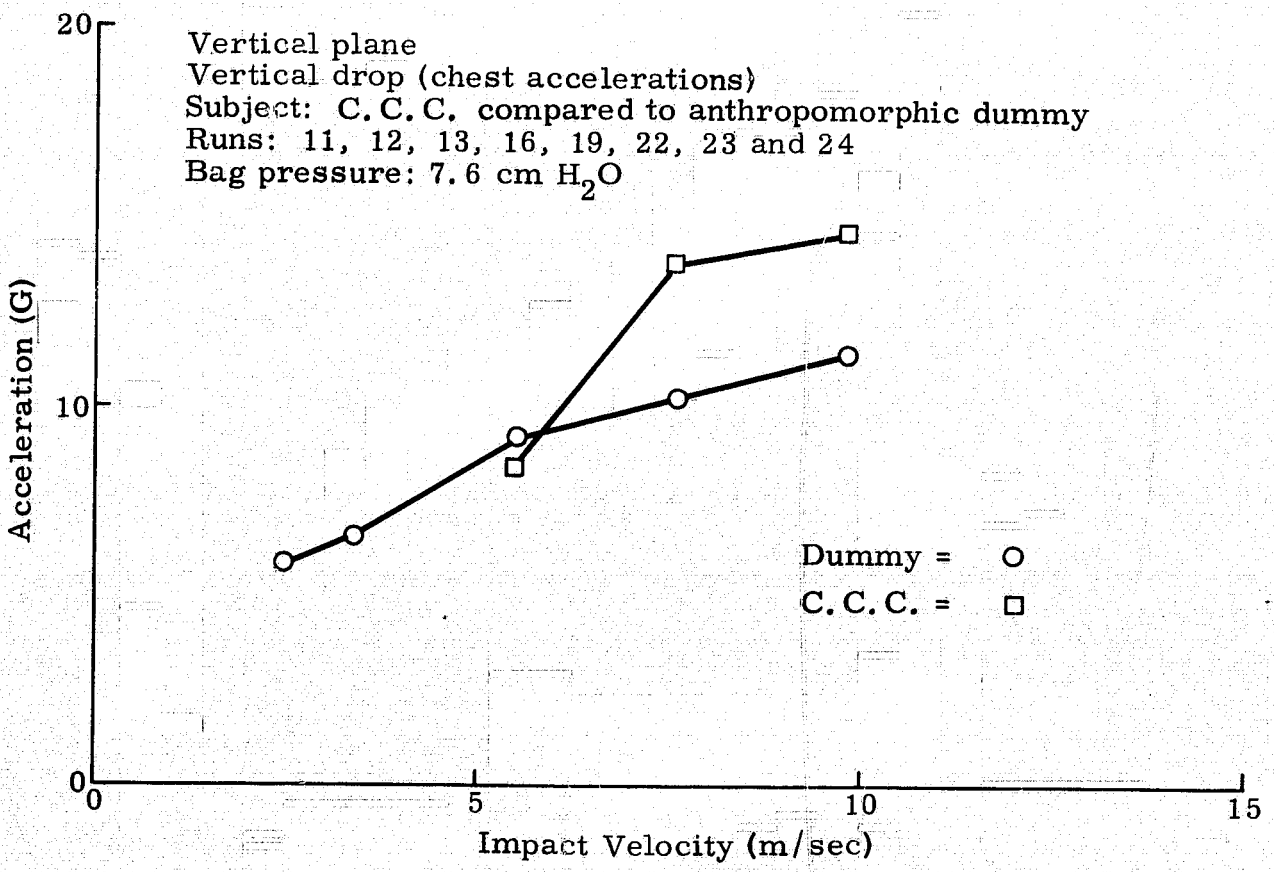

Fig. 48. Body Accelerations Versus Impact Velocity -- Anthropomorphic Dummy Compared to Human Subject

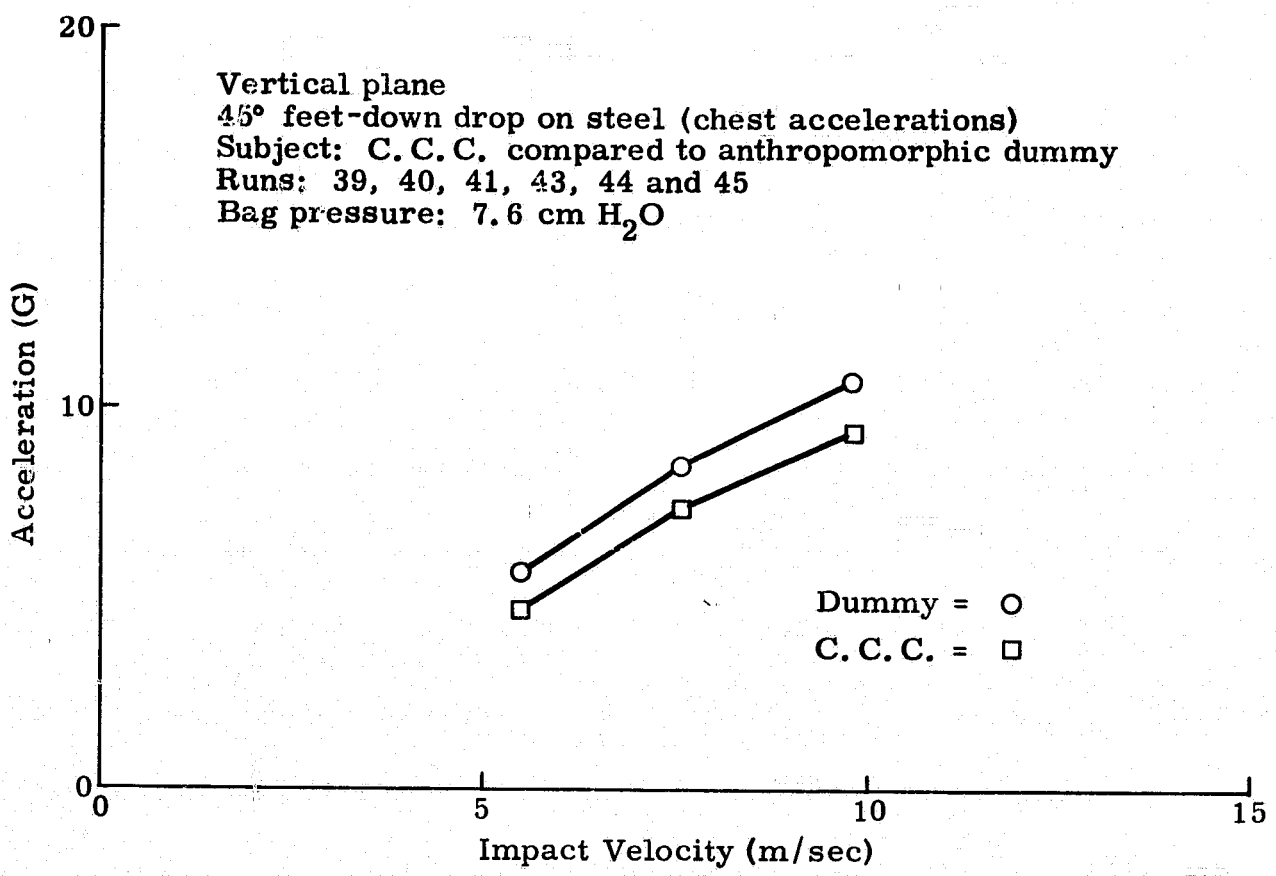

Fig. 49. Body Accelerations Versus Impact Velocity -- Anthropomorphic Dummy Compared to Human Subject

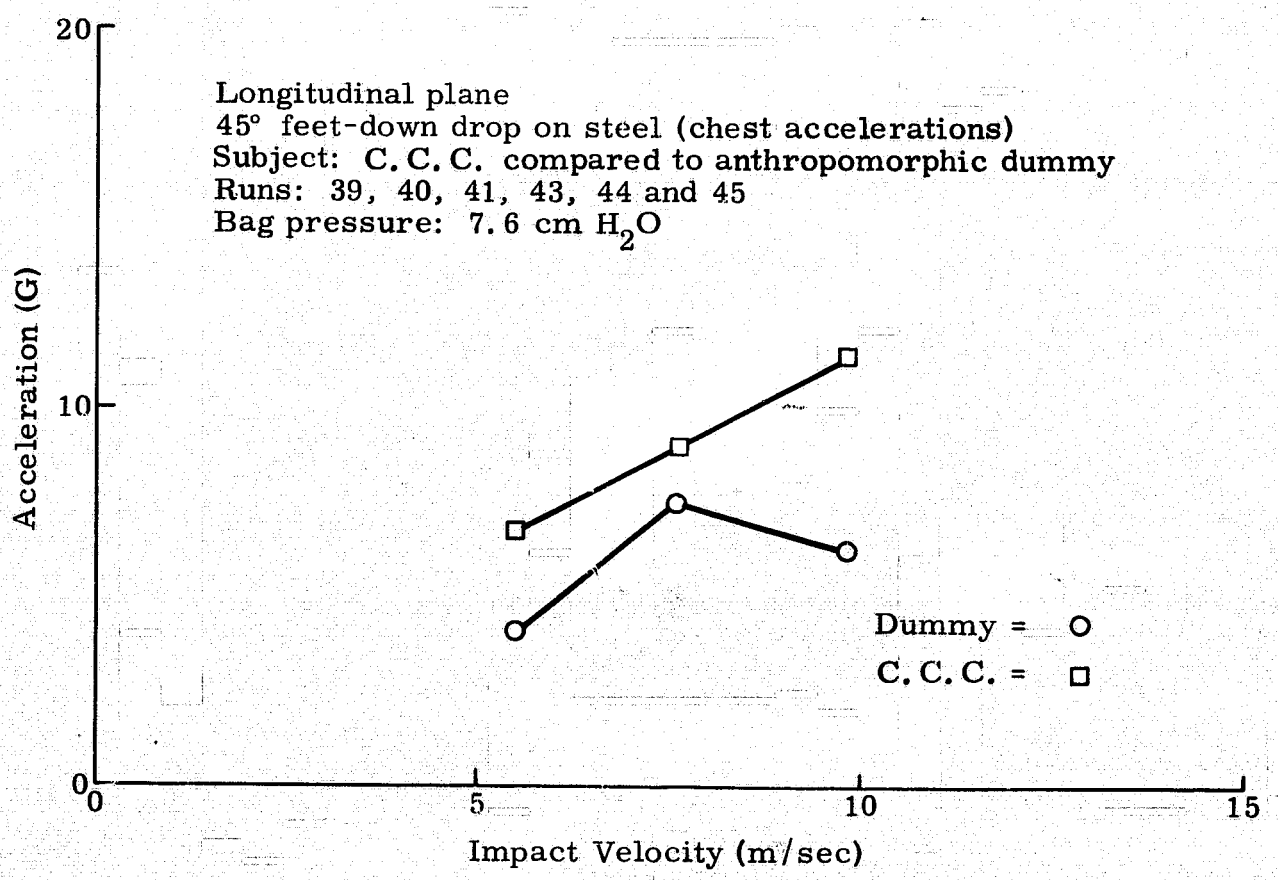

Fig. 50. Body Accelerations Versus Impact Velocity -- Anthropomorphic Dummy Compared to Human Subject

Vertical plane
45° left-side drop
Subject: anthropomorphic dummy
Runs: 50, 52 and 54
Bag pressure: 15 cm H_2O

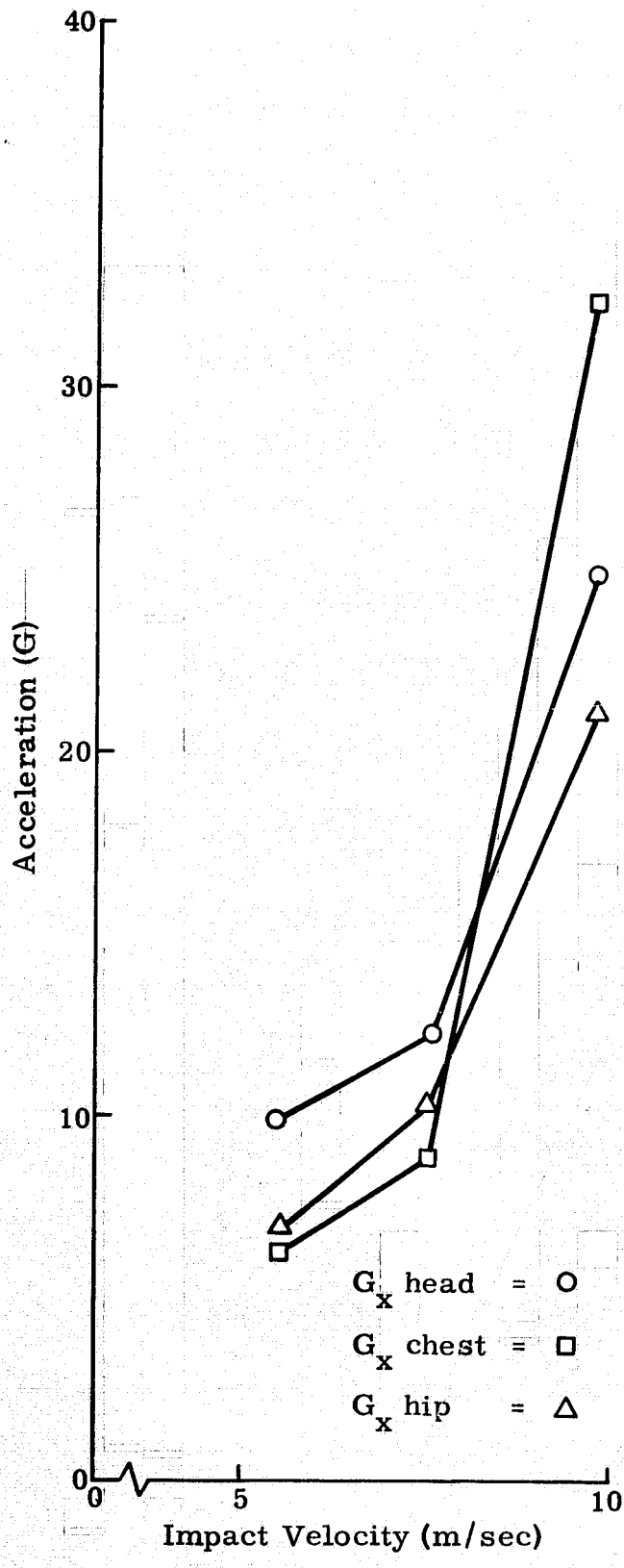

Fig. 51. Body Accelerations Versus Impact Velocity -- Anthropomorphic Dummy

Lateral plane
45° left-side drop
Subject: anthropomorphic dummy
Runs: 50, 52 and 54
Bag pressure: 15 cm H_2O

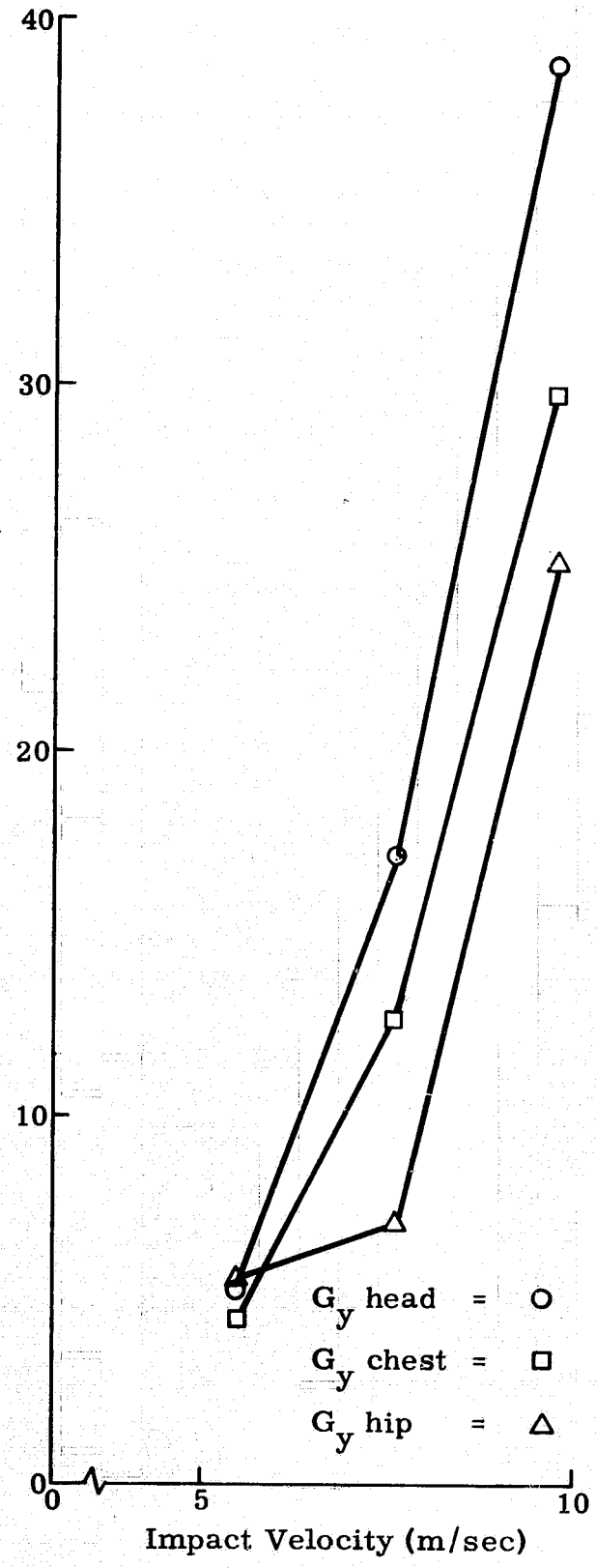

Fig. 52. Body Accelerations Versus Impact Velocity -- Anthropomorphic Dummy

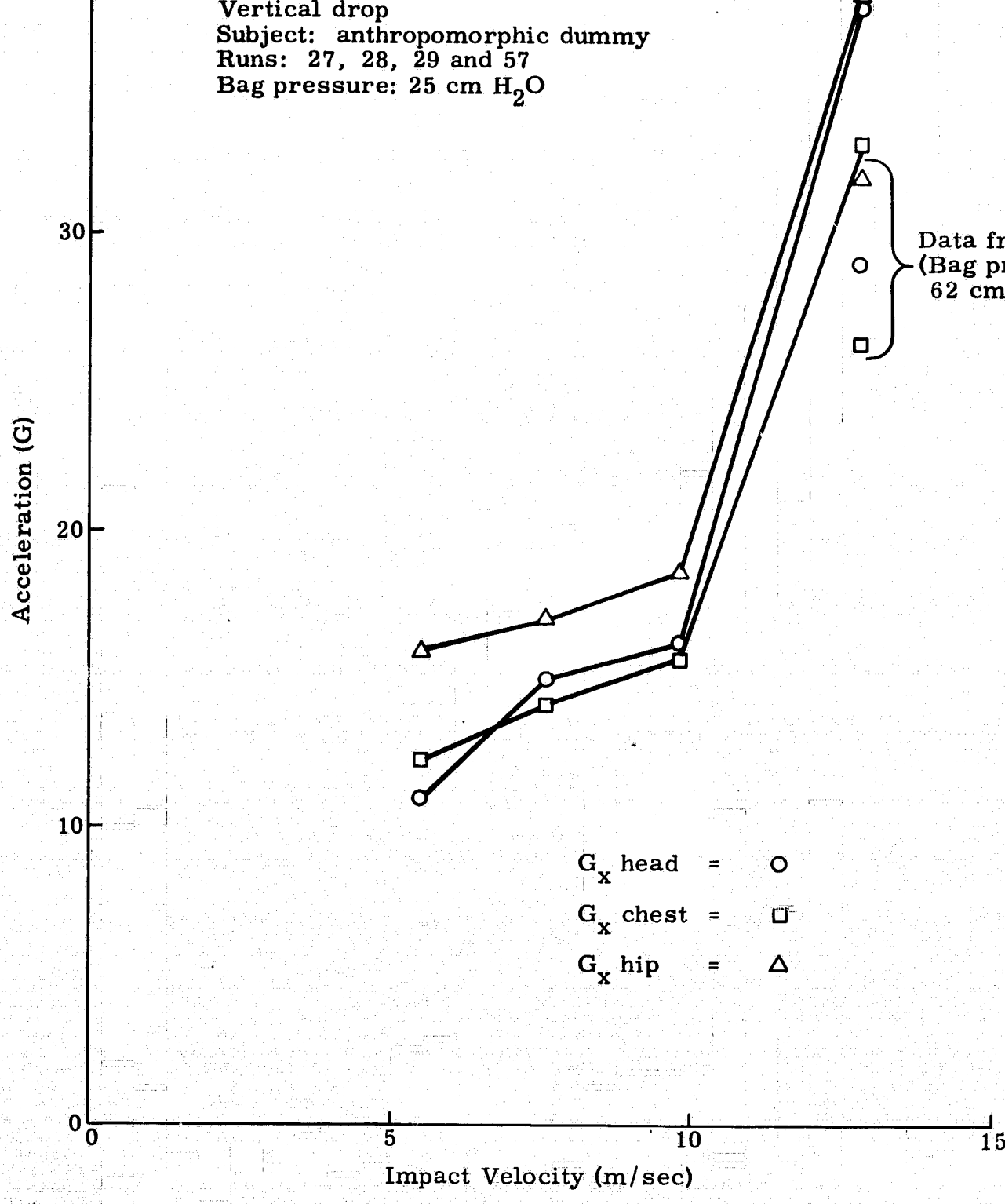

Fig. 53. Body Accelerations Versus Impact Velocity -- **Anthropomorphic Dummy**

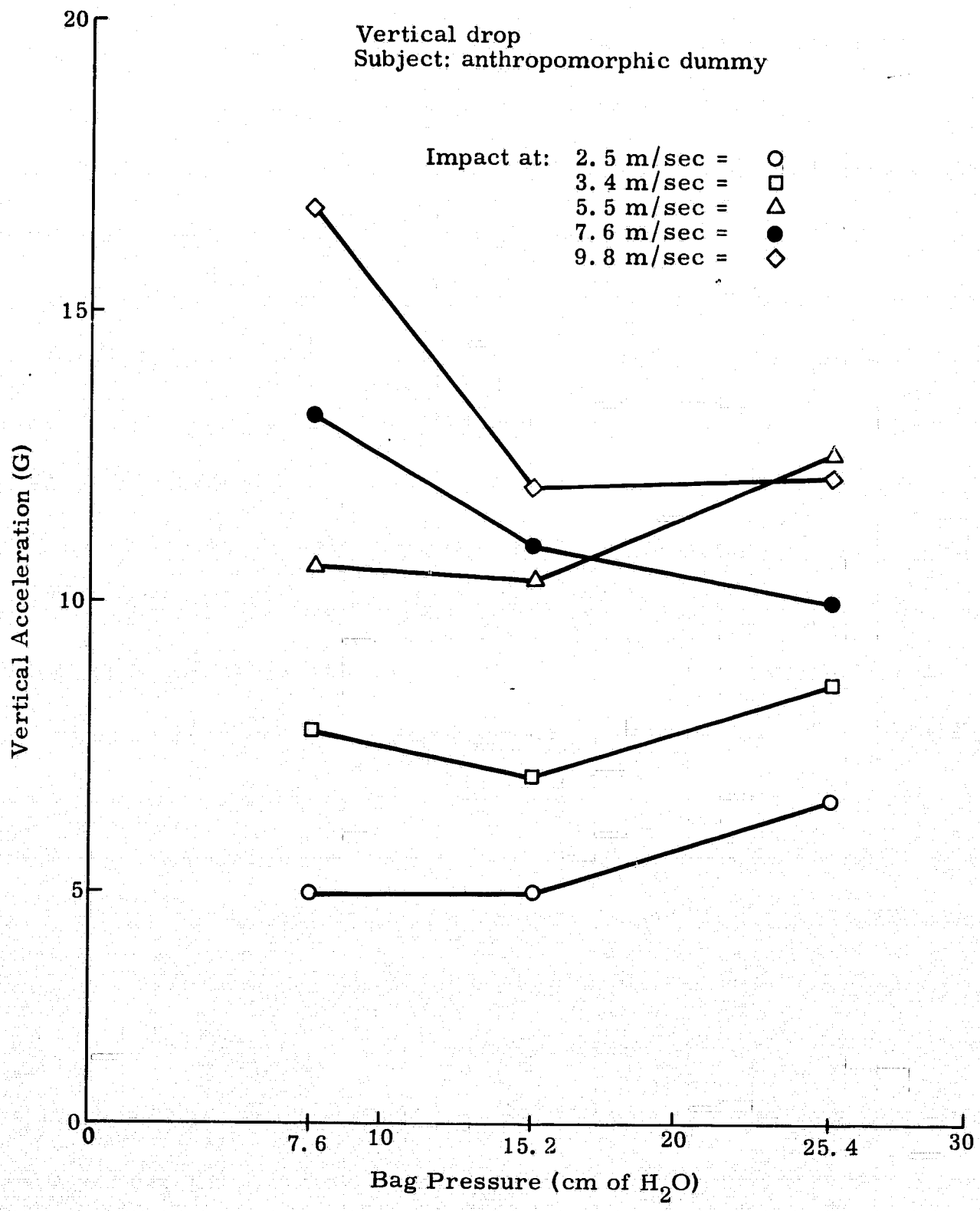

Fig. 54. Head (G_x) Accelerations Versus Airbag Pressure -- Anthropomorphic Dummy

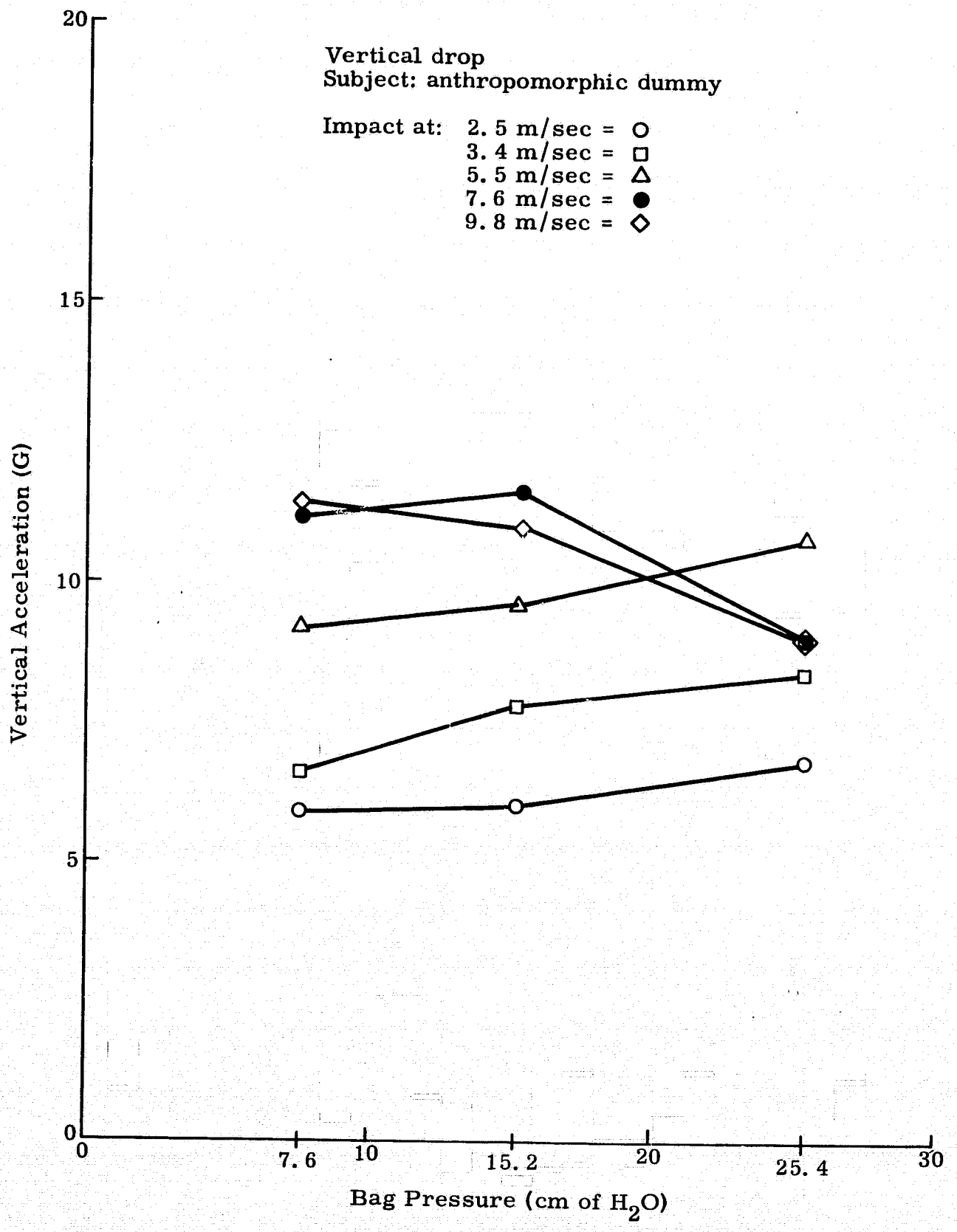

Fig. 55. Chest (G_x) Accelerations Versus Airbag Pressure -- Anthropomorphic Dummy

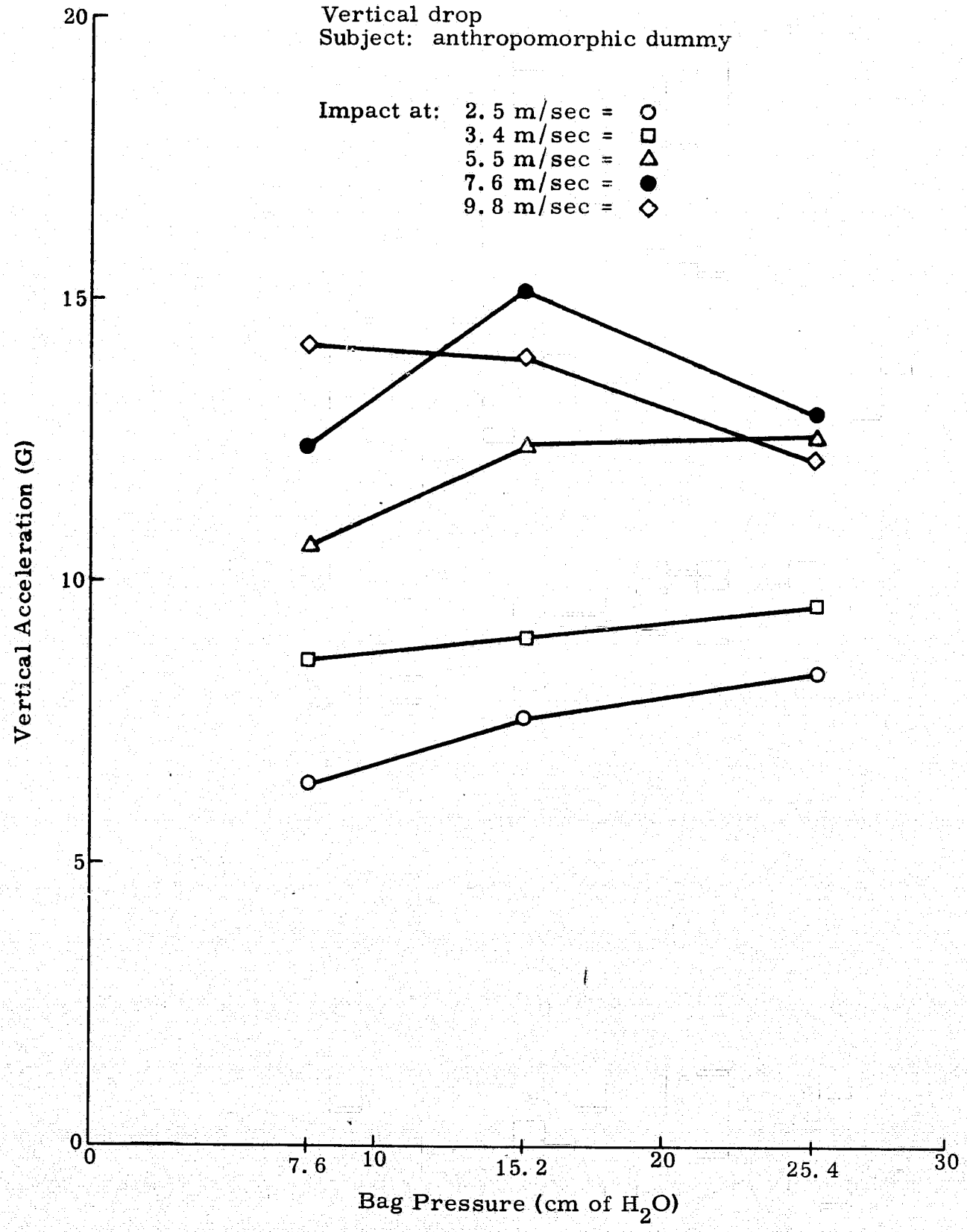

Fig. 56. Hip (G_x) Accelerations Versus Airbag Pressure -- Anthropomorphic Dummy

FOLDOUT FRAME 1

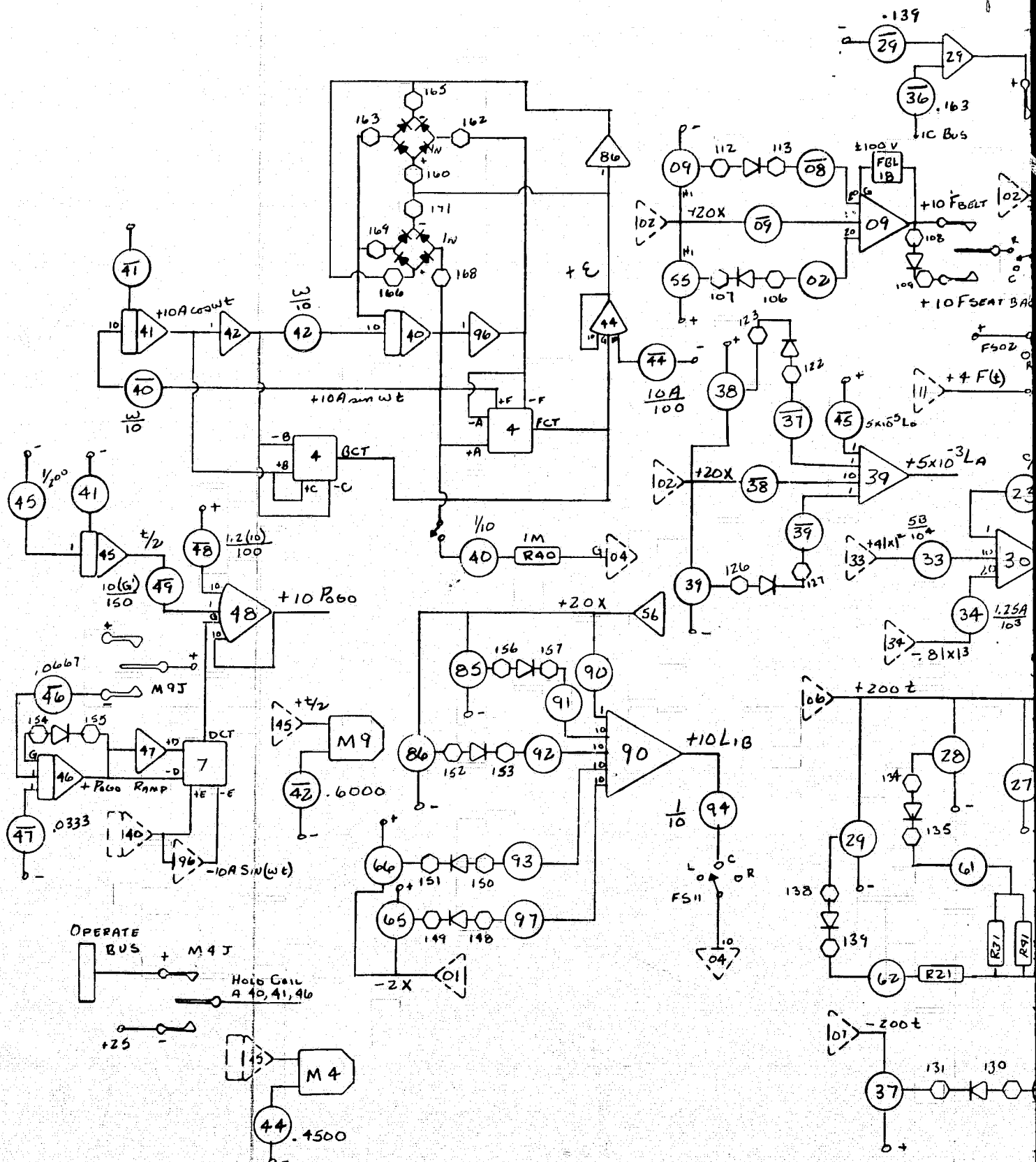

FOLDOUT FRAME 2

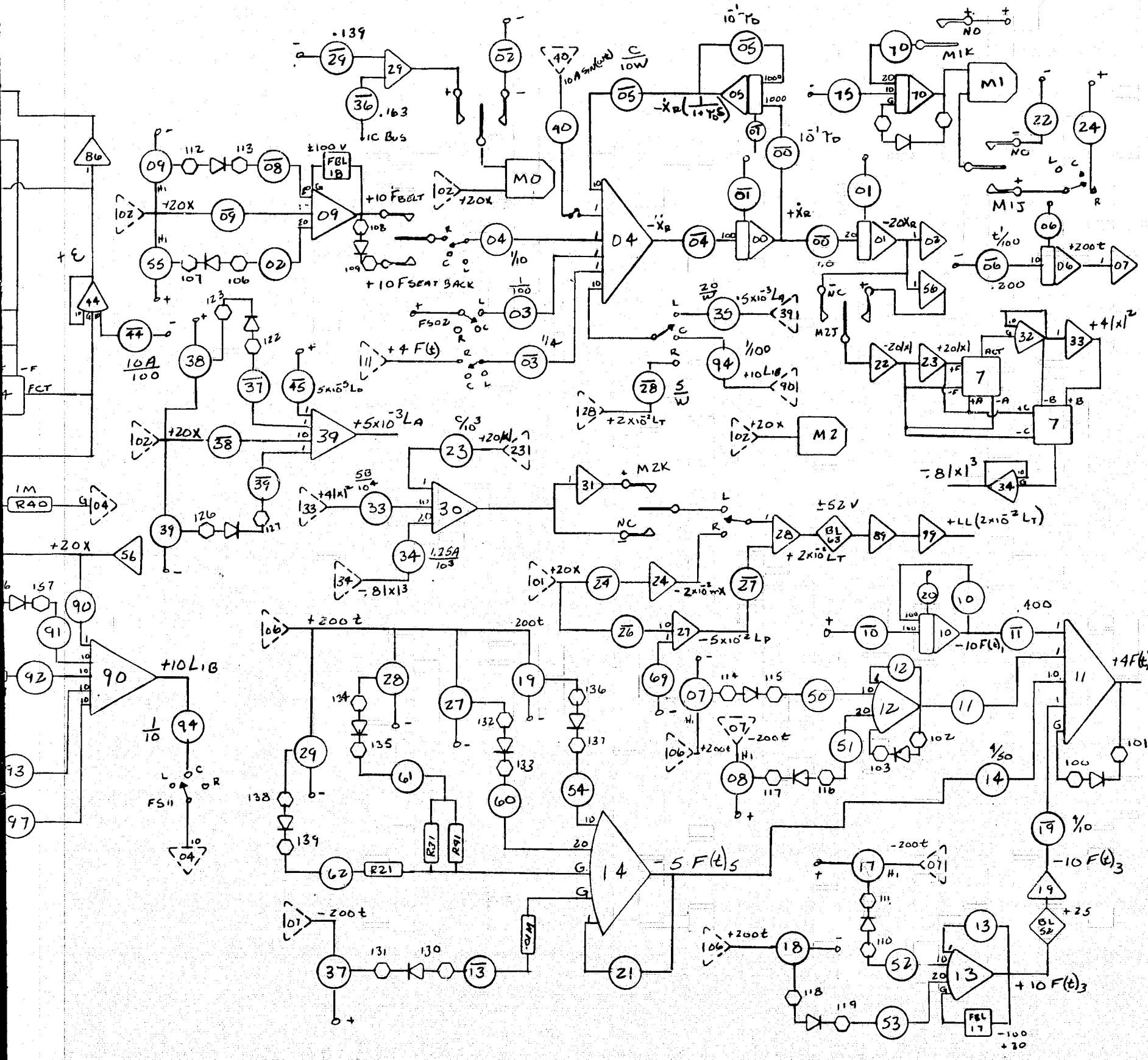

Fig. 57. Analog Schematic--Pilot Compartment Airbag Restraint System

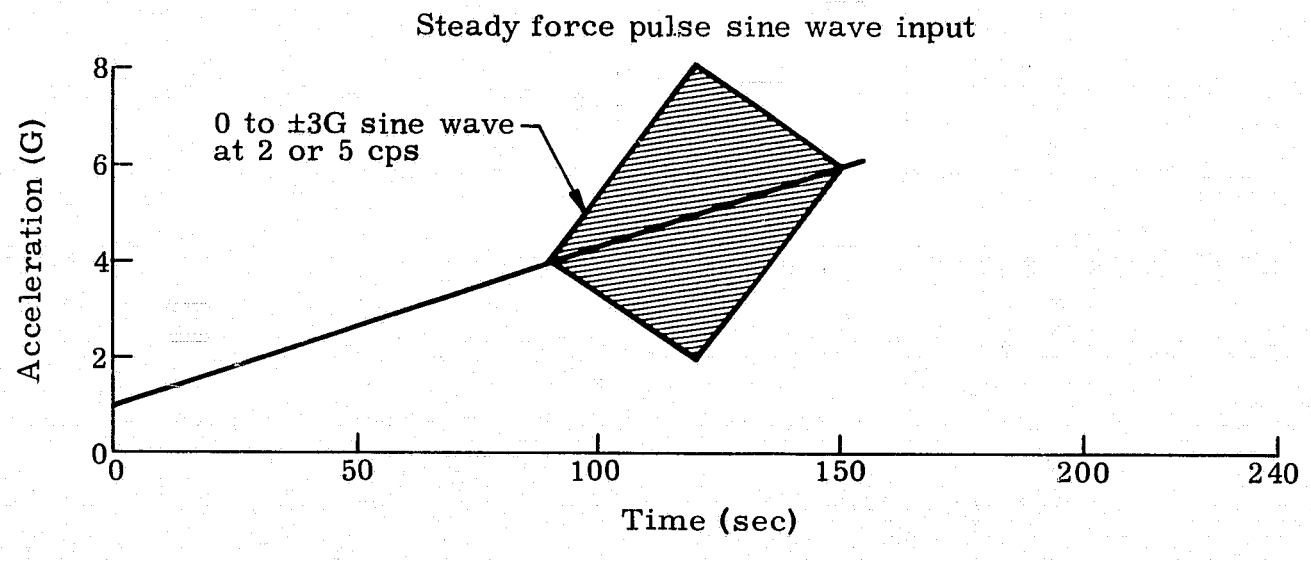

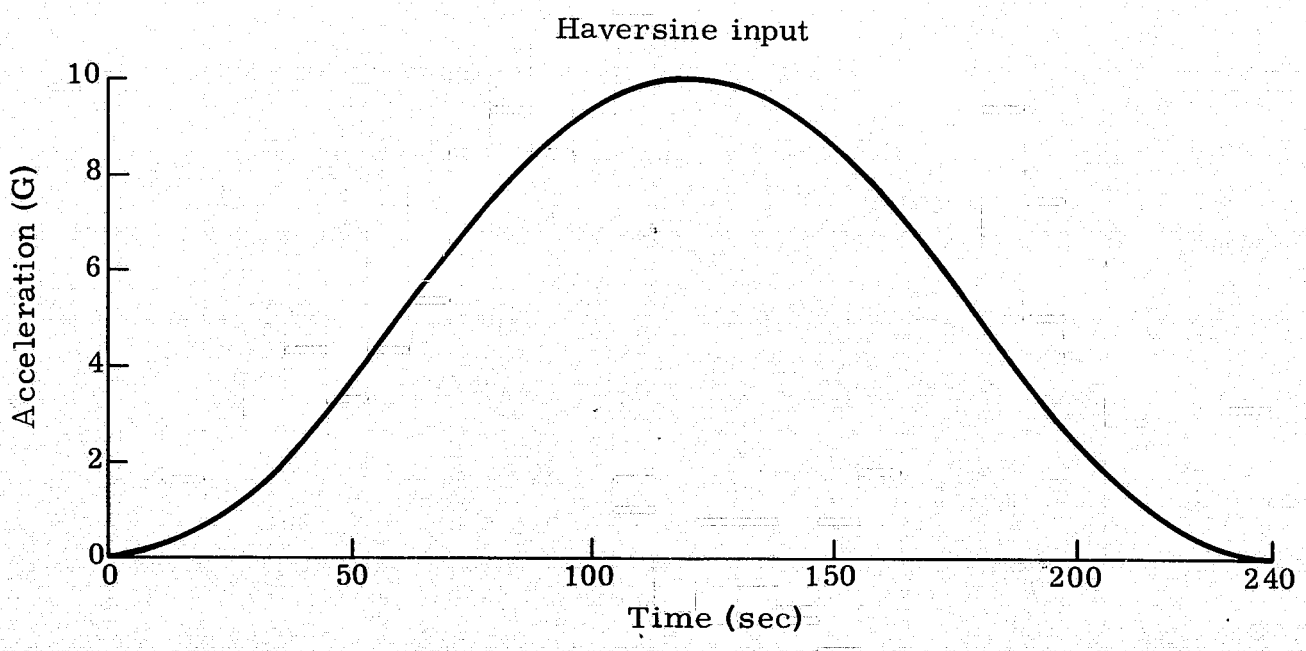

Fig. 58. Analog Airbag Restraint Study Inputs--Steady State Plus Sine Wave and Haversine--Pilot Compartment Airbag Restraint System

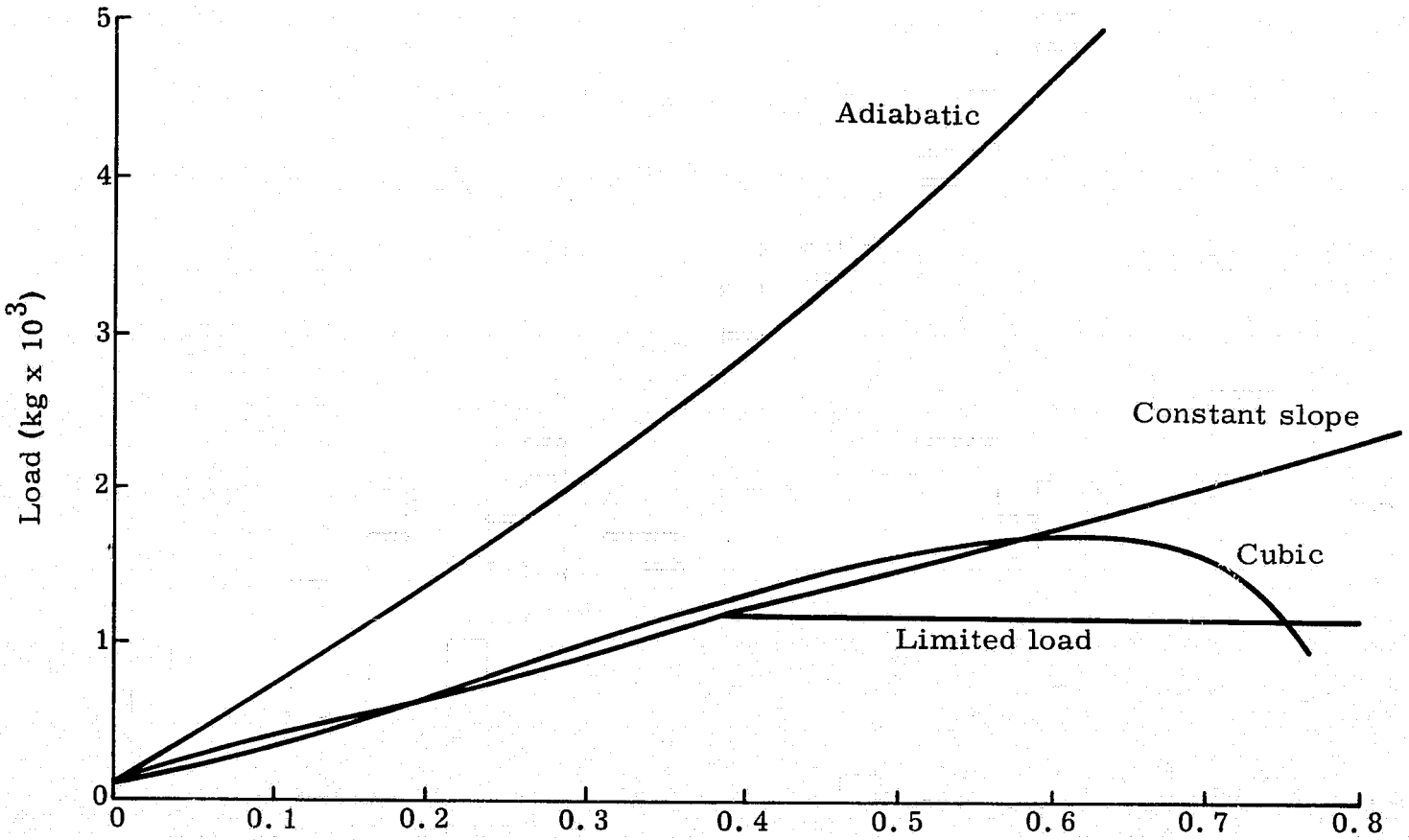

Fig. 59. Analog Airbag Restraint Study-Load Deflection Inputs-Pilot Compartment Airbag Restraint System

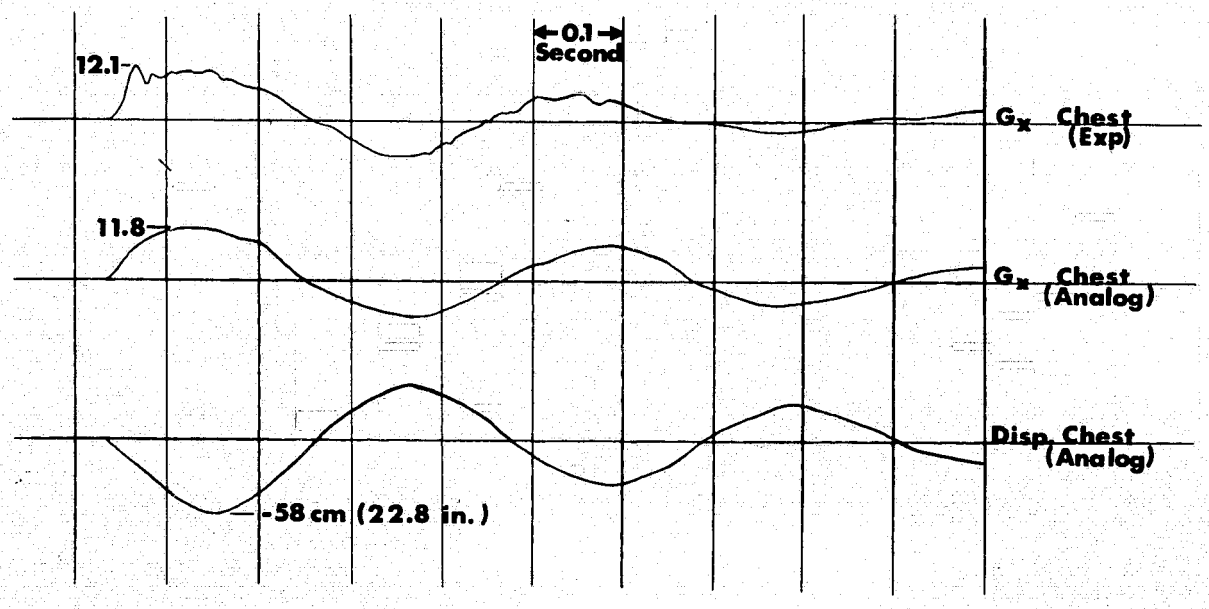

Fig. 60. Comparison of Experimental and Analog Data-Vertical Drop from 4.9 m (16 ft)--Pilot Compartment Airbag Restraint System

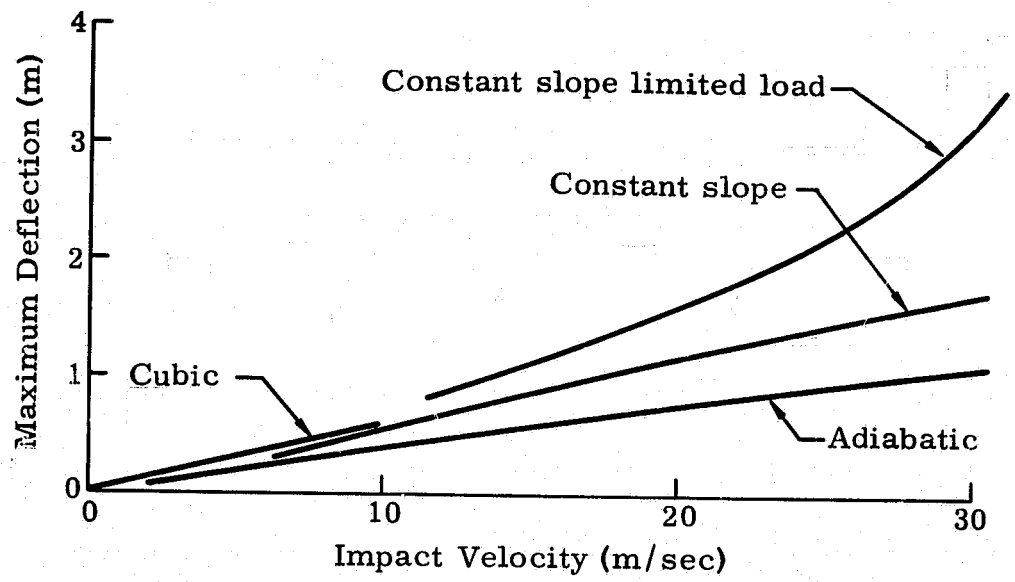

Fig. 61. Maximum Deflection Versus Impact Velocity for Various Restraint Systems--Analog Program--Pilot Compartment Airbag Restraint System

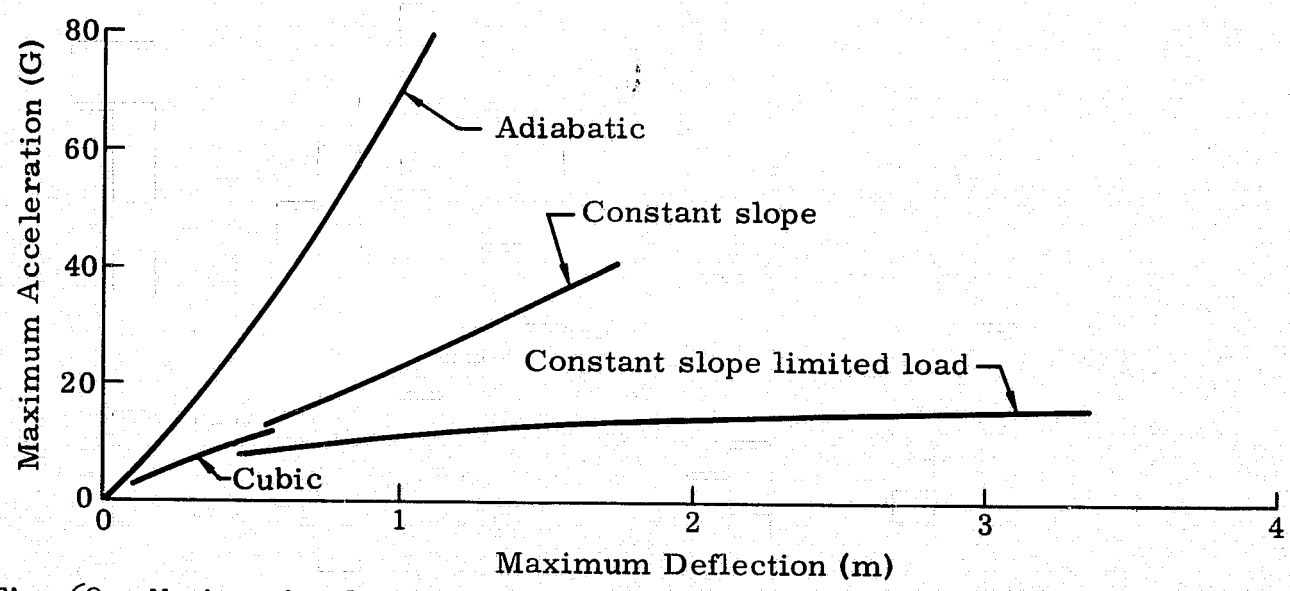

Fig. 62. Maximum Accelerations Versus Maximum Displacements for Various Restraint Systems--Analog Program--Pilot Compartment Airbag Restraint System

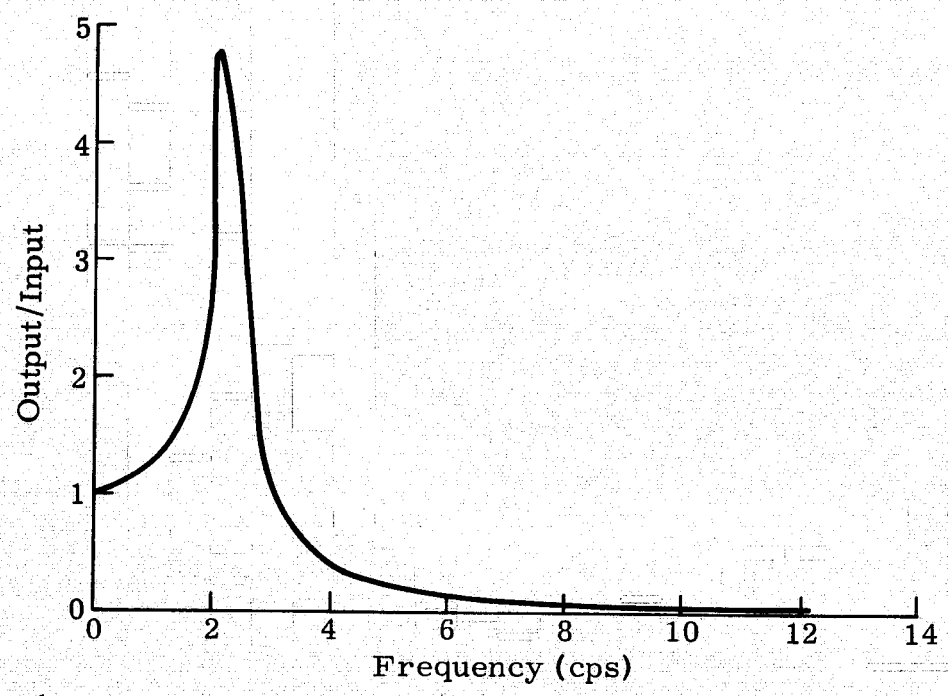

Fig. 63. System Response to Constant Amplitude 3-G Sine Wave--Analog Program--Pilot Compartment Airbag Restraint System

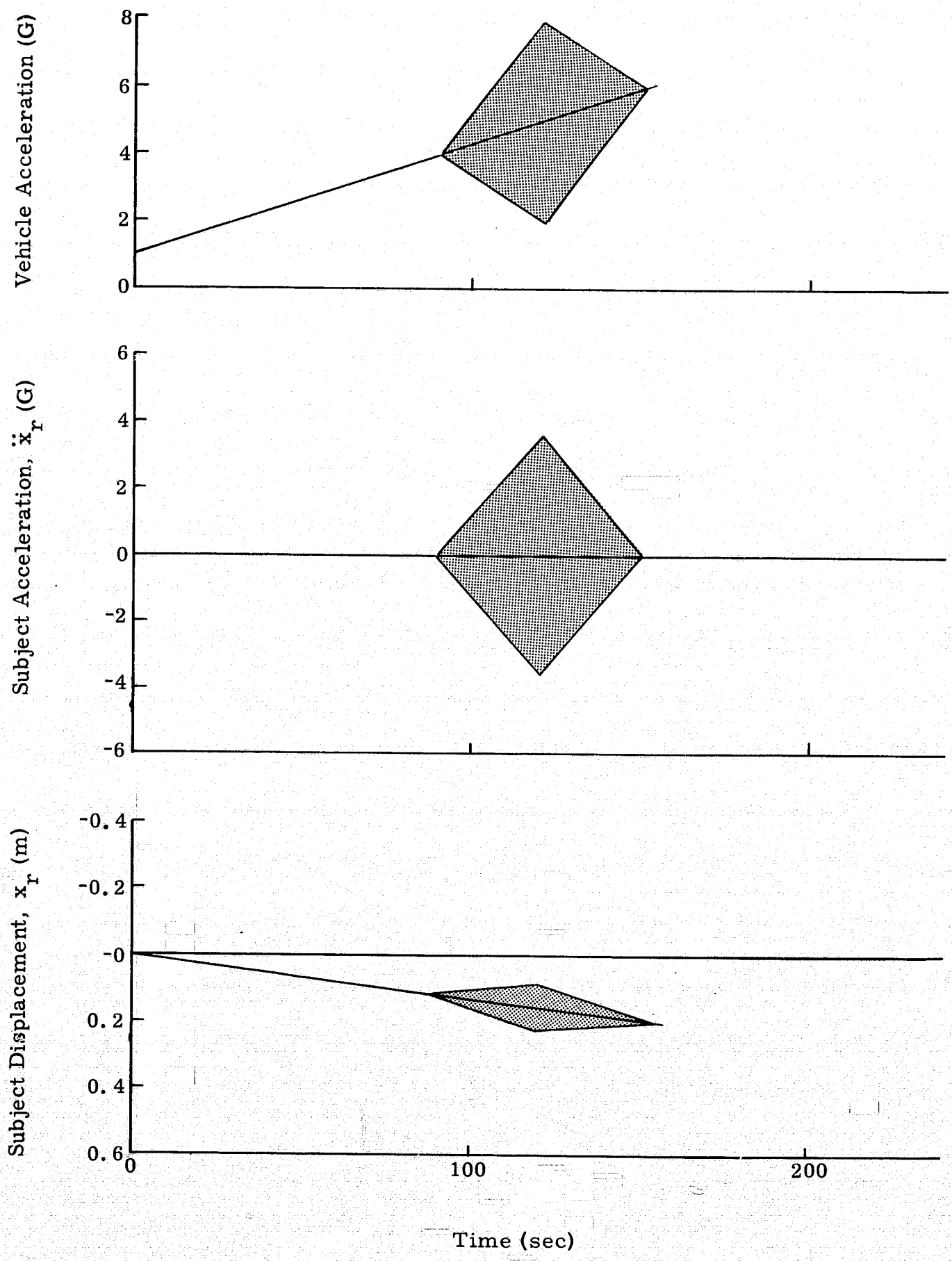

Fig. 64. System Response to Constant Force Plus Sinewave Input--Analog Program--Pilot Compartment Airbag Restraint System

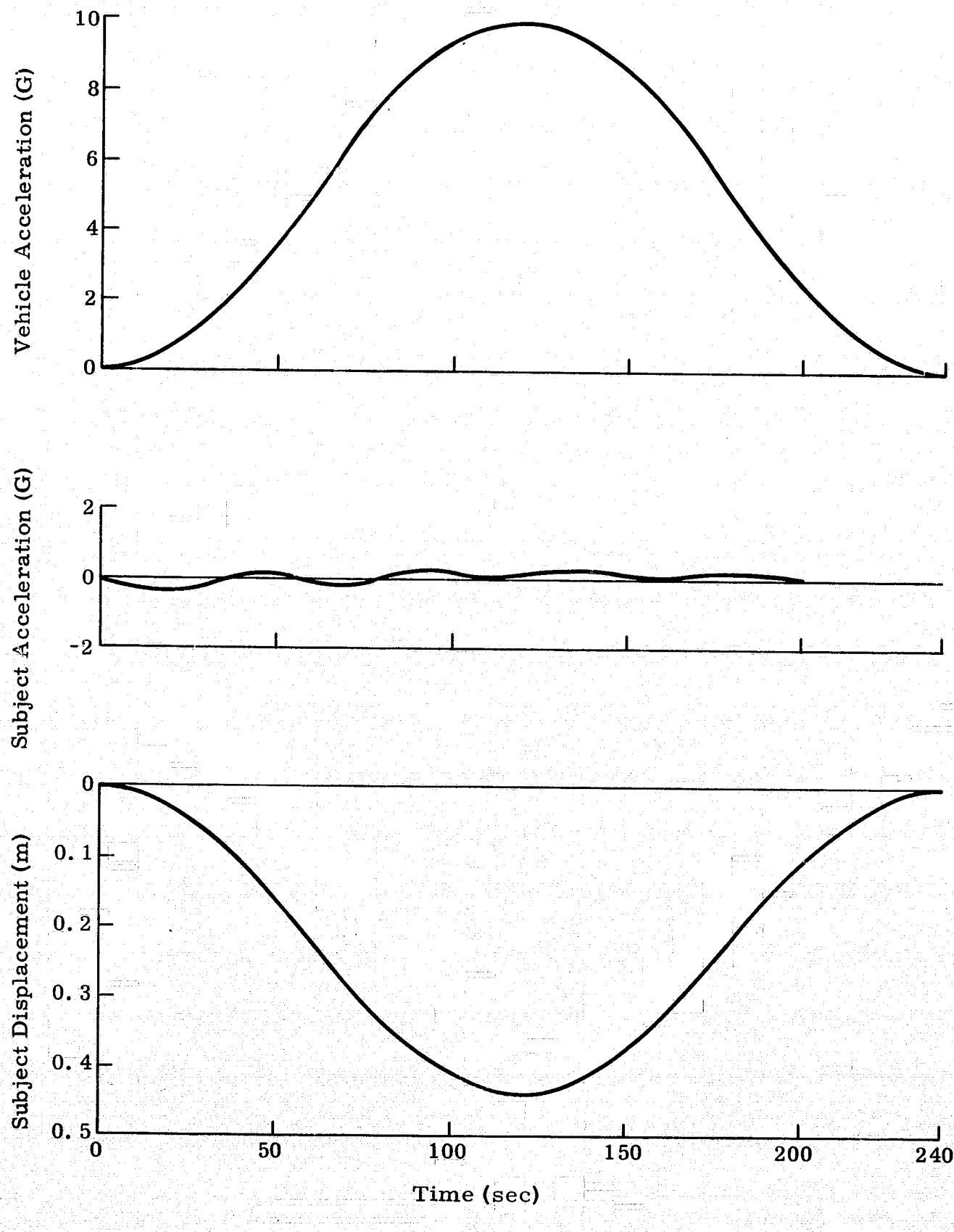

Fig. 65. System Response to Haversine Input--Analog Program--Pilot Compartment Airbag Restraint System

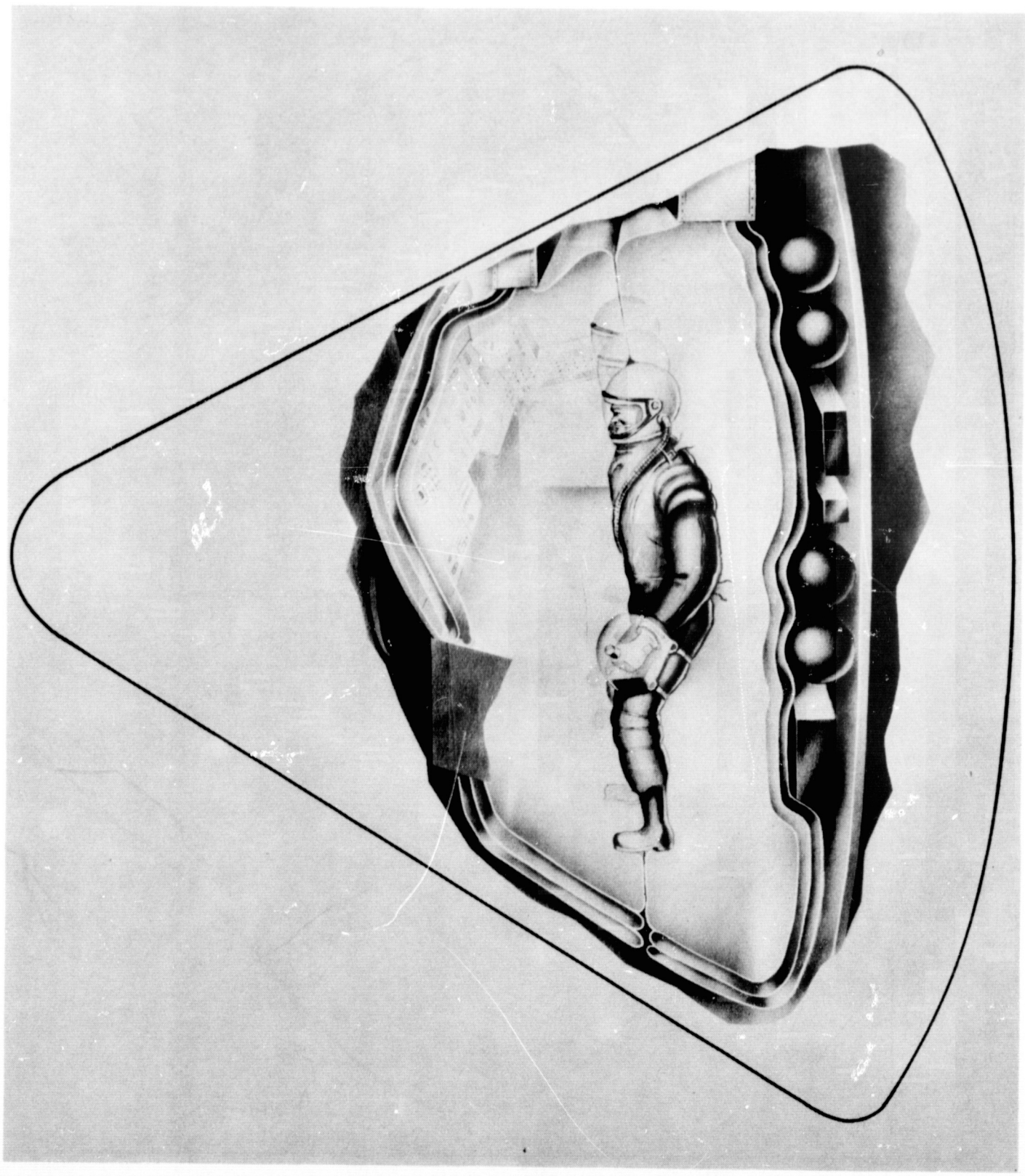

Fig. 66. Airbag Restraint System for a Multimanned Parachute Landing-Type Vehicle

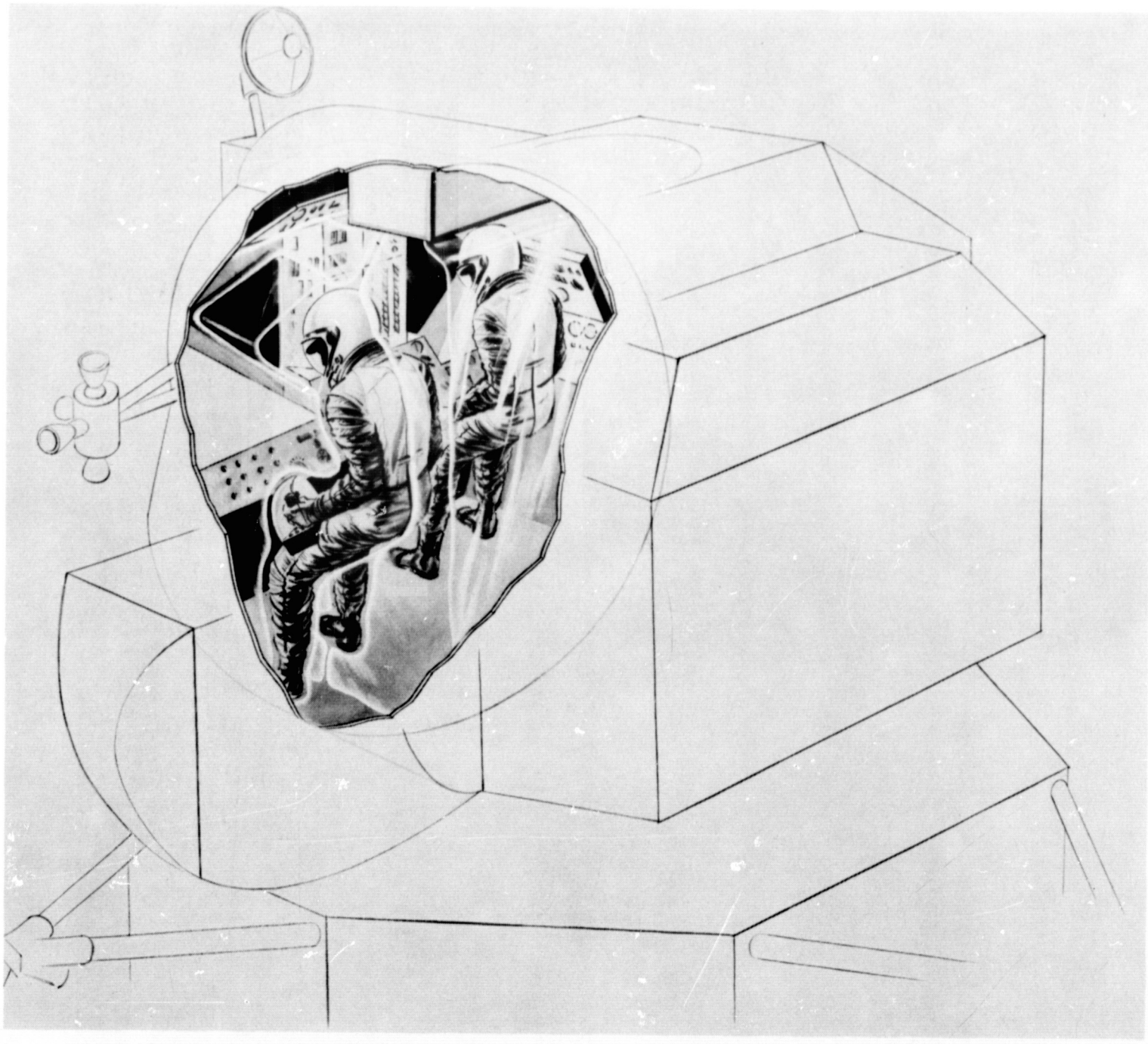

Fig. 67. Airbag Restraint System for a Multimanned Retrothrust Landing-Type Vehicle

Fig. 68. Airbag Impact Protection System for the Extravehicular Maneuvering Astronaut

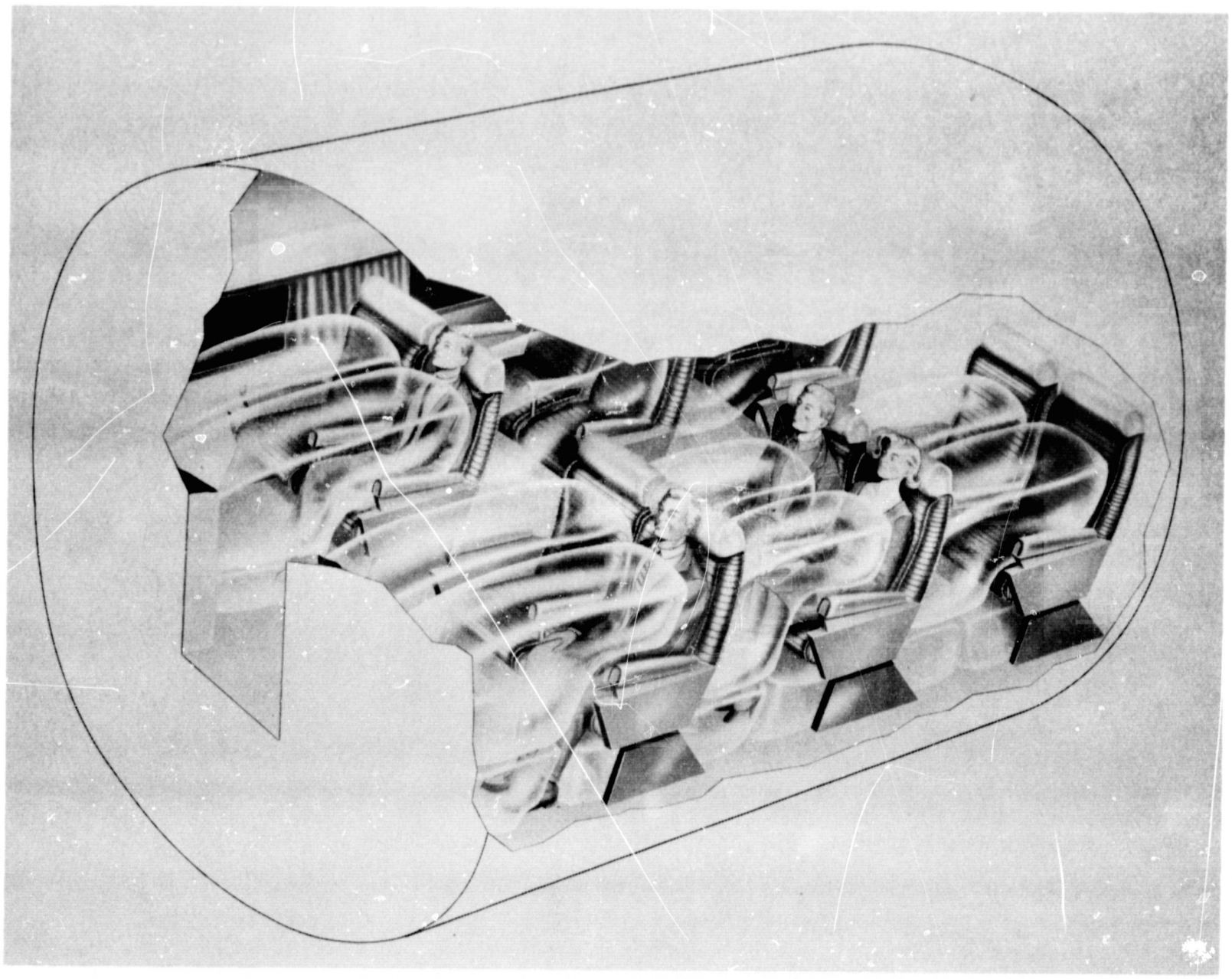

Fig. 69. "Airstop" Airbag Restraint System for Aircraft Crash Protection

FOLDOUT FRAME 1

TABLE 1

Impact Test Data--Pilot Compartment Airb

Test No.	Date	Orientation	Subject	Impact Medium	Drop Height (m)	Impact Velocity (m/sec)	Initial Press. (cm H_2O)	Max Acc, Vehicle*** (G)			G_x	
								G_x	G_y	G_z	Head	Chest
1	4-27-64	Vertical	Anthro. D.	Sand	0.3	2.5	15.0	19.0	--	--	5.0	6.0
2	↑	↑	↑	↑	0.6	3.4	15.0	20.0	--	--	7.0	7.8
3	↕	↕	↕	↕	1.5	5.5	15.0	27.0	--	--	10.4	9.6
4	↕	↕	↕	↕	0.3	2.5	25.0	13.0	--	--	6.6	6.8
5	↕	↕	↕	↕	0.6	3.4	25.0	27.0	--	--	8.6	8.4
6	↕	↕	Anthro. D.	↕	1.5	5.5	25.0	27.0	--	--	12.6	10.8
7	↕	↕	C. C. Clark	↕	0.3	2.5	5.1	22.0	--	--	--	--
8	↕	↕	C. C. Clark	↕	0.6	3.4	5.1	28.0	--	--	--	--
9	4-27-64	↕	C. C. Clark	↕	1.5	5.5	5.1	40.0	--	--	--	--
10	4-28-64	↕	Anthro. D.	↕	1.5	5.5	5.1	39.0	--	--	12.0	7.8
11	↕	↕	↕	↕	0.3	2.5	7.6	16.0	--	--	5.0	5.8
12	↕	↕	↕	↕	0.6	3.4	7.6	27.0	--	--	7.8	6.6
13	↕	↕	↕	↕	1.5	5.5	7.6	40.0	--	--	10.6	9.2
14	4-28-64	↕	↕	↕	3.1	7.6	15.0	45.0	--	--	11.0	11.6
15	4-29-64	↕	↕	↕	3.1	7.6	25.0	40.0	--	--	10.0	9.0
16	↕	↕	↕	↕	3.1	7.6	7.6	44.0	--	--	13.2	10.2
17	↕	↕	↕	↕	4.9	9.8	15.0	49.0	--	--	12.0	11.0
18	↕	↕	↕	↕	4.9	9.8	25.0	52.0	--	--	12.2	9.0
19	4-29-64	↕	↕	↕	4.9	9.8	7.6	62.0	--	--	16.8	11.4
20	4-30-64	↕	Anthro. D.	↕	1.5	5.5	7.6	29.0	--	--	8.4	9.0
21	5-4-64	↕	C. W. Blechschmidt	↕	0.3	2.5	7.6	13.0	--	--	--	--
22	↕	↕	C. C. Clark	↕	1.5	5.5	7.6	35.0	--	--	8.0	8.4
23	↕	↕	C. C. Clark	↕	3.1	7.6	7.6	40.0	--	--	14.8	13.8
24	5-4-64	↕	C. C. Clark	↕	4.9	9.8	7.6	69.0	--	--	21.8	14.6
25	5-5-64	↕	Anthro. D.	↕	4.9	9.8	7.6	65.0	--	--	17.5	12.1
26	↕	↕	↕	↕	4.9	9.8	7.6	52.0	--	--	20.2	12.5
27	↕	↕	↕	↕	1.5	5.5	25.0	40.0	--	--	11.0	12.3
28	↕	↕	↕	↕	3.1	7.6	25.0	40.0	--	--	15.0	14.2
29	5-5-64	↕	↕	↕	4.9	9.8	25.0	60.0	--	--	16.2	15.7
30	5-6-64	↕	↕	↕	1.5	5.5	51.0	28.0	--	--	11.6	11.5
31	↕	↕	↕	↕	1.5	5.5	64.0	29.0	--	--	11.8	11.9
32	↕	↕	Anthro. D.	↕	3.1	7.6	64.0	40.0	--	--	15.4	15.1
33	↕	↕	C. W. Blechschmidt	↕	0.3	2.5	7.6	13.0	--	--	--	4.4
34	↕	↕	C. W. Blechschmidt	↕	0.6	3.4	7.6	21.0	--	--	--	7.0
35	5-6-64	Vertical	C. W. Blechschmidt	↕	1.5	5.5	7.6	36.0	--	--	--	10.0
36	5-20-64	45° feet down	Anthro. D.	↕	1.5	5.5	7.6	17.0 & 12.0	--	6.0 & 4.0	3.9	4.7
37	5-20-64	↕	↕	↕	3.1	7.6	7.6	33.0 & 7.0	--	13.0 & 8.0	4.7	6.5
38	5-20-64	↕	↕	Sand	4.9	9.8	7.6	25.0 & 16.0	--	12.0 & 11.0	6.9	7.3
39	5-21-64	↕	↕	Steel	1.5	5.5	7.6	33.0 & 7.0	--	12.0 & 5.0	4.7	5.5
40	5-21-64	↕	↕	↕	3.1	7.6	7.6	66.0 & 9.0	--	50.0 & 17.0	6.1	8.3
41	5-25-64	↕	Anthro. D.	↕	4.9	9.8	7.6	69.0 & 13.0	--	34.0 & 15.0	11.7	10.7
42*	5-26-64	↕	None	↕	4.9	9.8	--	--	--	--	--	--
43	↕	↕	C. C. Clark	↕	1.5	5.5	7.6	31.0 & 10.0	--	11.0 & 5.0	8.0	4.7
44	↕	↕	C. C. Clark	↕	3.1	7.6	7.6	41.0 & 16.0	--	15.0 & 7.0	14.9	7.4
45	↕	↕	C. C. Clark	↕	4.9	9.8	7.6	72.0 & 17.0	--	27.0 & 12.0	16.5	9.4
46	5-26-64	45° feet down	None	Steel	4.9	9.8	--	50.0 & 18.0	--	23.0 & 7.0	--	--
								⊥ to impact plane				
47	6-11-64	45° left side	Anthro. D.	Sand	1.5	5.5	7.6	34.0			13.7	15.5
48	6-11-64	↕	↕	↕	3.1	7.6	7.6	64.0			39.9	20.3
49	6-11-64	↕	↕	↕	3.1	7.6	25.0	62.0			14.0	9.1
50	6-17-64	↕	↕	↕	1.5	5.5	15.0	35.0			9.9	6.3
51	6-17-64	↕	↕	↕	3.1	7.6	15.0	69.0			13.1	14.3
52	6-18-64	↕	Anthro. D.	↕	3.1	7.6	15.0	66.0			12.3	8.9
53	6-18-64	↕	C. C. Clark	↕	3.1	7.6	15.0	68.0			18.7	10.5
54	6-19-64	45° left side	Anthro. D.	Sand	4.9	9.8	15.0	89.0			24.9	32.3
								G_x	G_y	G_z		
55	6-19-64	Vertical	Anthro. D.	Sand	8.6	12.8	43.0	--	--	--	47.6	32.8
56	6-23-64	Vertical	Anthro. D.	Sand	8.6	12.8	64.0	101.0	--	--	29.0	26.3
57	6-23-64	Vertical	Anthro. D.	Sand	8.6	12.8	25.0	85.0	--	--	37.7	33.0

*This test made for demonstration purposes only.
**Second impact occurred only on 45° feet-down drops.
***Vehicle accelerations for 45° feet-down drops are in order of first and second impacts, respectively.

TABLE 1

ot Compartment Airbag Restraint System

icle***	Max Acc, Subject (G)															Remarks
	First Impact									Second Impact**						
	G_x			G_y			G_z			G_x			G_z			
G_z	Head	Chest	Hip	Head	Chest	Hip	Head	Chest	Hip	Head	Chest	Hip	Head	Chest	Hip	
--	5.0	6.0	7.6	--	--	--	--	--	--							
--	7.0	7.8	9.0	--	--	--	--	--	--							
--	10.4	9.6	12.4	--	--	--	--	--	--							
--	6.6	6.8	8.4	--	--	--	--	--	--							
--	8.6	8.4	9.6	--	--	--	--	--	--							
--	12.6	10.8	12.6	--	--	--	--	--	--							
--	--	--	--	--	--	--	--	--	--							No HD door
--	--	--	--	--	--	--	--	--	--							No HD door
--	--	--	--	--	--	--	--	--	--							No HD door
--	12.0	7.8	10.0	--	--	--	--	--	--							
--	5.0	5.8	6.4	--	--	--	--	--	--							
--	7.8	6.6	8.6	--	--	--	--	--	--							
--	10.6	9.2	10.6	--	--	--	--	--	--							
--	11.0	11.6	15.2	--	--	--	--	--	--							
--	10.0	9.0	13.0	11.8	--	--	--	--	--							
--	13.2	10.2	12.4	--	--	--	--	--	--							
--	12.0	11.0	14.0	--	12.0	--	--	--	--							
--	12.2	9.0	12.2	--	18.0	--	--	--	--							
--	16.8	11.4	14.2	--	--	--	--	--	--							
--	8.4	9.0	12.4	--	--	--	--	--	--							
--	--	--	--	--	--	--	--	--	--							No HD door
--	8.0	8.4	10.2	--	--	--	--	--	--							G_x ankle = 12.6
--	14.8	13.8	16.4	--	--	--	--	--	--							G_x ankle = 21.0
--	21.8	14.6	18.0	--	--	--	--	--	--							G_x ankle = 28.8
--	17.5	12.1	15.4	--	--	--	--	--	--							
--	20.2	12.5	16.6	--	--	--	--	--	--							
--	11.0	12.3	16.0	--	--	--	--	--	--							
--	15.0	14.2	17.0	--	--	--	--	--	--							
--	16.2	15.7	18.6	--	--	--	--	--	--							
--	11.6	11.5	14.6	--	--	--	--	--	--							
--	11.8	11.9	14.6	--	--	--	--	--	--							
--	15.4	15.1	18.6	--	--	--	--	--	--							
--	--	4.4	5.8	--	--	--	--	--	--							G_x knee = 5.4
--	--	7.0	7.0	--	--	--	--	--	--							G_x knee = 7.4
--	--	10.0	10.2	--	--	--	--	--	--							G_x knee = 11.8
6.0 & 4.0	3.9	4.7	5.9	--	--	--	5.7	4.1	4.3	9.4	6.2	5.6	11.8	-5.6	-4.6	
13.0 & 8.0	4.7	6.5	9.7	--	--	--	7.5	6.3	5.7	11.6	8.0	8.0	-14.2	-6.8	-6.0	
12.0 & 11.0	6.9	7.3	11.1	--	--	--	9.7	7.9	7.5	13.8	7.2	8.6	19.0	-10.8	-8.8	
12.0 & 5.0	4.7	5.5	5.1	--	--	--	5.7	4.1	4.3	6.2	5.0	7.4	7.8	-4.8	-4.4	
50.0 & 17.0	6.1	8.3	12.1	--	--	--	9.5	7.5	6.5	12.4	8.6	11.0	-19.0	-7.6	-7.2	
34.0 & 15.0	11.7	10.7	11.9	--	--	--	12.3	6.3	6.9	-11.8	5.0	6.8	-22.8	-11.0	-9.0	
--	--	--	--	--	--	--	--	--	--	--	--	--	--	--	--	
11.0 & 5.0	8.0	4.7	4.6	--	--	--	5.5	6.7	6.1	14.5	5.4	4.8	-6.7	-2.6	-4.8	
15.0 & 7.0	14.9	7.4	8.8	--	--	--	6.3	9.1	7.2	8.3	6.0	5.4	-5.4	-4.8	-5.4	
27.0 & 12.0	16.5	9.4	7.4	--	--	--	9.3	11.3	11.4	9.1	5.0	5.0	-8.6	-6.4	-5.7	
23.0 & 7.0	--	--	--	--	--	--	--	--	--	--	--	--	--	--	--	
ne																
	13.7	15.5	9.7	29.1	17.9	9.1	--	--	--							
	39.9	20.3	28.5	48.4	41.5	21.1	--	--	--							
	14.0	9.1	11.1	20.7	17.7	12.4	--	--	--							
	9.9	6.3	6.9	5.3	4.5	5.5	--	--	--							
	13.1	14.3	9.5	33.1	31.9	22.9	--	--	--							
	12.3	8.9	10.3	17.1	12.7	7.1	--	--	--							
	18.7	10.5	9.3	7.1	5.5	11.5	--	--	--							
	24.9	32.3	21.1	38.7	29.7	25.1	--	--	--							
G_z																
--	47.6	32.8	29.4	--	--	--	--	--	--							
--	29.0	26.3	32.0	--	--	--	--	--	--							
--	37.7	33.0	38.0	--	--	--	--	--	--							